INSIGHTS INTO THE PALAEOBIOLOGY OF SAUROPODOMORPH DINOSAURS THROUGH AN ANALYSIS OF THEIR BONE HISTOLOGY

By

Mohammed Fay-yaad Toefy

Department of Biological Sciences, University of Cape Town, Cape Town, South Africa

DISSERTATION

Presented for the degree of Master of Sciences in the Department of Biological Sciences,

University of Cape Town

September 2023

SUPERVISOR: Prof. Anusuya Chinsamy-Turan

Department of Biological Sciences, University of Cape Town, Cape Town

CO-SUPERVISOR: Dr. Emil Krupandan

Cenozoic Palaeontology, Iziko South African Museum, Cape Town

PLAGIARISM DECLARATION

I understand the meaning of plagiarism and declare that all the work in the following dissertation, except for that which has been acknowledged to others, is my own.

Signed by candidate

Mohammed Fay-yaad Toefy

Table of Contents

List of Figures

List of Tables

Acknowledgements

I would like to express my deep thanks to the following people and organisations for their support in the completion of my dissertation:

- The National Research Foundation and GENUS: DSI-NRF Centre of Excellence in Palaeosciences for funding this project.
- My supervisor Prof. Anusuya Chinsamy-Turan for sharing her abundance of knowledge and providing incredible guidance and opportunities. I would also like to thank her for her support, patience, and encouragement throughout this project.
- My co-supervisor Dr. Emil Krupandan for his assistance in histological section preparation, deep knowledge of sauropodomorph dinosaurs and guidance throughout this project.
- Claire Browning and Zaituna Skosan of Karoo Palaeontology at the Iziko South African Museum for access to specimens and allowing histological analysis on SAM-PK-K382, 3603, 3341, 2780.
- Dr. Jennifer Botha and the National Museum Bloemfontein, for providing permissions and access to specimens NMQR-1551 and 3314 for histological analysis.
- All my lab mates from the UCT Palaeobiology Research Group for their advice, support, and friendship.
- My family (Shaheed, Fayrooz, Shakeelah and Taamir) and friends for their unwavering love and support in everything I do. A special mention to my late grandfather, Moghamat, who was my biggest supporter to pursue postgraduate studies.

Abstract

The Elliot Formation (EF) of Southern Africa ranges from the Late Triassic to Early Jurassic. Many sauropodomorph dinosaurs such as *Massospondylus*, *Melanorosaurus* and *Antetonitrus* have been excavated from the EF. These dinosaurs range from basal Sauropodomorpha to the derived Sauropodiformes providing key insight into their evolution. Osteohistology studies are well recognised as providing much biological information about the growth dynamics of extinct animals, and several studies have focused on either basal Sauropodomorpha or derived Sauropoda. This research assesses the osteohistology of one basal Sauropodomorpha, *Plateosauravus* as well as three derived Sauropodiformes, Sauropodiforme indet., *Melanorosaurus* and Lessemsauridae indet. to better understand their growth dynamics of the transitionary Sauropodiformes *en route* to Sauropoda. Preparation and analysis of thin sections were undertaken on primarily long bones of *Plateosauravus* (SAM-PK-2780 – 3603), Sauropodiforme indet. (NMQR-3314), *Melanorosaurus* (NMQR-1551) and Lessemsauridae indet., (SAM-PK-K382). Histological descriptions and comparisons were completed within and between taxa. The general histology of all long bones was similar. In early to mid-stages of the ontogeny, fibrolamellar bone was the dominant bone type followed by parallel-fibred bone in late stages of ontogeny. *Melanorosaurus* elements differed by exhibiting a distinctive periosteal pathology and considerably more secondary remodelling in the femur. Although badly fragmented, Sauropodiforme indet. elements show similar histological features. Both *Plateosauravus* and Lessemsauridae indet. differ primarily in the degree of vascularisation around LAGs and secondary reconstruction. The number of growth marks varied between two to three in the fragmented Sauropodiforme indet., five to six in *Melanorosaurus* and *Plateosauravus* and up to ten in Lessemsauridae indet. LAGs in the basal taxon, *Plateosauravus*, were found throughout the compacta while the derived Sauropodiformes taxa primarily had growth marks in the outer half. The delayed deposition of LAGs differed between basal Sauropodomorpha and Sauropodiformes thus suggesting shifts towards more uninterrupted growth. Overall, the growth dynamics of these Sauropodomorph dinosaurs suggest an increase in growth rates and shift towards rapid, sustained growth as seen in the more derived Sauropoda, although they also show some variation in their individual growth dynamics.

Chapter 1 Introduction

1.1. Overview of Sauropodomorpha

Non-avian dinosaurs were one of the most diverse groups to roam the Earth spanning most of the Mesozoic for approximately 160 million years from the Middle Triassic to late Cretaceous periods (Nesbitt *et al*., 2013). Structural differences in the pelvic girdle have led to the classification of dinosaurs into Saurischia and Ornithischia (Langer *et al*., 2017). The saurischian pelvic girdle has a 3 pronged 'lizard hip' configuration in which the ilium faces forwards and downwards whereas ornithischians have a 'bird hip' arrangement in which the ilium faces backwards (Seeley, 1887). Pubis arrangement differs between the two groups via the forward-facing pubis in saurischians and the backwards facing pubis parallel to the ischium in ornithischians (Seeley, 1887).

Sauropodomorpha evolved from basal saurischians during the late Triassic (Langer *et al*., 1999; Müller & Garcia, 2020). Evolution of Sauropodomorpha from the basal taxa to the derived Sauropoda during the Jurassic led these dinosaurs to become the giants of the Cretaceous that reached lengths over 40m and weights of over 70 tons (Sander *et al*., 2011; Otero *et al*., 2020; Pol *et al*., 2021).

The global distribution of Sauropodomorpha fossils range from Middle Triassic to the Late Cretaceous. These localities vary geographically and temporally from the Late Triassic Elliot Formation, South Africa (McPhee *et al*., 2018), Ischigualasto Formation Argentina (Ezcurra, 2010; Ezcurra & Apaldetti, 2012), Klettgau Formation, Switzerland (Rauhut *et al*., 2020) to the Late Jurassic Morrison Formation, North America (Harris & Dodson, 2004; Tschopp & Mateus, 2013) and even the Early Jurassic Hanson formation of Antarctica (Smith & Pol, 2007; Cerda *et al*., 2012). In addition to the abundant dinosaur skeletal localities across all latitudes, many trackway sites have been located on every continent (Lockley *et al*., 1994)

Table 1: Phylogenetic nomenclature for the taxa mentioned in this study.

Clade	**Definition**	**Reference**
Sauropodomorpha	The most inclusive clade containing *Saltasaurus* but not *Passer* and *Triceratops*	Sereno, 2007
Massospoda	The most inclusive clade that contains *Saltasaurus* but not *Plateosaurus*	Yates, 2007a,b
Sauropodiformes	The least inclusive clade containing *Mussaurus* and *Saltasaurus*	Sereno, 2007
Sauropoda	The most inclusive clade that contains *Saltasaurus loricatus* but not *Melanorosaurus readi*	Yates, 2007a, b
Lessemsaurids	*Lessemsaurus* and *Antetonitrus*, and their common ancestor, and all its descendants	Apaldetti *et al*., 2018
Gravisauria	The most recent common ancestor of *Tazoudasaurus* and *Saltasaurus*	Allain & Aquesbi, 2008
Eusauropoda	The least inclusive clade containing *Shunosaurus* and *Saltasaurus*	Upchurch *et al*., 2004
Neosauropda	The least inclusive clade containing *Diplodocus* and *Saltasaurus*	Wilson & Sereno, 1998

Basal sauropodomorph dinosaurs, ranging from the basal Plateosauria and Massopodans to the intermediate Sauropodiformes, were the forerunners to more derived sauropods, and provide valuable insight into the evolution and transition from basal Sauropodomorpha to derived Sauropoda and Gravisauria (Sander *et al*., 2011). These basal forms in conjunction with transitional taxa, sauripodiformes such as such as *Aardonyx celeste* (Yates *et al*., 2010), *Sefapanosaurus zastronensis* (Otero *et al*., 2015), *Mussaurus patagonicus* (Bonaparte & Martin, 1979; Cerda, *et al*., 2022), *Melanorosaurus readi* (Van Heerden & Galton, 1997),

Antetonitrus ingenipes (Yates & Kitching, 2003), as well as other lessemsaurids (Pol *et al*., 2021) demonstrate the evolution of key traits and adaptations *en route* to Sauropoda.

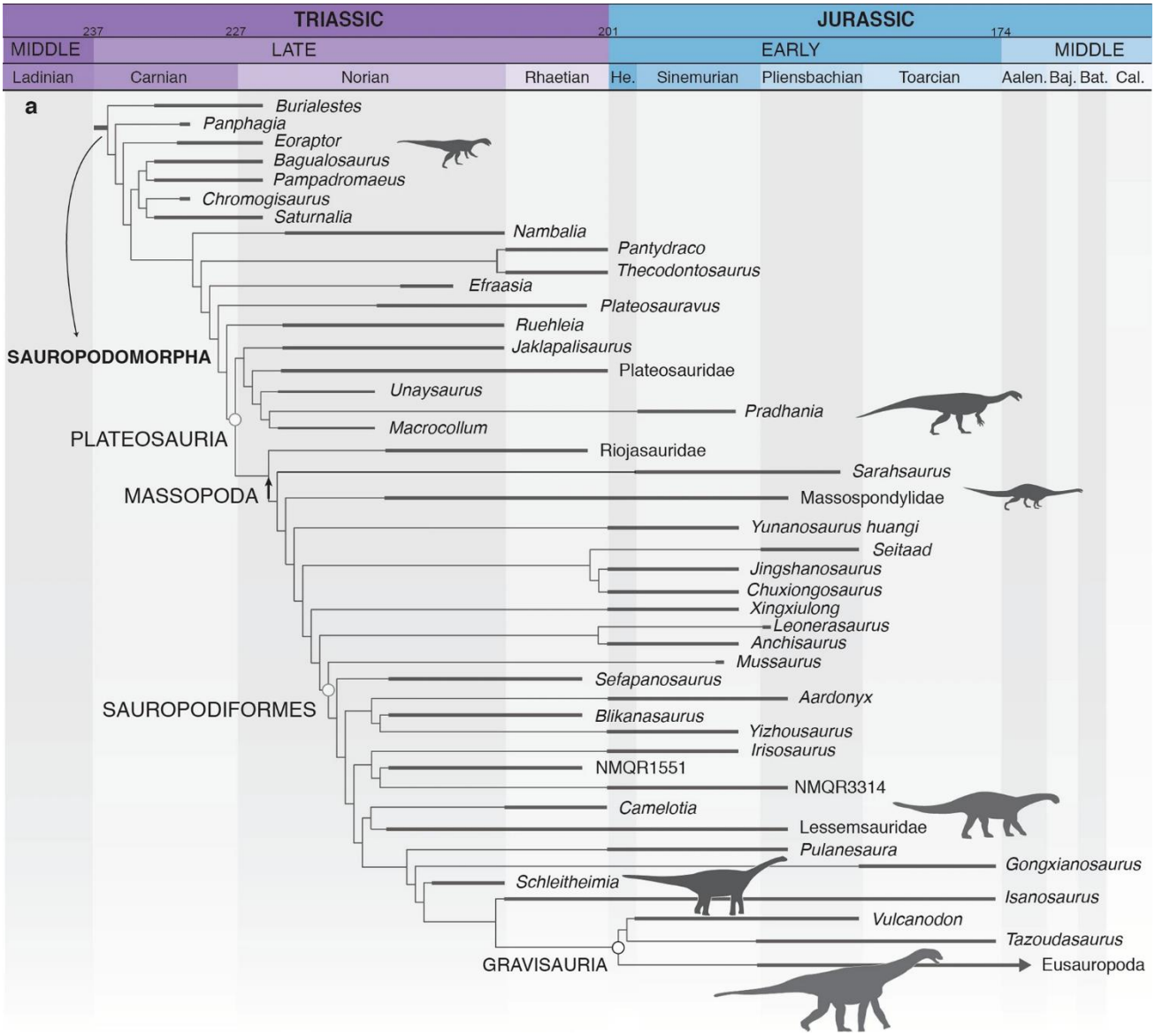

Figure 1: Time calibrated, most parsimonious phylogenetic tree for Sauropodomorpha from Apaldetti *et al.*, 2021.

In the transition from small, bipedal omnivorous basal Sauropodomorpha to the enormous, quadrupedal herbivorous Sauropoda the evolution of robust, columnar limbs, in addition to the elongation of neck, increases in growth among others emerged (Sander & Lallensack, 2018). Changes in posture, limb robusticity and shortening of the distal limb, primarily the femur, over time are indicative of the shifts towards large body

sizes and eventual gigantism (Carrano, 2001; 2005). The iconic gigantism seen in titanosaurs was possible, in part, through their herbivorous diet, enabling them to consume copious amounts of plant material to fuel their rapid growth (Sander & Clauss, 2008; Sander *et al*., 2011; Clauss *et al*., 2013). The evolution of lateral plates along tooth bearing bone of the mandible as well as the changes in cranial shape, increased breadth of snout and the expansion of the cheek region aided in the efficient stripping of foliage (Yates *et al*., 2010; Button et al., 2016). It is thought that the increase in bite size due to the loss of fleshy cheeks and U- shaped palate would have supported their voluminous diet (Barrett & Upchurch, 1994; Yates et al., 2010; Young et al., 2012). In addition, high metabolic rates and changes in growth dynamics (Sander *et al*., 2011; Cerda *et al*., 2017; Apaldetti *et al*., 2018; Krupandan *et al*., 2018) may have allowed for the evolution gigantism. The intensive deposition of fibrolamellar bone is associated with rapid early growth and supports the hypothesis of higher basal metabolic rate (BMR) of transitional Sauropodiformes and Sauropoda (Sander *et al*., 2011). Indeed, there are notable changes in growth strategies between basal Sauropodomorpha and highly derived Sauropoda, but only recently have we begun to get a more comprehensive overview of osteohistological changes into the changes in growth dynamics which would have occurred during this transition (Cerda *et al*., 2017).

1.1.1. Biology of Sauropodomorpha

The biology of sauropodomorph dinosaurs has been well studied with a wide variety of studies that have investigated their feeding methods and dietary choice (Sander *et al*., 2011) as well as a range of biomechanical studies that have focussed on their posture and locomotion (Apaldetti *et al*., 2021).

Many early Sauropodomorpha were small, bipedal and some weighed less than 100kg such as *Saturnalia* and *Eoraptor* (Apaldetti *et al*., 2021). Late Triassic Sauropodomorpha, like *Melanorosaurus*, illustrate the transition from bipedalism to the facultative quadrupedal locomotion prior to the evolution of full quadrupedal locomotion (Schwarz-Wings *et al*., 2010; Sander *et al*., 2011). The transition from bipedalism to quadrupedalism was linked to supporting increasing their size and mass (Carrano, 2005). Sauropodiformes such as *Lessemsaurus sauoropoides* (Bonaparte, 1999) and *Ledumahadi mafube* (McPhee *et al*., 2018) weighed as much as 5 tonnes whereas gravisaurian sauropods such as *Vulcanodon karibaensis* (Cooper, 1984)

and *Patagosaurus fariasi* (Bonaparte, 1999) weighed over 10 tonnes. The drastic increases in both size and mass in the evolution of the Sauropoda from the basal Sauropodomorpha did not occur linearly and appears to be a phylogenetically disparate trait (Rauhut *et al*., 2005; Sander *et al*., 2011; Apaldetti *et al*., 2021).

Size is an important factor in terms of how successful an organism can be (Makarieva *et al*., 2005). Growing larger is highly advantageous in avoiding predation pressure, and in more easily outcompeting other herbivores for resources (Hone & Benton, 2005). Gigantism of sauropods was possible through the evolution of faster growth rates among other adaptations (Sander *et al*., 2004; Chinsamy *et al*., 2016). The expansion into different ecomorphological spaces was key in their evolution of early gigantism in many sauropodiforms as well as later in the evolution of gravisaurian sauropods. This expansion allowed Sauropodiformes to occupy very specific niches whereas early Sauropodomorpha share a morphospace with small theropods (Pol *et al*., 2021).

The evolution of the bauplan of the derived Sauropoda can be traced through the acquisition of several key traits among the Sauropodiformes. For example, the changes to quadrupedality can be seen in their predecessors (Sander *et al*., 2011). More specifically, for example, the robust, columnar limbs seen in sauropods such as *Argentinosaurus huinculensis* (Bonaparte & Coria, 1993; Fowler & Sullivan, 2011) and *Diplodocus longus* (Young *et al*., 2012; D'Emic *et al*., 2013) can be traced to the facultative bipedal ancestral forms such as *Melanorosaurus readi* (Van Heerden & Galton, 1997) and *Saturnalia tupiniquim* (Bronzati *et al*., 2019).

Changes in posture and locomotion, while appearing sporadically, were key factors in the evolution of Sauropodomorpha. Proportional limb robusticity has been used for the inference of posture, with findings showing that quadrupedalism and bipedalism both evolved numerous times, prior to the dominance of quadrupedalism in derived Sauropoda (McPhee *et al*., 2018). Increases in robustness and shifts towards a more columnar build allowed sauropods to support and move their massive bulk (Lefebvre *et al*., 2022). Increases in the size and robustness of hindlimbs were found to be more gradual versus the more sporadic changes in forelimbs (Lefebvre *et al*., 2022). The relative shortening of the proximal limb segment, primarily the femur, and the transition from the cursorial to graviportal increased the load bearing capacity of limbs (Carrano, 2001, 2005; Rauhut *et al*., 2005; Sander *et al*., 2011).

The elongation of the neck that typifies sauropod dinosaurs can be traced to the early sauropodiform dinosaurs (Taylor & Wedel, 2013). The elongation of the neck facilitated their growth by the diversifying their feeding strategies (Yates *et al*., 2010; Bronzati *et al*., 2019). Sauropod necks can reach approximately 12 to 15m in length (Christian *et al*., 2013; Lacovara *et al*., 2014) and are biomechanically viable through the presence of pneumatic chambers within the elongated cervical regions (Taylor & Wedel, 2013). A long neck greatly increased the feeding range which allows for the sauropodiforms and sauropods to outcompete other herbivores (Sander *et al*., 2011; Taylor & Wedel, 2013). Additionally, the neck and small head of sauropods were somewhat inflexible towards the body and was primarily used in extended, sweeping motions (Stevens, 2013). Dental adaptations for mastication such as a spoon-like crown and enamel wrinkling are traits predominantly found in eusauropods but is also present among the basal sauropodiforms (Becerra *et al*., 2017). These changes in dentition suggest the beginning of a shift in diet towards that of the more derived Sauropoda.

In addition to the increase in variation in feeding strategies, it is likely that Sauropodomorpha and especially sauropods were able to process their food more efficiently through unique methods of digestion. Digestion in Sauropodomorphs has been suggested to be a gastric mill using gastroliths (Sander *et al*., 2011) or an extended digestive tract with long retention times based off the megaherbivores of modern times (Wings & Sander, 2007).

Sauropodomorph and sauropod respiratory systems are thought to have comprised multichambered air sacs, and flow-through lungs, and with the help of a powerful heart (or possibly multiple hearts) similar to that of their modern relatives: crocodilians and birds (Sander *et al*., 2011; Seymour, 2016). Extensive pneumatisation throughout the axial skeleton is indicative of modern avian-like respiration in addition to making use of dead space throughout the trachea, especially for sauropodomorphs with long necks (Sander *et al*., 2011; Taylor & Wedel, 2013). Postcranial skeletal pneumatisation (PSP) is well document in modern birds (Britt, 1994) and identified in multiple non-avian dinosaur taxa (Yates *et al*., 2012). Depressions within bone tissue, primarily vertebral elements, allow for attachment of respiratory air sacs in addition to their normal lung capacity. The presence of skeletal pneumatisation contributes to the hypothesis of sauropodomorphs having developed

higher rates of respiration as well as decreasing the weight of their bones (Yates *et al*., 2012; Apostolaki, 2019).

Juvenile sauropod dinosaurs are thought have experienced accelerated growth supported by a high BMR in conjunction with their specialised respiratory system (Sander *et al*., 2011). Additionally, they would be able to acquire and digest food more efficiently, supporting their extreme macronutritional requirements (Sander *et al*., 2011).

Numerous hypotheses have been proposed concerning how sauropodomorphs thermoregulated. Hypotheses such as tachymetabolic, constantly high metabolic rate, and bradymetabolic (high metabolic rate during activity) thermoregulation have been proposed strategies for the maintenance of stable body temperature in sauropodomorphs and sauropods (Hutchinson, 2005). Sauropodomorph dinosaurs are suggested to have had been able to consume enough food and sufficient respiratory ability to support high metabolic rates and thus the capacity for heat production (Christiansen, 1999; Yates et al., 2012; Butler *et al*., 2013). Both strategies would support the homeothermy hypothesis as these dinosaurs were so large that small scale temperature fluctuations would not cause any detrimental change in body temperature (Hutchinson, 2005; Hillenius, 2006).

The combination of these different factors which aided growth are preserved in their bone tissue and through osteohistology, it is possible to determine how these dinosaurs reached their large body sizes (Chinsamy-Turan, 2005).

1.1.2. Dinosaur osteohistology and growth dynamics

At a gross structural level, bone tissue can be classified into a dense component, (i.e., -compact bone) and a spongy or porous component (- cancellous bone) (Chinsamy *et al*., 1998; Chinsamy-Turan, 2005). Cancellous bone generally constitutes the core of the bone whereas the bone wall generally comprises of compact bone tissue. Bone growth occurs through appositional surface deposition. The main surfaces of bone growth are primarily the periosteum and endosteum, whereas an increase in length occurs through endochondral ossification (Francillon-Vieillot *et al*., 1990; Chinsamy-Turan, 2005). The latter process is achieved through the endochondral replacement of cartilage at the ends of the bone. Appositional growth results in an increase

in diameter of the bone wall in addition to the expansion of the medullary cavity. As the shape and axis of the bone changes during growth, drift occurs through the remodelling of the diaphysis (Enlow, 1962a; Chinsamy-Turan, 2005).

The process of secondary reconstruction occurs through the dual processes of the resorption of primary bone tissue and redeposition of secondary bone tissue (Francillon-Vieillot *et al*., 1990). Initially, osteoclasts breakdown and reabsorb bone leaving erosion cavities, osteoblasts then centripetally infill the empty space with lamellar bone tissue forming secondary osteons (Chinsamy-Turan, 2005). Secondary osteons, a type of secondary bone, are easily distinguishable by the cement line which marks the furthest extent of bone resorption. Secondary reconstruction occurs for several reasons such as stressors and environmental factors which include high mechanical loads and vitamin deficiency (McFarlin *et al*., 2016). Secondary reconstruction is additionally associated with old age (i.e., replacement of fatigued bone tissue and general growth of the bone), areas of high muscles attachment (i.e., bone surface reconstruction to allow more attachment points) and during periods of pregnancy and lactation (Cerda *et al*., 2014; Montoya-Sanhueza & Chinsamy, 2018). The amount of intra- and interskeletal secondary reconstruction can differ significantly in the same taxon and between different taxa. Secondary reconstruction occurs more frequently in bones of limbs which are used more intensely due to the increased biomechanical load. The constant biomechanical load leads to fatigued bone which then needs to be replaced by secondary reconstruction (Chinsamy *et al*., 2020). Due to the secondary reconstruction changing the bone texture via resorption and redeposition, as well as drift, important landmark features in the cortex such as growth marks and lines of arrested growth (LAGs) can be erased thereby affecting their efficacy in skeletochronology (Chinsamy, 1990; Nacarino-Meneses *et al*., 2016)

Bone tissue types in dinosaurs

In dinosaurs during early development, fibrolamellar bone (FBL) tissue is the predominant tissue type (Chinsamy-Turan, 2005; Sander & Klein, 2005; Pol *et al*., 2011). Fibrolamellar bone tissue is made of a woven or fibrous bone matrix in which the collagen fibres are haphazardly arranged and the bone tissue is deposited rapidly (De Margerie *et al*., 2004; Chinsamy-Turan, 2005). Post sexual maturity, the rate of

osteogenesis slows down and the deposition of bone becomes more organised. The slowing down in the rate of bone formation results in a change in the type of bone tissue deposited i.e., lamellar, or parallel-fibred bone (PFB) tissue are then deposited. Lamellar bone consists of consistently banded, lamellae of collagen fibres in layered arrangement and appears as stratified lines in the bone compacta. The stratification seen in lamellar bone is due to the slow deposition. Under polarised light, the fibre organisation of lamellar bone tissue appears highly homogenous (Chinsamy-Turan, 2005; Francillon-Vieillot *et al.*, 1990). Parallel-fibred bone is a result of a moderate rate of bone deposition and consists of tightly packed collagen fibres running in parallel to each other with often flattened osteocyte lacunae. The semi-constricted orientation of the fibres appears anisotropic under polarised light (Francillon-Viellot *et al*., 1990; Ziv *et al*., 1996; Chinsamy-Turan, 2005).

Other significant bone types are 1) lamellated, 2) dense Haversian, and 3) compacted coarse cancellous bone. 1) Lamellated bone tissue is stratified bone tissue with small scale cyclical variations and forms due to the variations in mineral microstructure (Reid, 1985). 2) Dense Haversian bone is a type of secondary bone tissue in which a large portion of the cortex has been resorbed and refilled by secondary bone tissue (Reid 1985; Chinsamy-Turan, 2005). Dense haversian bone is visually apparent by the bone between secondary osteons also being remodelled. 3) Compacted coarse cancellous bone is found near the medullary cavity. This type of bone normally forms once cancellous bone is compacted through the endosteal infilling of trabeculae at the medullary boundary (Chinsamy-Turan, 2005; Prondvai *et al*., 2012; Stein & Prondvai, 2014). The presence of compacted cancellous bone is an indicator this region of bone tissue was previously part of the metaphysis (Chinsamy-Turan, 2005).

Specialised types of bone tissue form when skeletal maturity has been obtained. Once the medullary cavity has fully formed, the inner circumferential layer (ICL) of bone is deposited as one of the three slowly deposited bone tissues: lamellar, lamellated or parallel-fibred bone tissue (Enlow, 1962a). The outer circumferential layer (OCL) forms once the appositional growth has slowed down and represents the onset of skeletal maturity. The OCL is generally made up of periosteally formed avascular lamellar bone (Enlow, 1962a; Chinsamy-Turan, 2005) and can sometimes be interrupted by LAGs.

Pathological bone can also be identified in fossil bones. The presence of a bony pathology is indicative of the individual having been inflicted with a particular disease or infection or injury (Chinsamy & Tumarkin-Deratzian, 2009; de Cerff *et al*., 2021). The nature of the pathological tissue can help diagnose the probable cause of death. Abnormal bone tissue often has distinctive features, such as radially organised fibrolamellar and densely distributed osteocytes (Cerda *et al*., 2017).

Cavities within the bone which contained vascular canals and other soft tissues are preserved during fossilisation (Chinsamy-Turan, 2005). These cavities in the fossil show the arrangement of the vascular canals during the life of the individual. The orientations of these vascular canals can be classified into three groups: longitudinal, circumferential and radial. (Chinsamy-Turan, 2005; Huttenlocker *et al*., 2013). Longitudinal vascular canals (running parallel to the diaphysis) appear as circular cavities in cross section. Circumferential vascular canals appear as cavities parallel to the bone periphery. Radial vascular canals traverse the compacta perpendicularly to the cross-sectional bone surface. The vascular canal arrangement can be classified into laminar, plexiform, and reticular (Francillon-Vieillot *et al*., 1990; Chinsamy-Turan, 2005): Laminar vascular canals appear in concentric layers around the cortex and consist of circumferentially arranged and longitudinally organised canals with few if any radial connections (Francillon-Vieillot et al., 1990; Chinsamy-Turan, 2005). Bone with a plexiform arrangement have an abundance of circumferentially and longitudinally organised vascular canals but there are frequent radial connections between the vascular canals (Francillon-Vieillot *et al*., 1990; Chinsamy-Turan, 2005). Reticular, unlike the previous two, show no regular organisation of the arranged vascular canals and there are frequent anastomoses between neighbouring layers of vascular canals (Francillon-Vieillot *et al*., 1990; Chinsamy-Turan, 2005).

Growth in dinosaur bone tissue

The types of growth marks in bone tissue can vary from periodically formed LAGs, to once off, birthing/hatching lines as well as those formed during the late stages of development called ‘rest lines’ (Ricqles De, 1983; Chinsamy-Turan, 2005). LAGs are hypermineralised portions of the cortex where bone deposition is halted periodically. LAGs appear avascular, parallel to the bone periphery and stratified from the rest of the bone matrix when viewed under cross section. In many vertebrates (dinosaurs included) regularly

formed growth marks interrupt the compact bone tissue due to periodic changes in growth rates. Cyclically formed growth marks (CGM) have been used to determine age through the application of skeletochronology (Castanet, 2006; Nacarino-Meneses *et al*., 2016; Woodruff *et al*., 2017). In addition, the OCL (often associated with rest lines) is useful as the indicator of the attainment of skeletal maturity. Like LAGs, rest lines appear visually stratified and are closely packed together near the outer periphery of the bone wall.

In dinosaurs, bone tissue is either deposited continuously (i.e., azonal growth) or is interrupted (i.e., zonal growth) and can change during an individual's life (Ricqles De, 1983; Horner *et al*., 2000; Chinsamy-Turan, 2005; Sander *et al*., 2011). Azonal growth is typically formed rapidly and in the absence of growth marks. Zonal growth is periodically interrupted by the presence of growth marks and is typical of moderate or slow rates of growth. Zonal bone can be grouped into fast growth periods, zones, and slow growth periods, annuli. The associated pauses in osteogenesis displayed by LAGs often precede, follow or are contained in annuli (Reid, 1985; Chinsamy-Turan, 2005).

1.1.3. Osteohistology of Sauropodomorpha

Our understanding of the bone histology of Sauropodomorpha has developed substantially over the past two decades. Based on the limited number of osteohistological studies at the time, Sander, and colleagues (2004; 2008; 2011) proposed a hypothesis that suggested different growth dynamics for sauropod versus non-sauropod sauropodomorph dinosaurs.

Sander and colleagues (Sander *et al*., 2004; 2008; 2011) proposed that sauropods would have maintained high growth rates throughout most of their ontogeny through the rapid rates of deposition of fibrolamellar bone tissue. Only late in ontogeny, once sexual maturity was obtained, did the deposition of growth marks occur, signalling the end of azonal growth. On the other hand, these researchers proposed that basal sauropodomorphs (non-sauropod sauropodomorphs) had zonal bone growth throughout their ontogeny and more variable types of primary bone tissue with the appearance growth marks very early in the ontogeny.

More recently, Cerda and colleagues (2017; 2022), proposed that this notion of dichotomous growth dynamic between basal sauropodomorphs and derived sauropods is invalid. There appears to be far more variation in

growth throughout the sauropodomorph clade than initially hypothesised. Indeed, the variation in growth dynamics of *Mussaurus* and other Sauropodiformes (Cerda *et al*., 2017; Krupandan *et al*., 2018; Botha *et al*., 2022) show that the previously proposed dichotomy in sauropodomorph growth dynamics (Sander *et al*., 2004) is too simplistic. While the general trend of cyclical zonal growth is somewhat common in early Sauropodomorpha, many transitional taxa such as *Mussaurus* and *Antetonitrus* (Krupandan *et al*., 2018) show the capacity to grow fast without interruptions in growth until later stages of their ontogeny.

Additionally, *Mussaurus* (Cerda *et al*., 2022) and basal sauropodomorphs, *Plateosaurus* (Sander & Klein, 2005) and *Massospondylus* (Chapelle *et al*., 2021), show much plasticity in their growth. *Mussaurus* shows both zonal and azonal growth as there is variation in whether LAGs are found in whole cortex versus being constrained to the regions near the bone periphery. Some *Mussaurus* specimens presented with primarily rapidly deposited fibrolamellar bone tissue and only had CGMs in the outer third of the cortex. Whereas other specimens presented with a relatively slower deposited parallel-fibred bone and had CGMs throughout their cortexes. Variation was also observed in the relation of element size to total number of growth marks. This variation is seen in *Plateosaurus* and *Massospondylus* where larger elements does not necessarily suggest older individuals. Further supporting this idea of plasticity is the OCL formation in the smaller specimens of *Mussaurus* which demonstrate that large body size and skeletal maturity are not mutually inclusive.

Basal sauropodiforms are the transitionary group between the basal sauropodomorphs and the derived sauropods. The growth dynamics of several Sauropodiformes have been previously studied (Table 2) and already there appears to be substantial variation in the growth dynamics of this clade. Thus, to fully describe the growth dynamics of the precursors to gigantism it is essential that more sauropodiforms are investigated.

Table 2: Summary of the osteohistological features from the basal Sauropodomorpha and the more derived Sauropodiformes up to basal Sauropoda. The dominant bone tissue is the most common throughout the compacta. The bone type transitions define the dominant tissue type at different ontogenetic stages. Abbreviations: FLB = Fibrolamellar bone; PFB = Parallel-fibred bone.

Taxa	**Dominant bone tissue**	**Bone type transitions**	**OCL presence**	**Primary LAG location**	**Reference**
Basal Sauropodomorpha					
Massospondylus	Fibrolamellar	Cancellous & woven → FLB → Lamellar	None	Entire cortex	Chinsamy, 1993, 1994; Cerda *et al.*, 2017; Chapelle *et al*., 2021; Chapelle *et al*., 2022
Ngwevu	Parallel-fibred	Cancellous & woven → PFB	None	Entire cortex	Chapelle *et al*., 2019
Plateosaurus	Fibrolamellar	Cancellous & woven → FLB → Lamellar zonal	None	Entire cortex	Sander & Klein, 2005; 2008; Klein & Sander 2007
Coloradisaurus	Parallel-fibred	Parallel-fibred bone (No inner cortex preserved)	None	Outer & mid cortex (inner not visible)	Cerda *et al*., 2017
Adeopapposaurus	Parallel-fibred	Cancellous & woven → PFB	None	Outer cortex	Cerda *et al*., 2017
Leyersaurus	Parallel-fibred	Cancellous & woven → PFB	None	Entire cortex	Cerda *et al*., 2017
Leonerasaurus	Parallel-fibred	Cancellous & woven → PFB	None	Entire cortex	Pol *et al*., 2011; Cerda *et al*., 2017
Basal Sauropodiformes					

Mussaurus	Fibrolamellar/ Parallel-fibred	Cancellous & woven → FBL	None	Entire cortex; Outer & mid cortex; None	Cerda *et al*., 2015, 2017, 2022
Aardonyx	Parallel-fibred	Cancellous & woven → PFB	None	Outer & mid cortex	Yates *et al*., 2010; Botha *et al*., 2022
Sefapanosaurus	Parallel-fibred	Cancellous & woven → PFB	None	Outer & mid cortex	Botha *et al*., 2022
Sauropoda					
Ingentia	Fibrolamellar	Cancellous & woven → FLB	None	Entire cortex	Apaldetti *et al*., 2018
Ledumahadi	Parallel-fibred	Cancellous & woven → PFB	Present	Outer & mid cortex	McPhee *et al*., 2018
Lessemsaurus	Fibrolamellar	Cancellous & woven → FLB → PFB	None	Entire cortex	Cerda *et al*., 2017
Antetonitrus	Fibrolamellar	Cancellous & woven → FBL	Present	Outer cortex	Krupandan *et al*., 2018
Volkheimeria	Fibrolamellar	Cancellous & woven → FBL	None	Outer & mid cortex	Cerda *et al*., 2017
Bothriospondylus	Fibrolamellar	Cancellous & woven → FBL	None	N/A	Ricqles, 1983

Notable variation can be seen between the dominant bone types of the Sauropodomorpha and Sauropodiformes. The frequency of parallel-fibred bone is higher in the basal Sauropodomorpha whereas fibrolamellar is most common within the Sauropodiforme clade. According to the previously proposed hypothesis (Klein & Sander, 2007; Griebeler *et al*., 2013) , it would be assumed that all taxa mentioned (Table 1) would show a transition from woven fibrolamellar bone to parallel-fibred bone or lamellar bone tissue early in ontogeny with cyclical growth marks throughout. However, some basal taxa do not show LAGs throughout ontogeny and almost all Sauropodiformes have LAGs present only in the mid- and outer cortex. Additionally, the number and location of growth marks as well as the size of skeletal

elements are not directly correlated as numerous taxa with growth line show some form of plasticity in their growth (Chinsamy, 1993; Sander & Klein, 2005; Chapelle *et al*., 2022).

The abundance of fibrolamellar bone, and the associated fast growth rate, is common throughout the basal sauropodomorphs and sauripodiformes, and rapid early growth rates is a developmental trait throughout the Sauropodomorpha (Table 2). Parallel-fibred bone tissue and its associated medium rate of bone deposition is the most common throughout ontogeny in the basal Sauropodomorpha whereas fibrolamellar bone and its rapid deposition is the most common of the Sauropodiformes from early to late ontogeny (Table 2). The overall trend as Sauropodomorphs evolve towards Sauropods is an increase in the rate of growth shown by azonal growth as well as the abundance of fibrolamellar bone. In Sauropodiformes growth marks are primarily found in the mid and outer cortex showing the primarily uninterrupted growth which is a typical characteristic of the Sauropoda (Sander *et al*., 2011; Sander & Lallensack, 2018; González *et al*., 2020).

Growth dynamics across basal Sauropodomorpha to basal Sauropoda

Growth dynamics of few Southern African Sauropodomorpha have been described in species such as *Massospondylus* (Chinsamy-Turan *et al*., 1990; 1994; Chappelle *et al*., 2021; 2022) and *Antetonitrus* (Krupandan *et al*., 2018). More recently, *Aardonyx* (Yates *et al*., 2010; Botha *et al*., 2022) and *Sefapanosaurus* (Botha *et al*., 2022) have also been histologically analysed, exhibiting the initial rapid growth common in the more derived sauropods. Typical growth patterns seen in early Sauropodomorphs were characterised as interrupted growth zonal growth with CGMs present throughout the ontogeny. While true for some, recent studies (Cerda *et al*., 2017; Krupandan *et al*., 2018; Botha *et al*., 2022) present a transition towards the more derived trait of early uninterrupted growth prior to the zonal growth present throughout transitionary Sauropodomorpha. Below we give brief descriptions of the growth dynamics of pertinent sauropodomorphs ranging from basal Sauropodomorpha to basal Sauropoda:

Plateosaurus (Klein & Sander, 2007)

A basal Sauropodomorph, *Plateosaurus*, presents with combination of basal and derived growth characteristics. Rapidly deposited fibrolamellar bone is the primary tissue throughout the cortex with LAGs present in all regions of the compacta. Later in ontogeny, bone deposition changes from fibrolamellar bone to either parallel-fibred bone or lamellar bone. Plasticity in growth is present in this taxon however, growth is rapid prior to sexual maturity. Following the first CGM, the typical zonal growth is observed. The amount of growth prior to this first CGM and the related size are often disjointed. This variation in growth rates is presented by Klein and Sander as the evidence for plasticity.

Massospondylus

The namesake of the Massopoda is one of the most basal Sauropodomorpha and of the most well studied in terms of osteohistology and ontogenic change (Chinsamy, 1993 & 1994; Cerda *et al*., 2017; Chapelle *et al*., 2021 & 2022). Growth patterns seen in *Massospondylus* are highly characteristic of Sauropodomorpha presenting with GCMs interrupting predominantly fibrolamellar or parallel-fibred bone throughout the cortex. Alternation of poorly vascularised lamellae and well vascularised zonal tissue show the seasonal growth of this basal sauropodomorph (Chinsamy, 1994). Later in ontogeny, fibrolamellar bone deposition is halted and parallel-fibred or lamellar bone is deposited (Chapelle *et al*., 2021). Number and proximity of LAGs vary greatly between different size femora displaying the plasticity of the taxa.

Ngwevu (Chapelle *et al*., 2019)

One of the massospodans, *Ngwevu* shows similar trends to that of *Massospondylus*. LAGs are present throughout the cortex, but intense resorption has occurred with numerous large cavities present. Growth dynamics of *Ngwevu* are similar to other basal Sauropodomorpha as it shows the zonal growth which is common in the early Sauropodomorpha. Parallel-fibred bone tissue is dominant tissue within the long bones with possible radial fibrolamellar bone pathology present in the outer cortex.

Aardonyx (Yates *et al*., 2010; Botha *et al*., 2022)

Aardonyx, a basal sauropodiform, shows combination of both typical sauropod and sauropodomorph characteristics. Woven fibrolamellar bone tissue stops being deposited nearing the middle region of the compacta followed by a transition to a fibrolamellar-parallel-fibred bone complex. Vascular canal arrangement varies between plexiform and reticular arrangements. Fibrolamellar and parallel-fibred bone is present in the outer bone wall. LAGs are common throughout the cortex, but numbers of LAGs vary between skeletal elements. Zonal growth with varying rates of growth is present within *Aardonyx*.

Sefapanosaurus (Botha *et al*., 2022)

A medium sized basal sauropodiform, closely related to *Antetonitrus*, presents with a mixture of common growth patterns. The initial rapid deposition of woven fibrolamellar bone for most of the early ontogeny is shared with many Sauropodomorpha. However, LAGs were found throughout the cortex early in the ontogeny of this dinosaur. After the first LAG was deposited there was a transition to well vascularised fibrolamellar-parallel-fibred bone complex, in either laminar or plexiform arrangement, except for an uncharacteristic portion of woven bone tissue in the outer cortex. The presence of LAGs varied greatly between the elements presented. Zonal growth with varying rates of growth is present within *Sefapanosaurus*.

Antetonitrus (Krupandan *et al*., 2018)

Antetonitrus, a lessemsaurid (McPhee *et al*. 2014; Apaldetti *et al*., 2018), is a key taxon for connecting the growth dynamics of basal sauropodomorphs to those of the sauropods. However, histological studies show *Antetonitrus* presents with typical derived growth traits such as consistent deposition of fibrolamellar and a delay in the deposition of LAGs (Krupandan *et al*., 2018). Fibrolamellar bone was the dominant tissue type throughout the compacta with variations in vascular arrangement. LAGs are seen in mid cortex but most LAGs were visible in outer cortex where bone texture shifts towards a laminar arrangement of vascular canals from a plexiform arrangement. The consistent deposition of fibrolamellar bone tissue and LAGs concentrated at the outer cortex is characteristic of derived sauropods (Klein &

Sander, 2008) whereas the presence of interrupted growth in early bone deposition is a trait seen in most early sauropodomorph dinosaurs (Cerda *et al*., 2017).

Ledumahadi (McPhee *et al*., 2018; Pol *et al*., 2021)

One of the largest lessemsaurids, *Ledumahadi* shows rapid early growth prior to the transition to mid ontogeny parallel-fibred bone. LAGs were only present within the mid and outer cortex but with intensive secondary reconstruction in the inner cortex. The accumulation of LAGs in the outer cortex parallel-fibred bone shows the presence of the EFS signifying a stop in appositional growth. Growth dynamics of *Ledumahadi* resemble that of the other sauripodiformes such as *Antetonitrus* and *Lessemsaurus* with an even larger Sauropod-like body size but did so at a slower rate shows the unique trait of rapid and then a moderate rate of uninterrupted growth prior to zonal growth.

Ingentia (Apaldetti *et al*., 2018)

Similarly, to the basal sauropodomorphs, *Ingentia* shows cyclical growth marks throughout ontogeny. However, these growth marks interrupt thick zones of highly vascularised fibrolamellar bone which would be tied to fast zonal growth as opposed to the proposed theory of relatively slower interrupted growth of the more basal taxa. The growth patterns and trajectory of *Ingentia* is very similar to that of *Lessemsaurus* (Pol & Powell, 2007; Cerda *et al*., 2017) and the abundance of rapidly deposited fibrolamellar bone is trait common in the Sauropoda, seen incipiently in this taxon.

Lessemsaurus (Cerda *et al*., 2017; Apaldetti *et al*., 2018)

Another lessemsaurid, *Lessemsaurus*, does not show the expected growth patterns of the more derived taxa. Like *Ingentia*, CGMs are present throughout the cortex, characteristic of Sauropodomorpha. However, most of the primary tissue is well vascularised, reticular fibrolamellar bone tissue evident of a high rate of growth. In outer portions of the cortex, parallel-fibred bone is well represented but is not the dominant bone tissue showing a slight decrease in rate of growth in late ontogeny.

1.2.Rationale

Sauropodomorph osteohistology is a growing field. However, the evolution of growth dynamics between Sauropodomorpha, Sauropodiformes and Sauropoda has not been fully established. Numerous sauropodomorph dinosaurs have been described systematically and taxonomically but osteohistological studies have only been conducted on some of these taxa. The focus of this research is to analyse osteohistology of the available Sauropodomorph specimens, *Plateosauravus* (SAM-PK 3603, 3341, 2780), an unidentified basal Sauropodiforme (NMQR 3314), *Melanorosaurus readi* (NMQR 1551) and Lessamsauridae indet. (SAM-PK-K382) in order to fully describe the transition of growth patterns from Sauropodomorpha to basal Sauropods.

Plateosauravus (Charig *et al*., 1965) is currently being re-described and is a basal sauropodomorph (Krupandan *pers. comm*). An unidentified sauropodiform dinosaur, Sauropodiforme indet., from the EF, specimen NMQR-3314 is currently undescribed. *Melanorosaurus readi* (NMQR-3314) (Van Heerden & Galton, 1997) has been studied anatomically and revised (De Fabrègues & Allain, 2016) but there is a lack of knowledge surrounding the growth dynamics and osteohistology of the *Melanorosaurus* taxa. The close relation of *Melanorosaurus*, as the immediate outgroup to Sauropoda (Wilson &Sereno, 1998), to *Antetonitrus* and other basal Sauropods would give vital osteohistological information as to the evolution of the rapid growth and eventual gigantism in the Sauropoda. The Telle River dinosaur, referred to as Lessemsauridae indet. is also closely related to the *Melanorosaurus* and basal Sauropoda and thus would also contribute to transitionary growth changes between basal and derived Sauropodomorpha.

The histological analysis of these Southern African sauropodomorph dinosaurs would undoubtedly contribute to our understanding of the evolution, biology, and growth dynamics of the Sauropodomorpha. The osteohistology of these dinosaurs would contribute to creating a more complete view of the growth dynamics of the Sauropodomorpha as well as contribute to the understanding of the evolutionary steps from basal Sauropodomorphs to derived Sauropoda.

1.2.1. Hypotheses

The overarching hypothesis that is being tested in the study is whether the osteohistology of the *Plateosauravus* will show similar growth dynamics to *Massospondylus* and *Plateosaurus* whereas the Sauropodiforme indet. *Melanorosaurus* and Lessemsauridae indet. will show growth dynamics like that of other derived Sauropodiformes previously studied such as *Antetonitrus, Ledumahadi, Ingentia* and *Lessemsaurus*. It is expected that these basal sauropodomorphs would present with interrupted growth throughout ontogeny whereas more derived species would show the initial fast uninterrupted growth prior to the cyclical growth patterns.

More specifically, I hypothesise that:

I. Different elements within each taxon will display similar growth dynamics.
II. There will be notable intraspecific and interspecific histological variation between elements.
III. *Plateosauravus* will show the characteristic zonal growth dynamics previously observed in majority of basal sauropodomorph taxa.
IV. Sauropodiforme indet., *Melanorosaurus* and Lessemsauridae indet. will show the characteristic azonal to late zonal shift in growth dynamics as observed in other sauropodiform dinosaurs.

If these hypotheses are true, I expect:

1. Comparisons between the specimens will yield overall similarities in growth dynamics with notable inter-taxa differences.
2. *Plateosauravus* to have typical zonal growth throughout its lifetime with cyclical growth marks present throughout the compacta.
3. Sauropodiforme indet., *Melanorosaurus* and Lessemsauridae indet. to have initial rapid growth, azonal growth, until sexual maturity followed by zonal growth of either parallel-fibred bone or lamellar bone tissue in late ontogeny.

1.2.2. Aims & Objectives

The aim of this study is to describe the long bone osteohistology of four southern African sauropodomorph taxa to obtain information regarding their palaeobiology and to provide insights into the evolution of growth dynamics in the Sauropodomorpha. The growth dynamics of these taxa will contribute to our understanding of the evolution of gigantism in the Sauropoda.

Research objectives

1. Describe the bone microstructure of *Plateosauravus* (SAM-PK 3603, 3341, 2780s), Sauropodiforme indet., (NMQR-3314), *Melanorosaurus* (NMQR-1551) and Lessemsauridae indet. (SAM-PK-K382) to assess their palaeobiological significance.
2. Compare the intraspecific and interspecific histological variation between different skeletal elements.
3. Compare the osteohistological characteristics of the above taxa with that of other sauropodomorphs and basal sauropods to create a more comprehensive overview of sauropodomorph growth dynamics.

Chapter 2 Materials and Methods

2.1. Specimen information

Specimens used in this study are the basal sauropodomorph *Plateosauravus* (SAM-PK-2780, 3341, 3603), and three sauripodiformes: Sauropodiforme indet. (NMQR-3314) *Melanorosaurus readi* (NMQR-1551), and Lessemsauridae indet. (SAM-PK-K382). All four taxa were excavated from the Elliot Formation which borders South Africa and Lesotho. Exact locations and GPS coordinates are unavailable as excavations were done pre-1950. The Elliot Formation ranges from the Late Triassic (Lower EF) to the Early Jurassic (Upper EF) and dates from approximately 220 to 140 million years ago. In the current study, long bones were all sectioned in the midshaft area as this portion of the bone best preserves the histology of the growth dynamics (Chinsamy & Raath, 1992; Chinsamy-Turan, 2005). Sampling permits and permissions for destructive analysis were obtained from SAHRA and Iziko South African museums and the National Museum Bloemfontein (Permit numbers: 2865; 3091; 3567).

Plateosauravus (SAM-PK-2780, 3341, 3603)

Plateosauravus is a basal sauropodomorph close the basal Sauropodiformes but not a massospodan. One of many dinosaurs classified as *Euskelosaurus*, a garbage bin taxon, *Plateosauravus* like other taxa have been redefined (Krupandan *per comms*). The elements of *Plateosauravus* sampled include the midshaft of a complete femur (Fig. 2.1.1A), the posterior end of a rib (Fig. 2.1.1B) and the distal end of a fragmented femur (Fig. 2.1.1C).

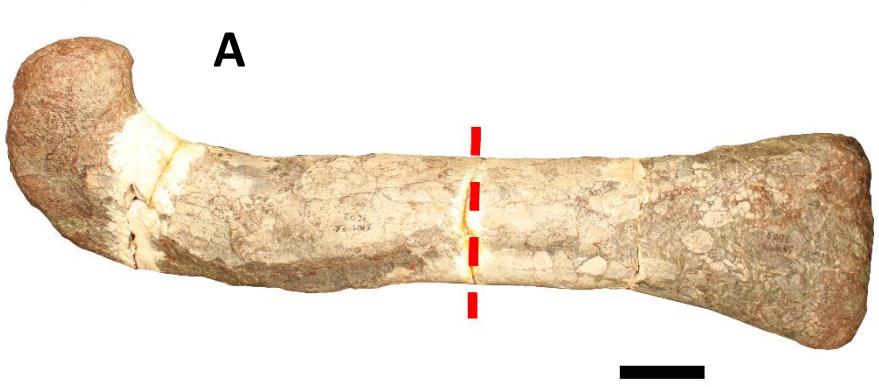

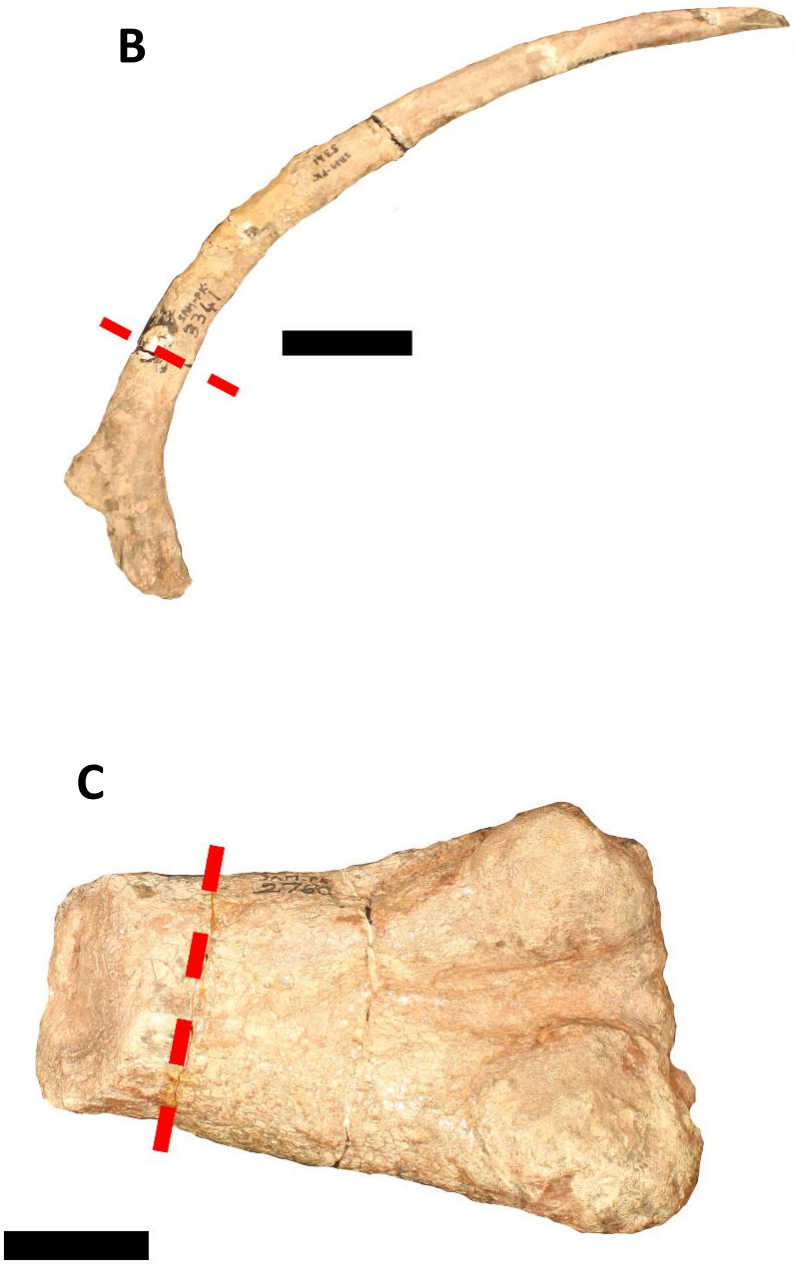

Figure 2.1.1: Photographs of *Plateosauravus* (SAM-PK-2780, 3341, 3603) (A) femur and (B) rib and (C) distal end of a femur. Dashed red lines show the area which was sectioned and described. Scale bar = 5cm.

Sauropodiforme indet. (NMQR-3314)

Sauropodiforme indet. is an unidentified sauropodiform dinosaur and is thought to be related to *Melanorosaurus*. The midshaft of a fibula (Fig. 2.1.2A) and tibia (Fig. 2.1.2B) were sampled.

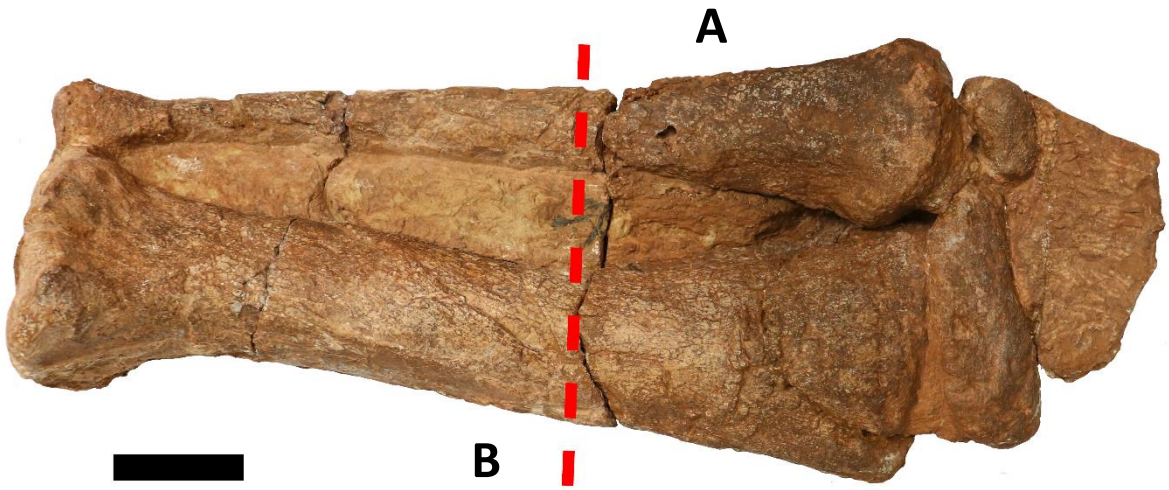

Figure 2.1.2: Photographs of Sauropodiforme indet. (A) fibula and (B) tibia. Dashed red lines show the area which was sectioned and described. Scale bar = 5cm.

Melanorosaurus (NMQR-1551)

Melanorosaurus is a Sauropodiforme closely related to well-studied *Antetonitrus* (Yates & Kitching, 2003; Yates *et al*., 2012; Mcphee *et al*., 2014; Krupandan *et al*., 2018) and *Mussaurus* (Cerda et al., 2014; Otero *et al*., 2019; Cerda *et al*., 2022). The only Sauropodomorpha found in both the Triassic and Jurassic deposits of the EF (De Fabrègues & Allain, 2016) *Melanorosaurus* is an important taxon in the evolution of Sauropodomorpha as the direct outgroup to Sauropoda (Fig. 1). Previously two species of *Melanorosaurus* were identified, *M. readi* and *M. thabensis* however *Melanorosaurus thabanensis* has been revised to *Meroktenos thabanensis* and thus *M. readi* is the only *Melanorosaurus* species. This Sauropodiforme is estimated to have reached 12m and weighed over 1500kg putting it near many basal Sauropods in terms of

size. Elements of *Melanorosaurus* sampled include multiple sections from the midshaft of a femur (Fig. 2.1.3A) and tibia (Fig. 2.1.3B).

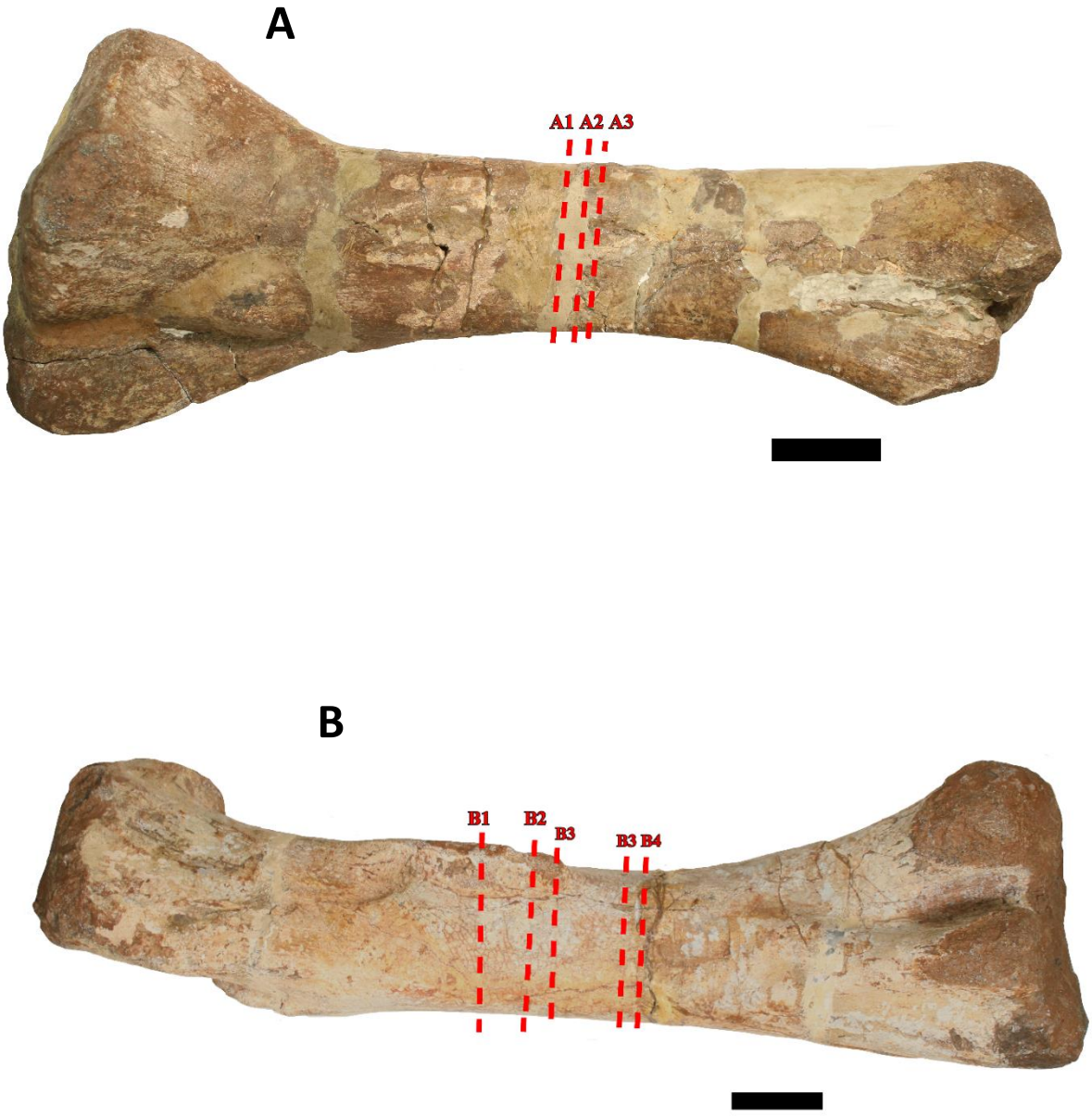

Figure 2.1.3: Photographs of *Melanorosaurus* (NMQR-1551) (A) femur (top) and (B) tibia (bottom). Dashed red lines show the area which was sectioned and described. Labels on the images correspond to the headings in Chapter 3.3. Scale bar = 5cm

Lessemsauridae indet. (SAM-PK-K382)

The so called “Telle River dinosaur” (Fig. 2.1.4A – C) was excavated from the EF, and dates approximately to the Late Triassic. This dinosaur is suggested to be a derived Sauropodiforme from the Lessemsauridae clade and is referred to as Lessemsauridae indet. onwards. Two femora, a tibia, a fibula, and the spinal process of a fragmented caudal vertebra were sectioned as shown below (Fig. 2.1.4A – CD. The long bone elements (Fig. 2.1.4A – C) were sectioned along broken areas of the midshaft, and the caudal vertebrae was sampled as indicated by the red dashed lunes on the image (Fig. 2.1.4D). All the following long bones were sampled once in the midshaft region.

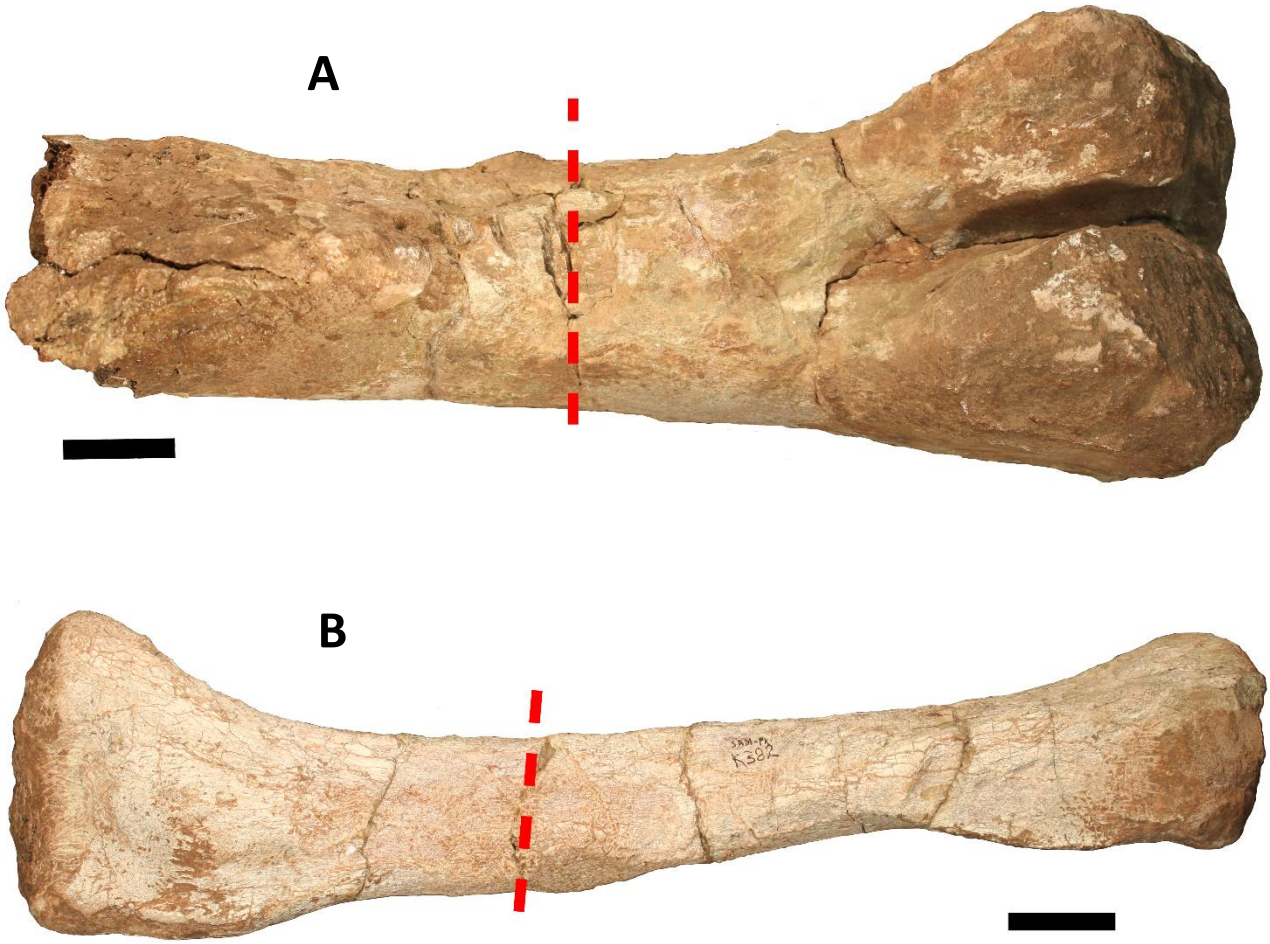

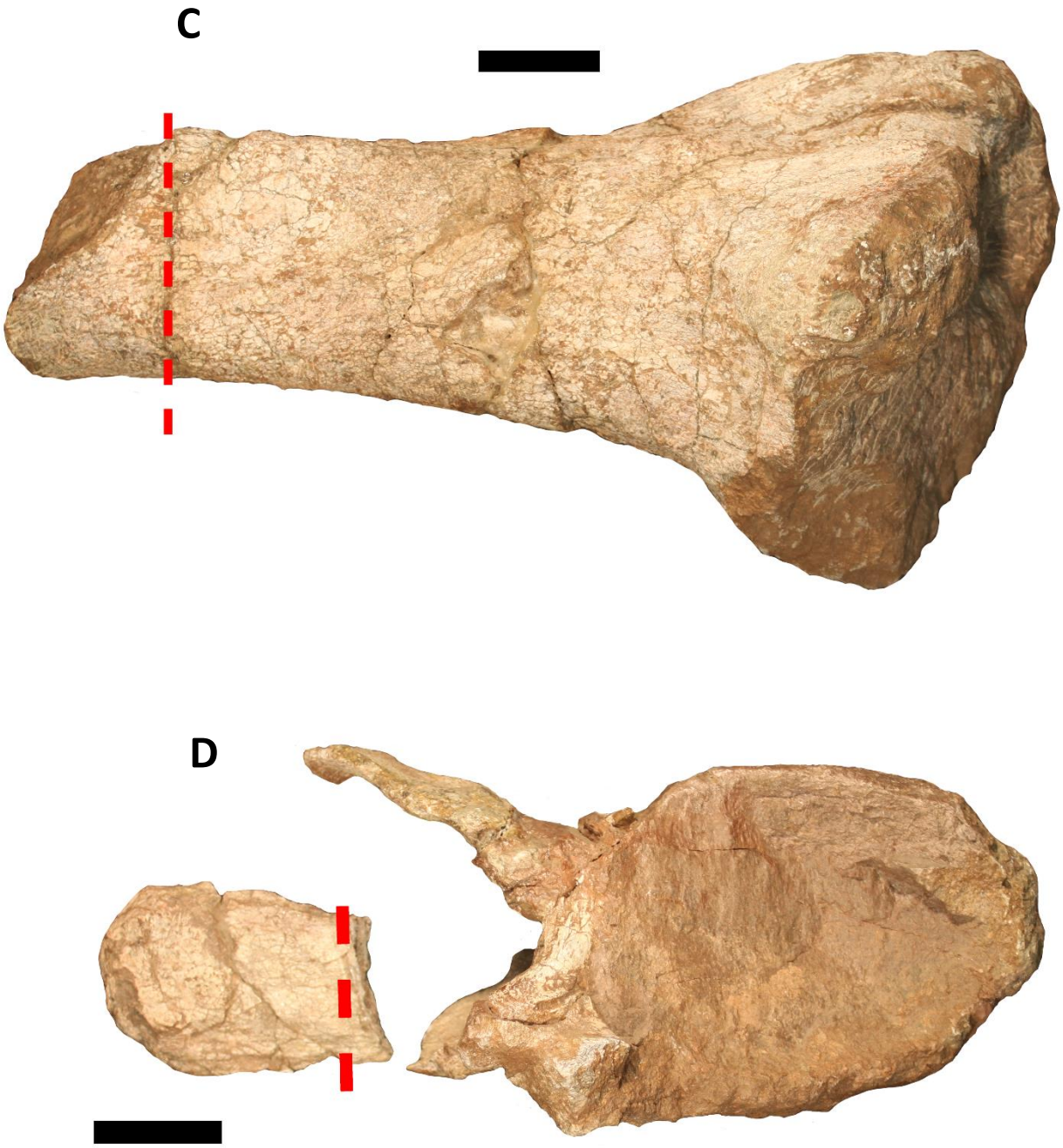

Figure 2.1.4: Photographs of Lessemsauridae (SAM-PK-K382) (A) femur, (B) fibula, (C) tibia and (D) caudal vertebrae. Dashed red lines show the area which was sectioned and described. Scale bar = 5cm.

2.2. Measurements and 3D scanning

Destructive analysis leads to the loss of anatomical features and to preserve as much of the information, standard measurements (such as length, midshaft circumference, diameter etc.) of the fossil bones were recorded (Appendix table 1 & 2). In addition to these measurements, the entire bone was also 3D scanned using an Artec Space Spider (Artec3D). The Artec Spider is a high-resolution light scanner with accompanying software Artec Studio. The General SOP provided by Artec was sufficient in producing high quality scans. The scans preserve all the surface taxonomic and diagnostic features that could be valuable for future taxonomic study.

All fossils were scanned multiple times to preserve the integrity of the surface details. To ensure continuity of features when scanning sometimes homogenous surfaces, such as bones, one needs to find monumental features (landmarks) such a large crack in the fossil or a clear suture or the fourth trochanter but can be anything of visual surface significance. These monumental features allow for the software to align multiple scans by using it as a landmark point. Once the scan is complete, excess 3D material within each scan needs to be erased manually. The scanner mistakenly pickups numerous orbiting pixels which can lead to floating 'dead particles' present in the scan. These floating dead pixels and the surface you place the object on need to be removed prior to the processing of the image. The multiple scans taken should then be aligned which can be done manually if there are not enough landmarks for the automatic alignment feature. Once the scans are aligned, the 3D co-ordinates of each separate scan needs be determined. This registration process uses the monument features to create the parent co-ordinate system that the scans can be assigned prior to fusing the scans together. Note that registration time can range from 5 minutes for small fossils (<5cm diameter, 2 cm length) to 1 hour for larger fossils (~ 40cm diameter, >1m in length) and is dependent on hardware quality, primarily the graphics processing unit. Once registered, image outliers should be removed using the Outlier removal function, but these can also be removed manually. Once the scan is cleaned of outliers then the frames can be fused to obtain the final model which can be saved in several formats, in this study the object (obj.) and shape (shp.) file formats were used for printing and future taxonomic analysis. The sections (Fig. 2.1.1 – 2.1.3) removed for histological analysis were also 3D scanned using the above methodology. The

section scans were each printed for reattachment to the fossil specimen from which the histological sample was removed.

Fig. 2.2: Interactive 3D model of the femur of Lessemsauridae indet. pictured in Fig. 2.1.4.

2.3. Histological sectioning

Fossil samples were cleaned prior to sectioning to prevent any particulates from also being embedded in the embedding medium (-polyester resin). Osteohistological sectioning followed the general procedure outlined in Chinsamy & Raath (1992). Approximately 2 to 4 cm length (due to the size of larger fossils, a consistently sized portion could not be removed from all bones) of the sample were removed from the midshaft of fossil specimens or otherwise indicated in figures 2.1.1 – 2.1.4. The smallest section was taken out (Fig. 2.3A) without impacting the structural integrity of the fossil and to minimise the damage to the bone. Each bone was given a letter label (Fig.2.3B) and the orientation at which the tissue is viewed (P for proximal or D for distal). When multiple thin sections were made from a single bone, numbers were used to distinguish between the different sections of the bone (Fig. 2.3B)

Samples were embedded in clear resin made from Epoxycast resin and Epoxycast hardener (100:30) and left to set 24 – 48 hours depending on the size of the fossil embedded. Once hardened, the resin-fossil block was

cut with a diamond-encrusted cutter (Abrasive cutter Imptech C 10) to fit petrographic microscope slides (55mm x 75mm) (Fig. 2.3C). The exposed side (i.e., the side with exposed fossil material) of the resin-fossil blocks were polished on grinder polisher on 320p, 800p and 1200p carbide grinding discs on the Eura Drives Grinder Polisher (Fig. 2.3D). The increasing grit leads to higher abrasion and a smoother finish prior to mounting onto the microscope slides (Fig. 2.3D). Microscope slides were frosted using the grinding wheel of the Struers Accutom-50. The polished side of the sectioned bone was mounted onto the frosted side of the microscope slides using Epoxycast resin and Epoxycast hardener (100:30). The microscope slide attached to the embedded resin bone blocks were left to harden for 24 hours prior to the thin sectioning. Using Accutom-50, specimens attached to the microscope slides were cut to approximately 300um thickness with the diamond edged blade (Fig. 2.3E). The thin sections were then ground down to approximately 200um prior using the Accutom-50 grinding wheel before the final grinding and polish. The thin sections slides were then ground and polished on abrasive carbide sandpaper on the Eura Drives Grinder Polisher. The grinding begun on lower grit sandpaper which is rougher and the finished on higher grit for polishing. The grit paper was used the order 320p, 600p, 800p and 1200p. The petrographic slides were then polished by hand using 1200p abrasive carbide sandpaper. The final polish was done on the Eura Drives Grinder Polisher using silicon carbide powder on a fabric wheel.

Once thin sections reached an appropriate thickness (approximately 30 microns; Fig. 2.3F) and the detailed histology could be seen under the Zeiss AX10 light microscope, the thin sections were ready for study. Photographs were taken under normal and polarised light using the Zeiss Blue software and Axiocam 208 Colour camera and editing was done using Clip Studio Paint. Composite photomicrographs were obtained using AutoPano Giga to stitch high resolutions photographs into panorama views of the entire bone cortex.

The histology of the sections were described using terminology from Francillon-Vieillot *et al*. (1990) and Chinsamy & Hurum (2006). Each section was described separately, and all photographed portions are mapped onto thin section drawings. Since the bone wall of the specimens were quite large, the histology of the thin section was split into thirds for histological descriptions (i.e., Outer, mid, and inner cortexes). When specific

portions are not preserved in the thin section, the same terminology is used as the regions are relative to the entire bone wall shown in the thin section schematics.

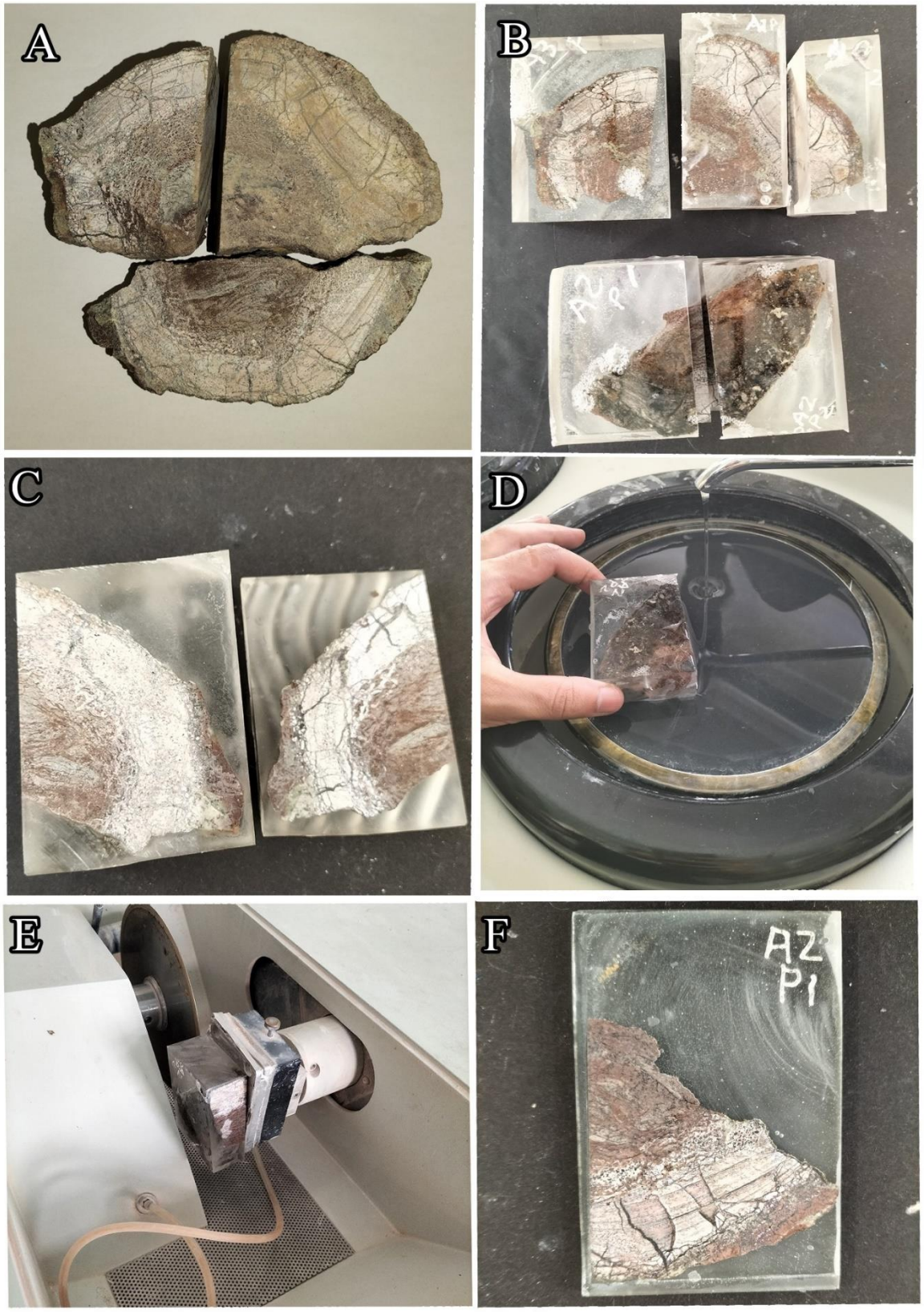

Figure 2.3: Preparation of fossils for thin sectioning. A) Section of femora mid-shaft cut into three parts to fit the petrographic microscope slides. B) Cut femoral sections are embedded in resin and engraved with labels A1 - A3. The same letters shown indicate that the sections are from the same element. P or D indicate whether it is the proximal or distal view. The numbers are for identification purposes for when more than one section is made per bone sample. C) Resin block containing the fossil sample is cut prior to polishing of the larger exposed specimen which is mounted onto the petrographic slide. D) Polishing exposed side prior to mounting onto microscope slide. The polishing starts at low 320 grit and finishes on a high 1200p grit for a smooth surface to mount. E) Cutting of excess material post mounting. Cutting excess sample allows for more efficient grinding and polishing and reuse of the cut-off larger block for extra thin sections. F) Thin section of proximal side of femora mid-shaft for viewing under the petrographic microscope.

Chapter 3 Results

3.1. *Plateosauravus*

A rib, complete femur, and distal femur head of *Plateosauravus*, were sampled. The sections were taken from the proximal portion of the rib, midshaft of the complete femur and from the distal end of the detached femur head (Fig. 2.1A – C).

3.1.1 Rib histology of *Plateosauravus* (SAM-PK-3341)

The thin section shows the histology of the proximal end of the rib. The bone wall of section (Fig. 3.1.1A) consists of intensively secondarily reconstructed bone tissue except for the outermost portion of the bone wall which comprises of some primary bone tissue in between well-developed secondary osteons and erosion cavities (Fig. 3.3.1B). The primary bone tissue tends to be parallel-fibred bone tissue.

The medullary cavity is surrounded by cancellous bone tissue (Fig. 3.1.1C) which makes up a considerable portion of the inner compacta. Long trabeculae extend into the medullary cavity.

The mid cortex comprises of exclusively secondarily reconstructed bone tissue (Fig. 3.1.1D) with numerous secondary osteons which often forms dense Haversian tissue. The abundance of secondary osteons is only interrupted by moderate sized resorptive cavities (Fig. 3.3.1D). Moderately sized resorption cavities are common throughout the mid cortex, and some have endosteal deposits of lamellar bone tissue.

Parallel-fibred bone is present in the outermost portion of bone tissue. Secondary osteons are present within and around the portions of parallel-fibred bone tissue (Fig. 3.1.1E). LAGs are visible despite the intensive amounts of secondary reconstruction (Fig. 3.1.1E & F). Eight LAGs are present within the mid and outer portions for the compacta. In some areas, it is obvious that the secondary reconstruction completely removes some of the LAGs that were present (Fig. 3.1.1B).

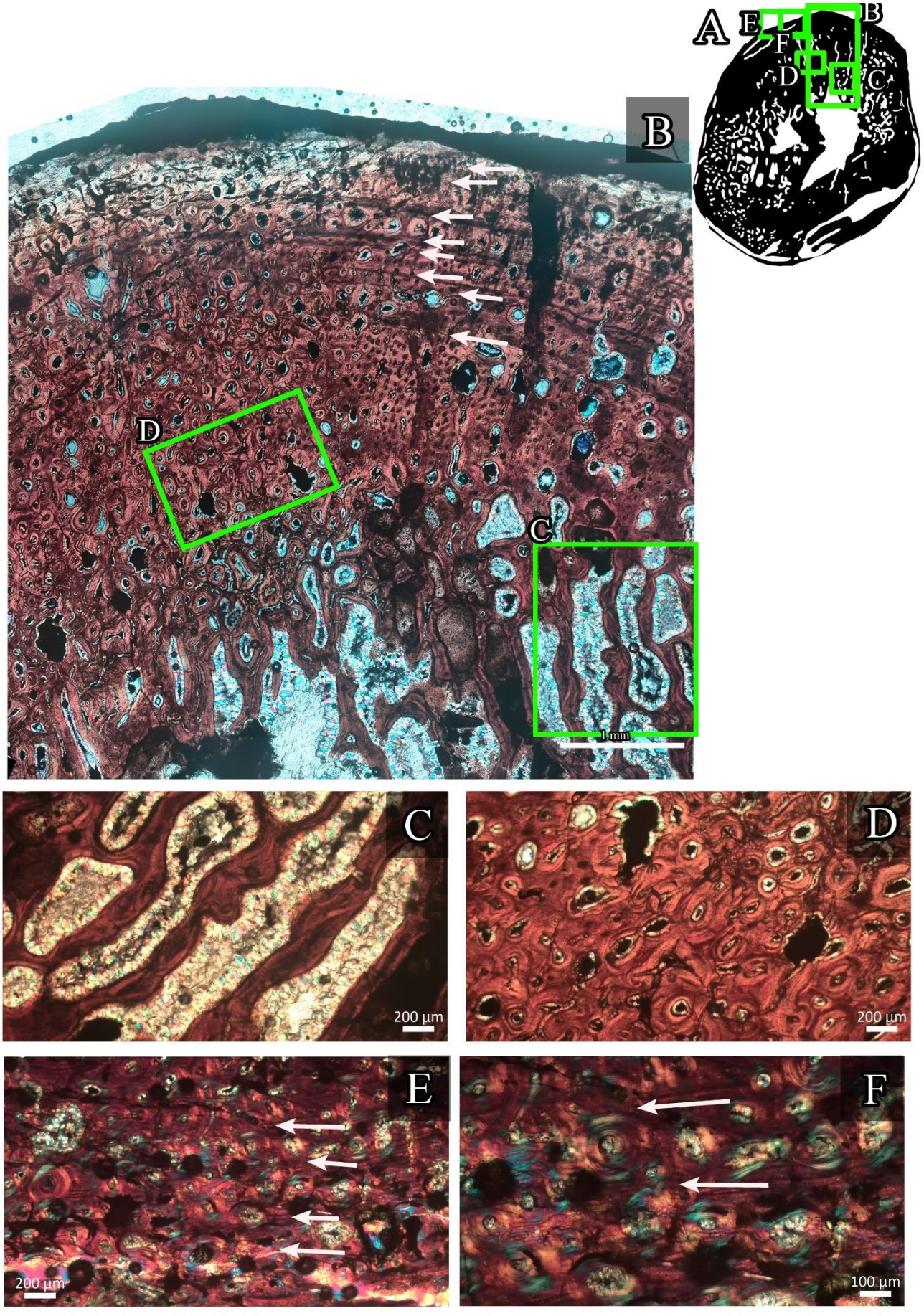
A
B
C
D
E
F
1 mm
200 µm
200 µm
200 µm
100 µm

Figure 3.1.1: Histological section of the *Plateosauravus* rib. A) Schematic of the preserved bone tissue of the thin section. The black area indicates the preserved part of the bone wall. Green boxes show the location of the higher magnification photographs. B) Composite micrograph showing the general histology of the rib from medullary cavity to the bone periphery. White arrows indicate the growth marks. C) Struts of cancellous trabeculae bordering the medullary cavity. D) Dense Haversian bone in the inner cortex with few moderately sized resorptive cavities. E) Higher magnification view of multiple growth marks preserved despite intensive secondary reconstruction. F) Close up of view of E. Two LAGs can be seen amongst fully formed secondary osteons.

3.1.2 Femoral histology of *Plateosauravus* (SAM-PK-3603)

The thin section (Fig. 3.1.2A) represents the mid-diaphyseal section of the complete femur of *Plateosauravus* (Fig, 2.1A). The general histology of HD shows mostly well-preserved tissue, but some cracks are present in the compacta. The section consists of a transition from secondarily reconstructed and fibrolamellar bone tissue in the perimedullary regions towards parallel-fibred bone in the outer cortex (Fig. 3.1.2B).

The perimedullary regions comprises of well vascularised fibrolamellar and some cancellous bone tissue (Fig. 3.1.2C). Arrangement of intrinsic fibres show mass birefringence. There is a moderate amount of secondarily reconstructed tissue within the inner compacta, but the region still tends to have a cancellous texture. Small secondary osteons and resorptive cavities are present but generally, the inner cortex is not heavily reconstructed. Growth marks can be seen in the inner cortex where there are lesser amounts of secondary reconstruction. Lamellar bone tissue is deposited around the growth marks forming an annulus.

The well vascularised fibrolamellar bone is the dominant bone tissue throughout the mid cortex (Fig. 3.1.2D). The arrangement of vascular canals is primarily in a laminar arrangement throughout the cortex in addition to localised areas of plexiform-reticular vascular arrangement. Vascularity is commonly high throughout the mid cortex but a decrease in vascular canal abundance occurs near the growth marks. Two to three growth marks surrounded by lamellar bone tissue are visible in the mid region of the compacta. Secondary remodelling is uncommon as only small secondary osteons and very few resorptive cavities are found in the mid cortex. Intrinsic fibre arrangement ranges from a moderate (Fig. 3.1.2E) to mass birefringence. Growth marks start being deposited in the mid cortex (Fig. 3.1.2B & D).

The outer cortex consists of primary moderately vascularised parallel-fibred bone and well vascularised fibrolamellar bone tissue (Fig. 3.1.2F). The circumferential and longitudinal vascular canals are present in a laminar arrangement. There are very few radially orientated vascular canals in the outer portion of the compacta. Secondarily reconstructed bone is minimal nearing the outer bone wall as few small secondary osteons are seen. Additionally, not many resorptive cavities are present. Intrinsic fibre arrangement shows a moderate degree of arrangement. Four LAGs are seen in outer region and vascularity decreases near these LAGs as lamellar bone tissue is deposited.

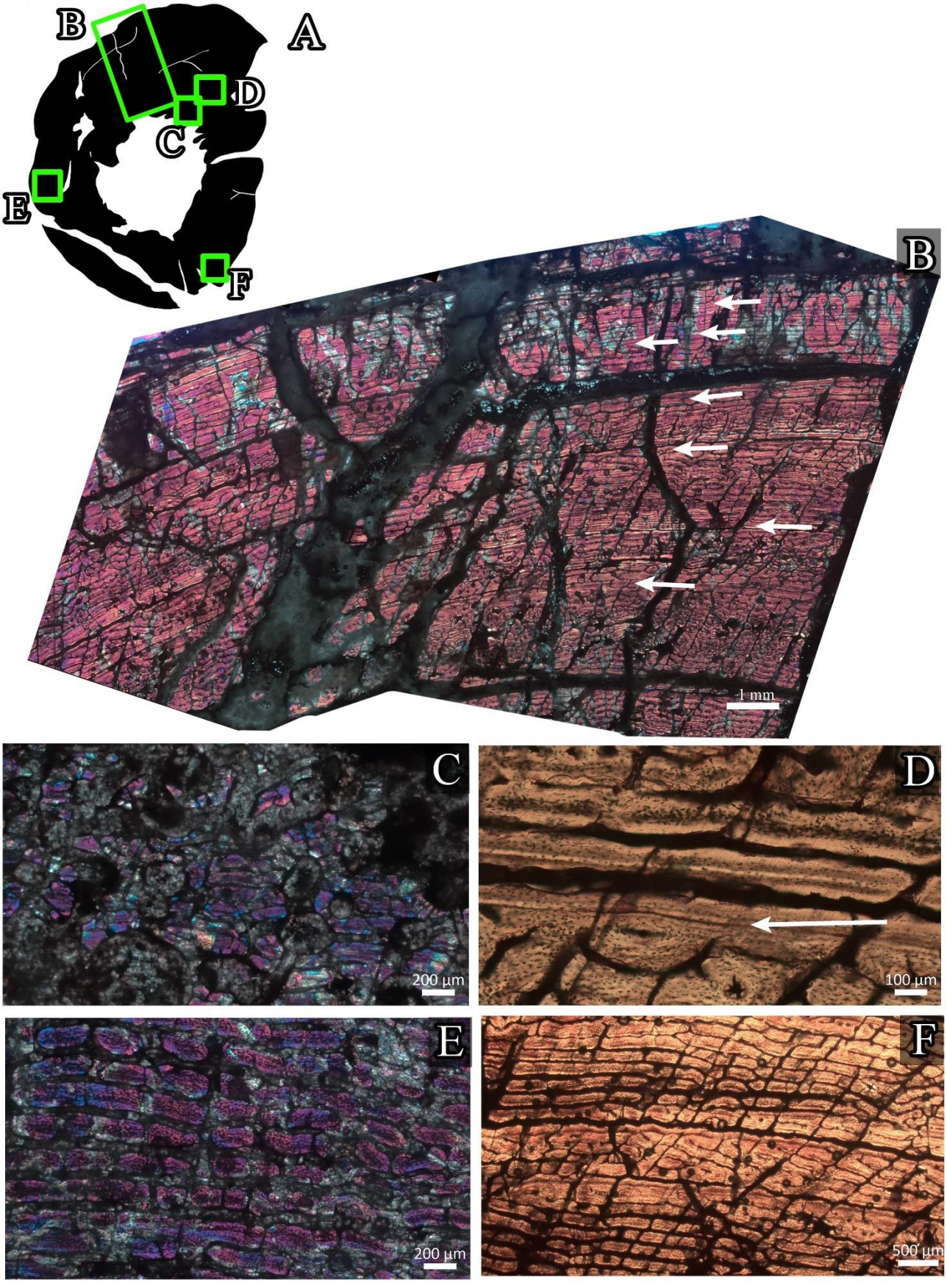
A
B
C
D
E
F
1 mm
200 µm
100 µm
200 µm
500 µm

Figure 3.1.2: Histological section of the *Plateosauravus* right femur. A) Schematic of the preserved bone tissue of the thin section. The black area indicates the preserved part of the bone wall. Green boxes show the location of the higher magnification photographs. B) Composite micrograph of the posterior portion of the bone compacta. White arrows indicate the growth marks. C) High magnification view of the poorly preserved inner cortex consisting of fibrolamellar bone and resorptive cavities. D) Close up view of a growth mark in the mid cortex which comprised of mostly fibrolamellar tissue. E) High magnification view of the well vascularised fibrolamellar bone tissue found throughout the mid and outer areas of the bone. Polarisation shows the moderate birefringence of the intrinsic fibres. F) Low magnification view of the fibrolamellar bone with vascular canals in a plexiform arrangement.

3.1.3 Femoral histology of Plateosauravus (SAM-PK-2780)

Two thin sections were made from the tibia of the distal end of the *Plateosauravus* femur as shown below in figure 3.1.3.

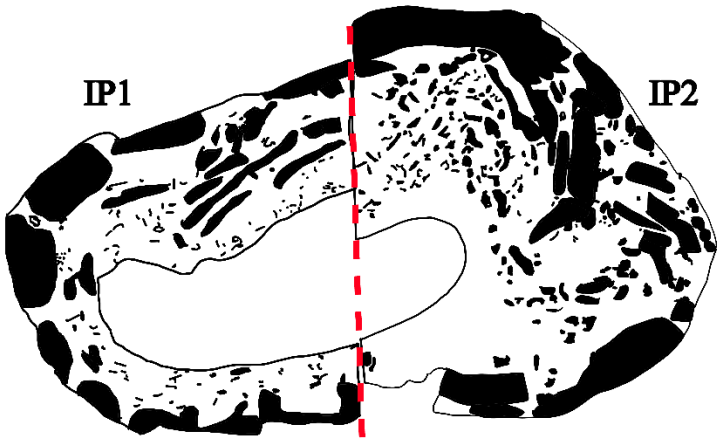

Fig. 3.1.3: Drawing of the distal end of a *Plateosauravus* indicating how the fragmented bone sample was cut for thin section analysis. The dashed line represent how the bone section was cut for mounting onto the petrographic slides.

3.1.3.1 Lateral femoral section

The thin section IP2 shows the histology of the lateral half of the distal end of the femur head of *Plateosauravus*. The section is poorly preserved, and the bone wall is highly fragmented, with some parts of the compacta displace inwards towards the medullary (Fig. 3.1.3.1A). The compacta comprises of cancellous textured and fibrolamellar bone tissue in the inner cortex and parallel-fibred and fibrolamellar bone (Fig. 3.1.3.1B) in the outer two thirds. The fragmentation prevents any definitive LAG identification as there is minimal continuity between the compact tissue.

The inner cortex is poorly preserved but appears to be highly cancellous in texture (Fig. 3.1.3.1C). The portions of fibrolamellar bone tissue within the inner third are all well vascularised with high variation between intrinsic fibres. Secondary remodelling is common throughout the inner cortex with abundant fully formed secondary osteons throughout in addition to large resorption cavities.

The mid cortex consists of parallel-fibred and fibrolamellar bone tissue (Fig. 3.1.3.1D) and a small amount of secondarily reconstructed bone tissue. Vascular canal arrangement tends to be in either a laminar or plexiform arrangement. Intrinsic fibres tend to have moderate birefringence. Many resorptive cavities are visible and are being infilled with lamellar bone tissue. The fragmented parts of the bone wall comprises of fibrolamellar bone with numerous osteocytes in a loose arrangement and a haphazard arrangement of vascular canals. A LAG can be seen in a fragmented portion of bone tissue, but the total number of LAGs cannot be observed due to the overall poor preservation (Fig. 3.1.3.1E).

The outer cortex consists of predominantly parallel-fibred bone (Fig. 3.1.3.1F). The parallel-fibred bone shows an abundance of vascular canals. The vascular canals of the outer cortex tend to be mostly circumferentially orientated. Small secondary osteons and dispersed resorption canals are visible. No growth marks can be discerned due to extremely poor preservation.

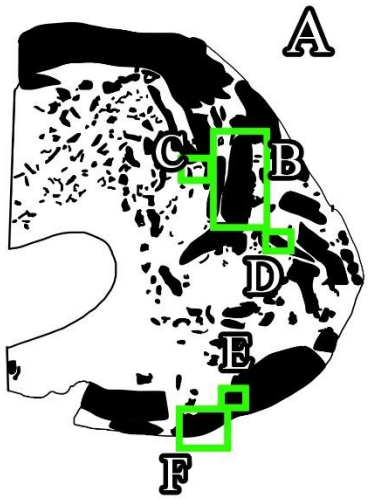
A
C
B
D
E
F

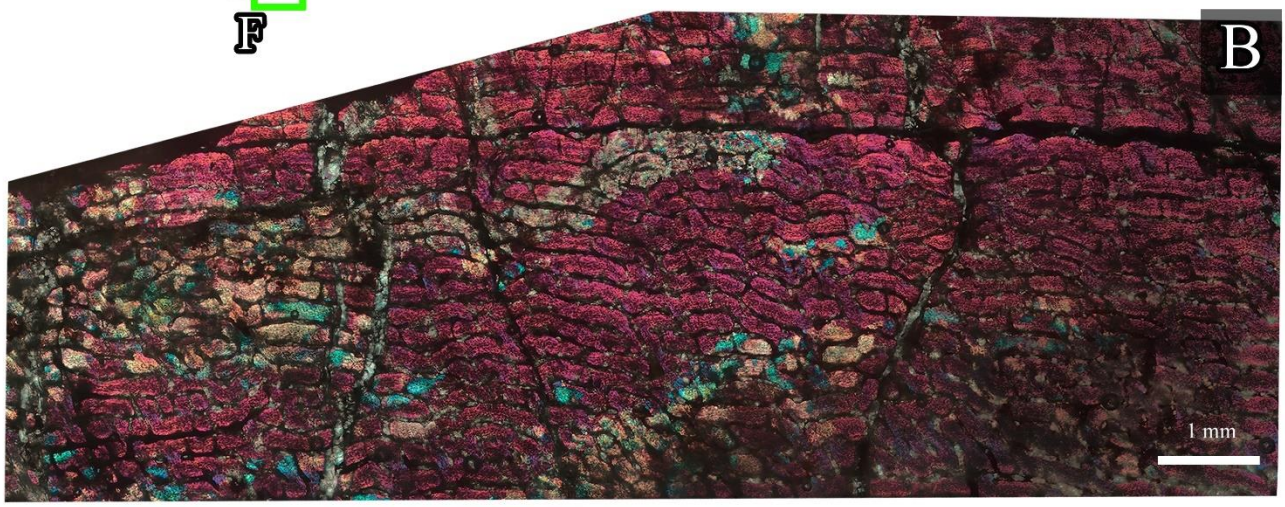
B
1 mm

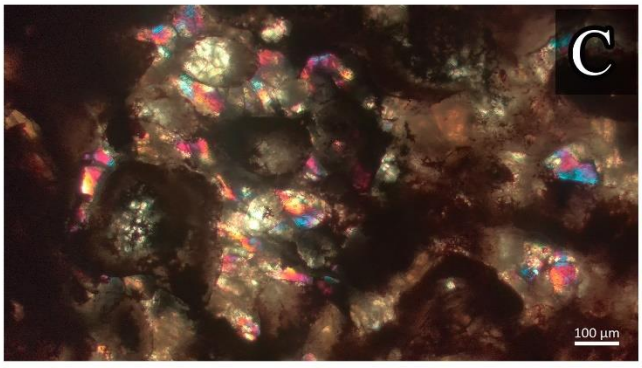
C
100 µm

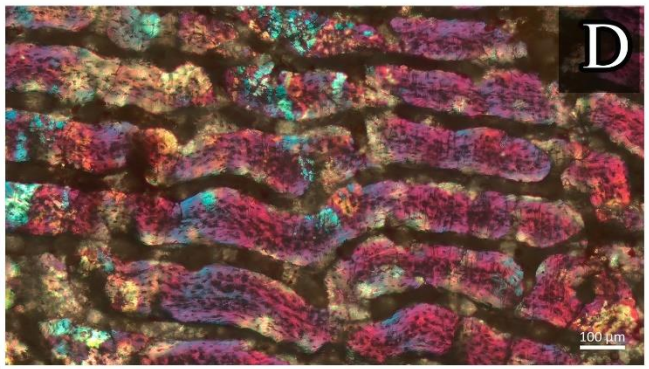
D
100 µm

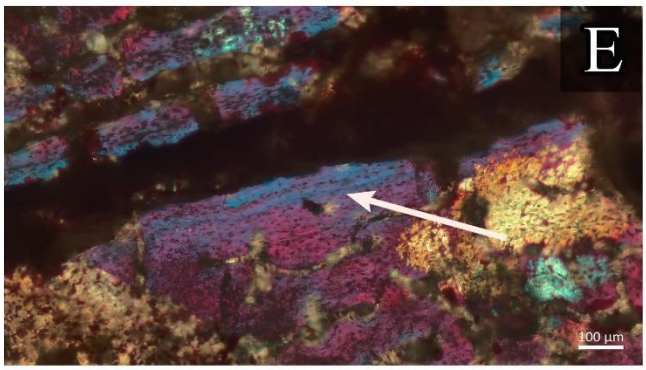
E
100 µm

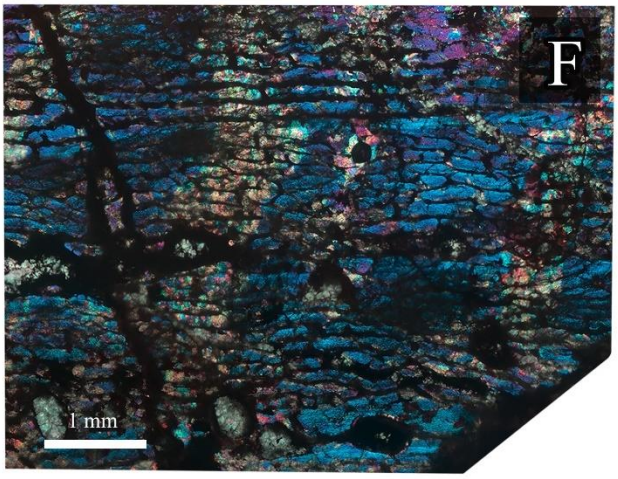
F
1 mm

Figure 3.1.3.1: Histological section of the lateral cortex of the distal end of the *Plateosauravus* femur. A) Schematic of the preserved bone tissue of the thin section. The black area indicates the preserved part of the bone wall. Green boxes show the location of the higher magnification photographs. B) Micrograph of the inner cortex fragment showing predominantly fibrolamellar bone and parallel-fibred bone in the outermost region. White arrows indicate the growth marks. C) Close up view of the poorly preserved inner cortex which consisted of fibrolamellar bone and numerous large resorptive cavities. D) Close up view of the predominant fibrolamellar bone tissue showing clear birefringence of the intrinsic fibres in the inner cortex. E) High magnification view of the only possible LAG found throughout the fragmented cortex. F) Micrograph of an outer cortex fragment showing parallel-fibred and fibrolamellar bone tissue with low birefringence in intrinsic fibres and several resorption canals.

3.1.3.2 Medial femoral section

The thin section IP1 shows the histology of the medial half of cross section of femur head of *Plateosauravus*. The general histology shows the overall bone wall is highly fragmented but the different regions of the compacta can be described (Fig. 3.1.3.2A). The inner cortex of the compacta consists of cancellous and fibrolamellar bone tissue which then transitions towards fibrolamellar and parallel-fibred bone in the outer cortex.

The inner region of the compacta consists of mostly secondarily reconstructed bone tissue giving the preserved tissue a cancellous texture. Large resorptive canals are common throughout the perimedullary zone and continues into the mid cortex (Fig. 3.1.3.2B & C). Secondary osteons are common throughout the perimedullary region of the cortex. Large resorptive cavities are lined with thick bands of lamellar bone tissue. Fibrolamellar bone tissue is the predominant primary bone tissue in the fragmented portions. The fibrolamellar bone tissue is well vascularised and in a reticular arrangement of the vascular canals.

The central area of the compacta is made up of well vascularised parallel-fibred and fibrolamellar bone tissue (Fig. 3.1.3.2D). Intrinsic fibres show moderate variation in arrangement with slight regional variation. The parallel-fibred bone (Fig. 3.1.3.2E) vascular canals are primarily circumferentially orientated in a laminar arrangement with very few longitudinal and radial vascular canals. Some regions of the mid cortex have a plexiform arrangement with long, radial vascular canals connecting circumferential vascular canals. A small portion of fibrolamellar is seen in the most medial portion of the bone wall. The fibrolamellar bone shows mass birefringence and is well vascularised with numerous haphazardly arranged vascular canals (Fig. 3.1.3.2E).

The outer cortex consists of predominantly well vascularised fibrolamellar tissue and some portions of moderately vascularised parallel-fibred bone tissue. Vascular canals of the parallel-fibred tissue are observed to be a laminar arrangement. Both bone tissue types within the outer third is well vascularised but orientation and shape of osteocyte lacunae vary throughout. The extent of secondary reconstruction is unclear due to the fragmentation but generally the outer cortex is mostly primary bone tissue with some resorptive cavities (Fig.

3.1.3.2D). The preservation of LAGs is extremely poor in the outer regions and no clear LAGs can be identified but one possible growth mark is seen in outer cortex (Fig. 3.1.3.2F).

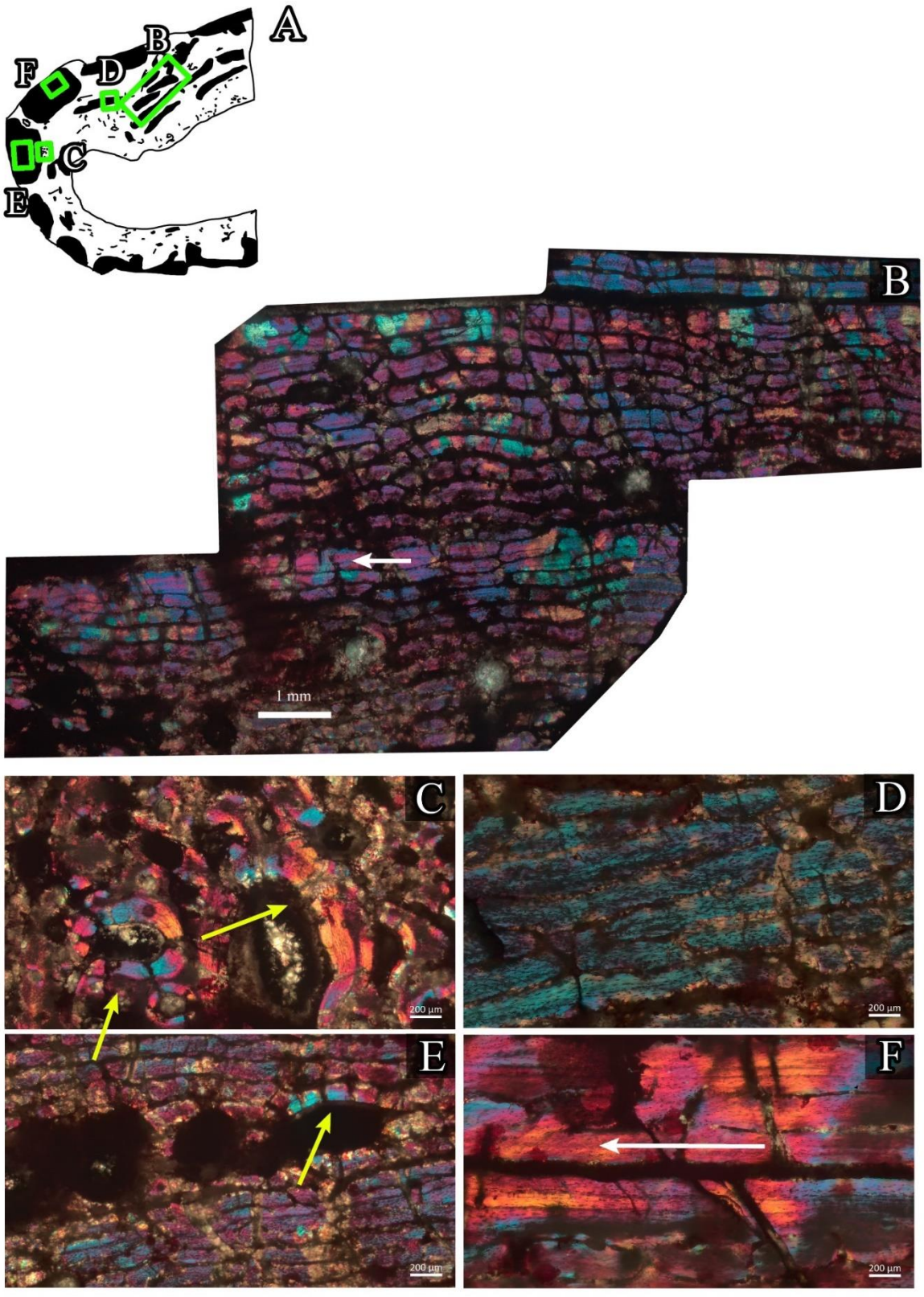

Figure 3.1.3.2: Histological section of the medial cortex of the distal end of the *Plateosauravus* femur. A) Schematic of the preserved bone tissue of the thin section. The black area indicates the preserved part of the bone wall. Green boxes show the location of the higher magnification photographs. B) Micrograph of a mid-cortex fragment showing predominantly fibrolamellar tissue in a plexiform arrangement and parallel-fibred bone in laminar vascular arrangement in outer area. White arrows indicate the growth marks. C) Low magnification view of the large secondary osteons showing thick bands of endosteally formed lamellar bone deposits shown by the yellow arrows.. D) Close up view of parallel-fibred bone in a laminar vascular canal arrangement. E) Low magnification of large resorptive cavities visible in the mid cortex. The endosteal deposition of lamellar bone is underway along the inner margins of the erosion cavities shown by the yellow arrows. F) High magnification of one possible growth mark found in the middle cortex.

3.2. Sauropodiforme indet.

A fibula and tibia of the indeterminate Sauropodiforme were sampled. One section was taken from the fibula (Fig. 2.2A) and the tibia midshaft (Fig. 2.2B) and are described here.

3.2.1 Fibular histology of Sauropodiforme indet. (NMQR-3314)

The thin section (Fig. 3.2.1A) represents the fibula of Sauropodiforme indet. The general histology of the section while incomplete, presents with a transition from cancellous and fibrolamellar bone tissue, in the inner half of the compacta, to parallel-fibred and fibrolamellar bone tissue, in the outer regions.

Secondarily reconstructed tissue is abundant in the fragments surrounding the medullary cavity. The degree of secondary reconstruction varies between moderate and the presence of many erosion cavities gives a cancellous texture to the bone tissue (Fig. 3.2.1B & C). Fibrolamellar bone is the primary bone of the inner regions evident by the intrinsic fibre arrangement observed. Majority of the enlarge erosion cavities are not infilled, although a few well-formed secondary osteons are present (Fig. 3.2.1E).

Parallel-fibred bone and fibrolamellar bone tissue is found in mid- and outer cortex. The fibrolamellar bone (Fig. 3.2.1C & D) tissue is well vascularised whereas the small portion of parallel-fibred bone is moderately vascularised. Intrinsic fibres show a looser degree of arrangement within the fibrolamellar regions of the compacta. A small amount of secondary reconstruction can be seen represented by a few fully formed secondary osteons and small resorptive cavities. Three LAGs (Fig. 3.2.1B) were observed within the larger portion of compact bone but due to the fragmentation, they could not be followed throughout the rest of the compacta.

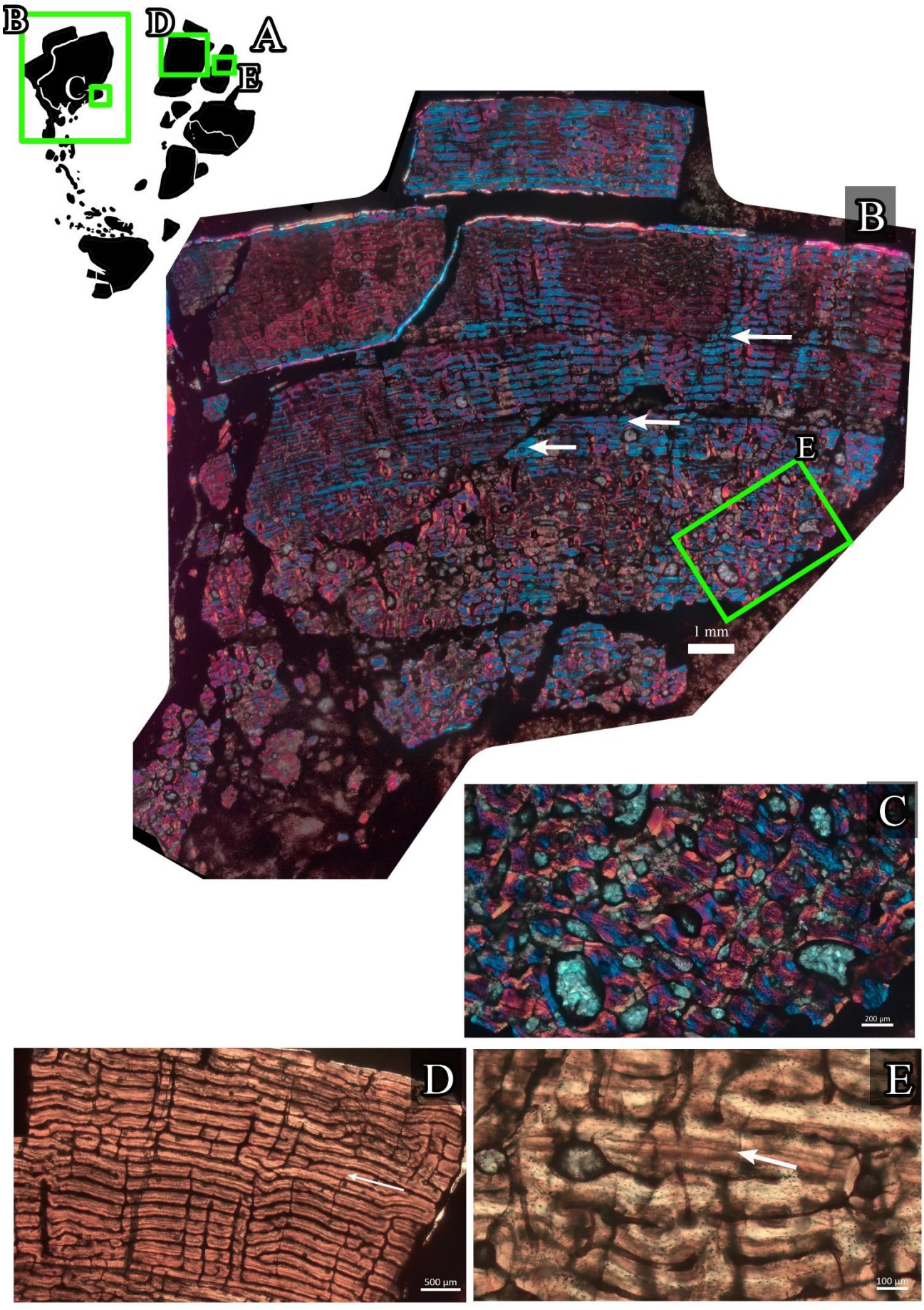
B
D
A
E
C
B
E
1 mm
C
200 µm
D
500 µm
E
100 µm

Figure 3.2.1: Histological section of the Sauropodiforme indet. fibula. A) Schematic of the preserved bone tissue of the thin section. The black area indicates the preserved part of the bone wall. Green boxes show the location of the higher magnification photographs. B) Composite micrograph of the largest fragment on the anterior side of the fibula. Green frames indicate the location of the following photographs. White arrows indicate the growth marks. C) Intensively reconstructed bone tissue in the inner regions of the mid cortex. Large secondary osteons are formed around several large resorptive cavities. D) Low magnification view of the fibrolamellar bone tissue with vascular canals in a plexiform arrangement. E) Close up view of a LAG interrupting the deposition of fibrolamellar bone tissue.

3.2.2 Tibial histology of Sauropodiforme indet. (NMQR-3314)

The section (Fig. 3.2.2A) shows the general histology of the tibia. The bone wall is generally well preserved although there are some poorly preserved areas in the outer cortex. The inner cortex consists of cancellous textured tissue and fibrolamellar bone tissue. The mid cortex also comprises of mostly fibrolamellar and secondary bone tissue which then transitions to well vascularised parallel-fibred and fibrolamellar bone in the outer cortex (Fig. 3.2.2B). Two LAGs are observed in the mid- and outer cortex.

The inner cortex comprises of fibrolamellar and secondarily reconstructed bone tissue. Secondary osteons and resorptive canals occur regularly throughout the poorly preserved fibrolamellar bone tissue. The numerous resorptive cavities give the perimedullary region a cancellous texture (Fig. 3.2.2C) but there are also many cracks throughout the inner compacta. The abundant fibrolamellar bone is well vascularised with a reticular arrangement of vascular canals and is more abundant towards the mid cortex. The intrinsic fibres are observed mostly having a lower degree of organisation and varies between the medial and lateral sides of the inner cortex. The innermost compact tissue appears to be a lamellar bone tissue which makes up an ICL (Fig. 3.2.2D).

The mid cortex is comprised of fibrolamellar bone (Fig. 3.2.2E & F). Well vascularised fibrolamellar bone is the most abundant bone tissue in the mid cortex. Vascular canals of the fibrolamellar bone tissue are numerous and in a reticular arrangement. The arrangement of the intrinsic fibres varies throughout mid cortex as fibrolamellar tissue shows mass birefringence whereas the parallel-fibred bone shows moderate birefringence of the fibres. Secondary reconstruction occurs as occasional secondary osteons and resorptive cavities are visible in the mid cortex.

The outer cortex consists of predominantly fibrolamellar bone tissue present. The well vascularised parallel-fibred bone has alternating vascular arrangements as the arrangements tend to either be in a reticular or a laminar arrangement of the vascular canals. The bone tissue is not well preserved in the outer cortex and only two LAGs are visible.

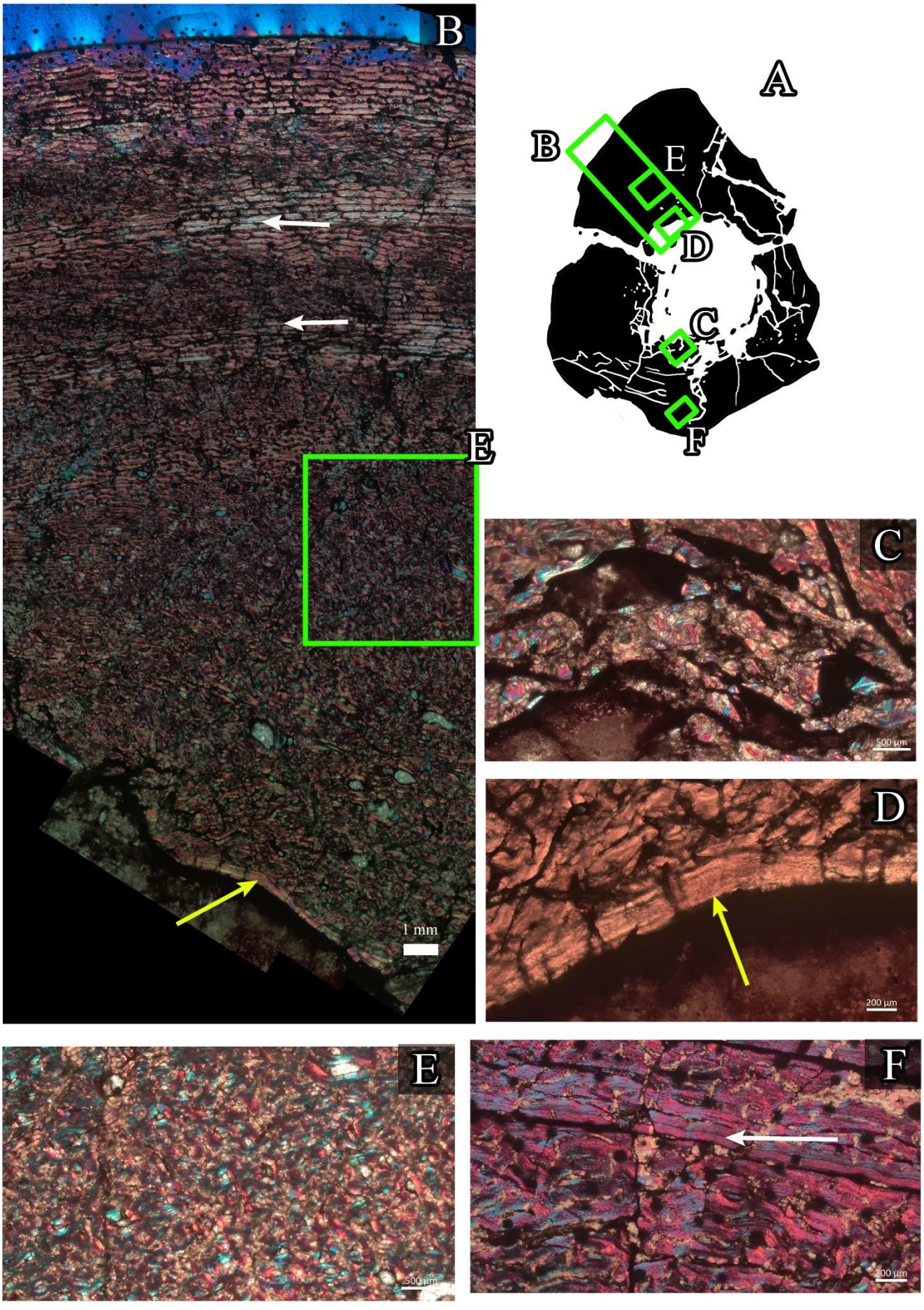
B
E
1 mm
A
B
E
D
C
F
C
500 µm
D
200 µm
E
500 µm
F
200 µm

Figure 3.2.2: Histological section of the Sauropodiforme indet. tibia. A) Schematic of the preserved bone tissue of the thin section. The black area indicates the preserved part of the bone wall. Green boxes show the location of the higher magnification photographs. B) Composite micrograph of the general histology of the femur from the inner cortex of the femur to the peripheral bone tissue. White arrows indicate the growth marks. C) Large resorptive cavities present in the cancellous bone tissue surrounding the medullary cavity. D) Lamellar bone tissue lining the medullary cavity shown by the yellow arrows. This band of lamellar bone tissue is not present in other regions of the compacta. E) Low magnification view of the poorly preserved fibrolamellar bone tissue with some small resorptive canals spread throughout the mid cortex. F). One growth mark in thin band of lamellar tissue forming a small annulus surrounded by fibrolamellar bone tissue.

3.3. *Melanorosaurus readi*

Two elements of *Melanorosaurus*, a femur and tibia, were sampled for histological processing. Three sections from the femur midshaft (Fig. 2.1.3A) and four sections from the tibia midshaft (Fig. 2.1.3B) are described here. The descriptions are from the most proximal section to the most distally located sections.

3.3.1 Tibial histology of *Melanorosaurus* (NMQR-1551)

The histology of three thin sections A1, A2 and A3 are described here. All three sections are taken from the central region of the midshaft (Figure 2.1.3B).

3.3.1.1 Tibial section A1

The most proximally located section of tibia, A1 (Fig. 2.1.3B), shows the histology from the mid cortex to the outer bone wall (Fig. 3.3.1.1A). The general histology (Fig. 3.3.1.1B) shows fibrolamellar tissue in the inner regions and laminar parallel-fibred bone in outermost periphery.

This tibial section did not preserve the innermost portion of the bone wall and thus only the mid and outer cortex are described. In the mid-cortex, the osteocyte arrangement within the inner portion of the preserved cortex (Fig. 3.3.1.1B) is less organised than that of the rest of the compacta and represent the earlier fibrolamellar bone transitioning to laminar parallel-fibred bone (Fig. 3.3.1.1C) or a localised area of woven bone.

In the mid cortex, secondary osteons (Fig. 3.3.1.1D) are dispersed throughout the moderately vascularised parallel-fibred and fibrolamellar bone tissue. Occasionally, vascular canals show resorption which results in small erosion cavities. These resorption cavities are irregularly dispersed throughout the mid cortex. Within this region of the compacta, there are consistently more resorption cavities and secondary osteons. The primary bone tissue in the mid cortex comprises of parallel-fibred bone in a laminar arrangement in the outer area and fibrolamellar bone in the inner region.

The outer cortex also presents with moderately vascularized parallel-fibred bone with vascular canals in a laminar arrangement with a few radial connections. There are primarily circumferential and longitudinal

vascular canals in the peripheral region. The intrinsic fibre arrangement of the outer region shows a high degree of organisation. There is minimal secondary reconstruction within the outer periphery apart from small, isolated resorption canals. Six LAGs are visible in the outer zonal bone of the cortex and one LAG within the mid-cortex. The LAGs are all present towards the peripheral margin and occur within primary bone tissue. The distance between the LAGs tend to decrease when approaching the outer bone wall (Fig. 3.3.1.1E).

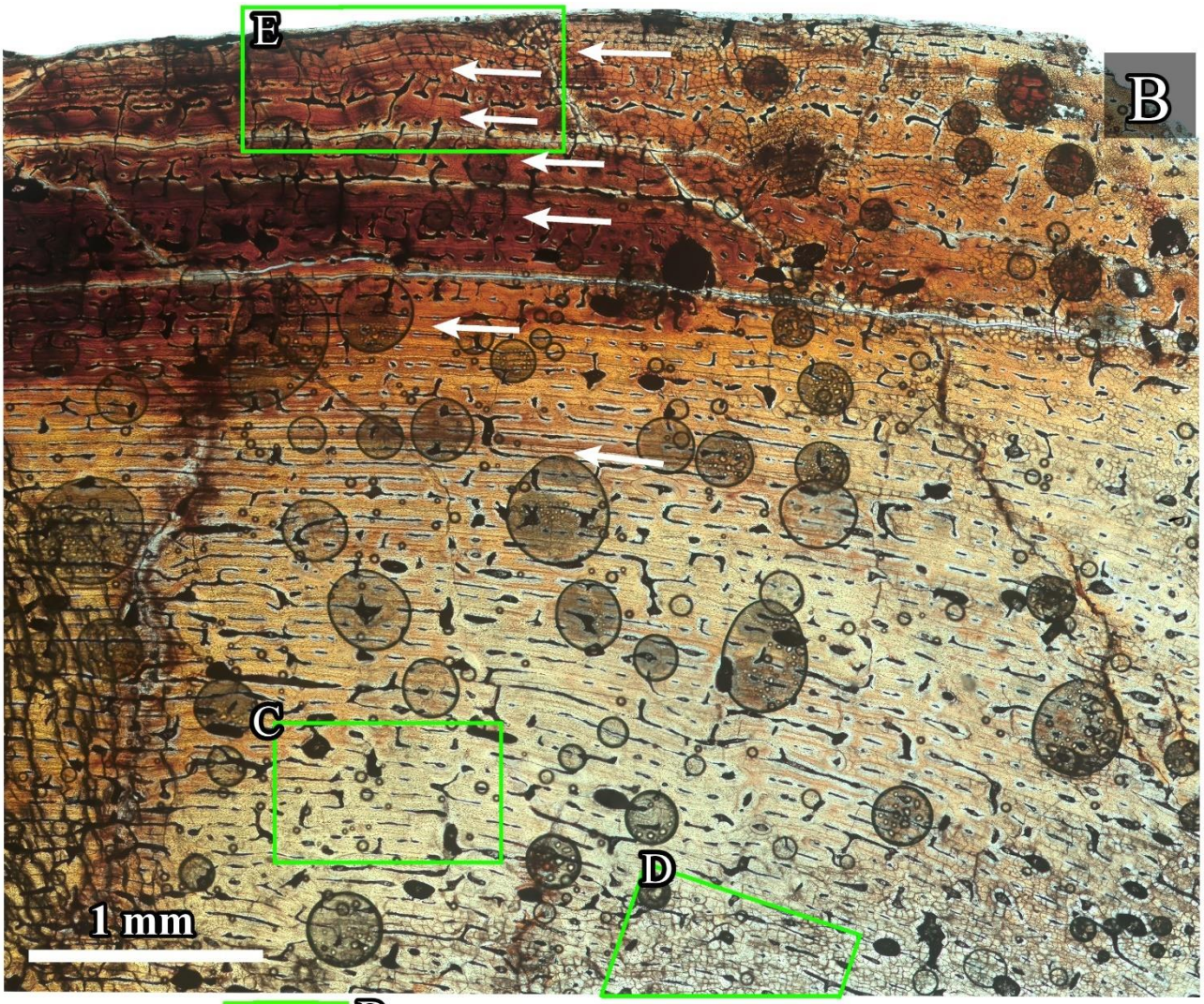
E
B
C
D
1 mm

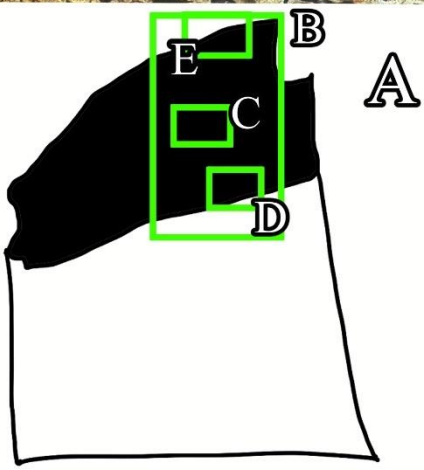
B
E
C
D
A

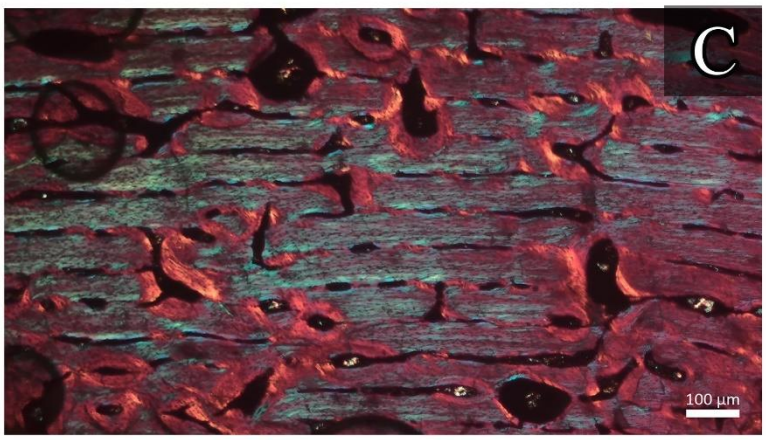
C
100 µm

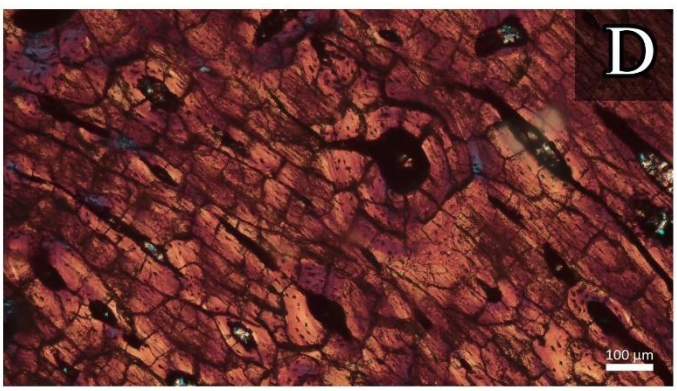
D
100 µm

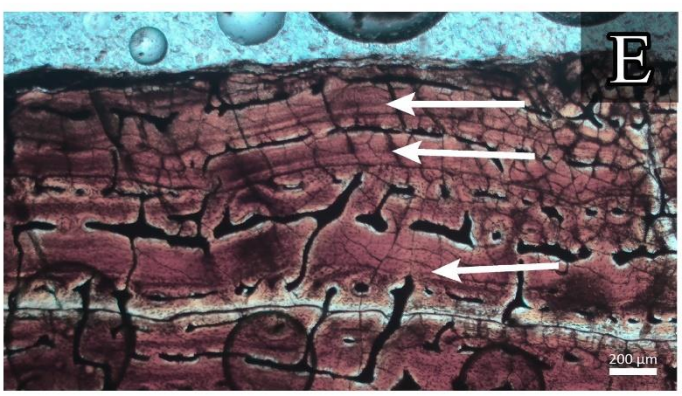
E
200 µm

Figure 3.3.1.1: Histological section of the outer half of *Melanorosaurus* tibial section A1. A) Schematic of the preserved bone tissue of the thin section. The black area indicates the preserved part of the bone wall. Green boxes show the location of the higher magnification photographs. B) Composite micrograph of the mid to outer cortex. White arrows indicate the growth marks. C) Higher magnification view of laminar arranged vascular canals and secondary osteons in fibrolamellar bone in the mid cortex. D) High magnification view of fully formed and small secondary osteons in the fragmented mid cortex. E) High magnification view of the closely associated growth marks in parallel-fibred bone in the outer cortex.

3.3.1.2 Tibial section A2

Section A2 (Fig. 2.1.3B) represents a midsection (between sections A1 and A3) and shows a complete view from perimedullary to the outer bone wall (Fig.3.3.1.2A). The general histology (Fig. 3.3.1.2B) shows a transition from cancellous and fibrolamellar bone tissue in the inner cortex to highly vascularized parallel-fibred bone towards the peripheral region of the bone wall.

The perimedullary zone is comprised of predominantly cancellous bone composed of many secondarily enlarged erosion cavities (Fig. 3.3.1.2C). Bone tissue between erosion cavities appear to be remnants of woven textured primary bone tissue. The intrinsic fibre arrangement was relatively woven throughout the fibrolamellar bone in the inner areas of the compacta. The fibrolamellar bone tissue comprised of a high density of osteocytes lacking regular arrangement.

The mid-cortex is a mixture of well vascularised primary parallel-fibred bone, fibrolamellar bone and many secondary osteons (Fig. 3.3.1.2D). The laminar arrangement of the bone tissue is maintained throughout the central compacta but occasionally regions of reticular fibrolamellar bone occur. The intrinsic fibres of the parallel-fibred bone show some birefringence but most variation is on the regional scale. Fibrolamellar tissue in a plexiform arrangement in dispersed throughout the mid cortex.

There are five growth marks present in the outer third of the compacta (Fig. 3.3.1.2B). The outer cortex shows similar bone types and vascular canal arrangement as compared to the mid cortex and comprises of predominantly primary fibrolamellar with vascular canals in a laminar arrangement. There are very few radial vascular canals throughout the compacta. The intrinsic fibre arrangement of the outer cortex shows consistently a higher degree of arrangement when compared to the inner regions. Vascularity ranges from moderate to high within the outer cortex but the density of both osteocytes and canals decreases in the immediate regions surrounding growth marks (Fig. 3.3.1.2E).

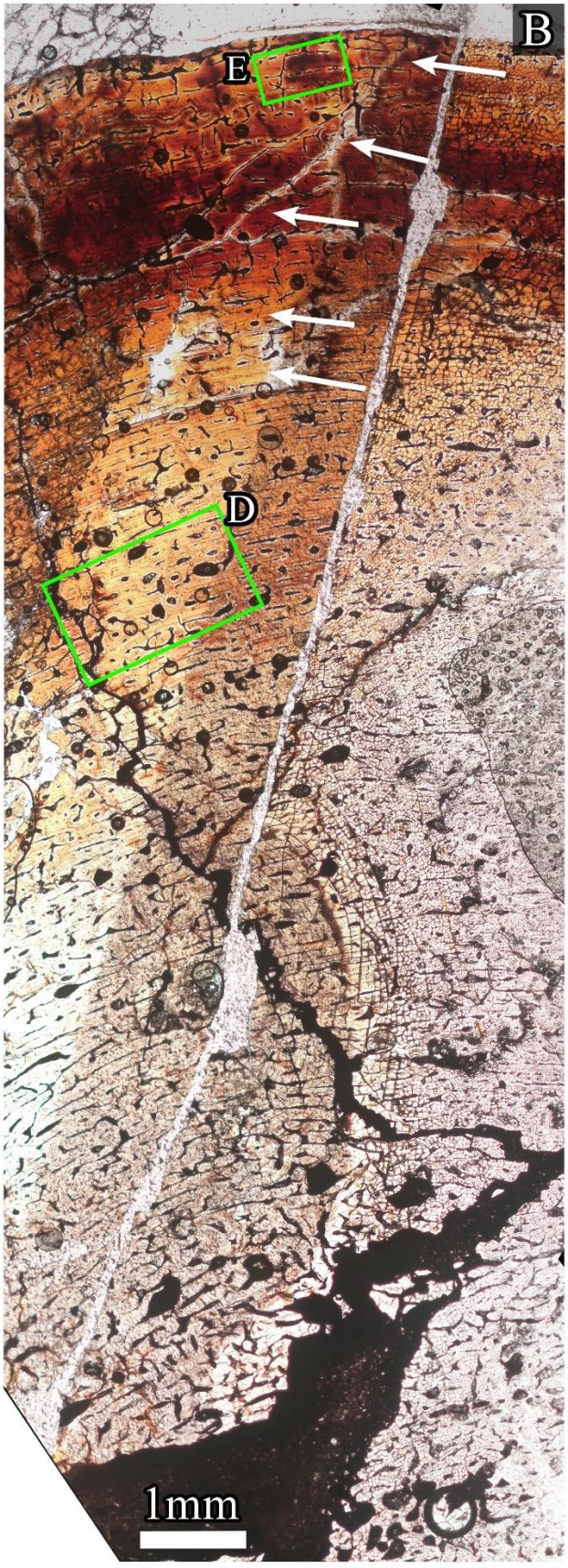
B
E
D
1mm

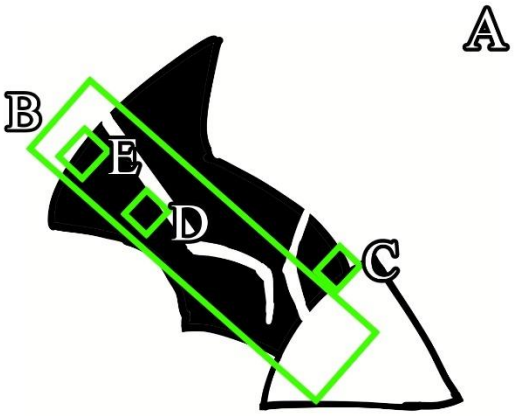
A
B
E
D
C

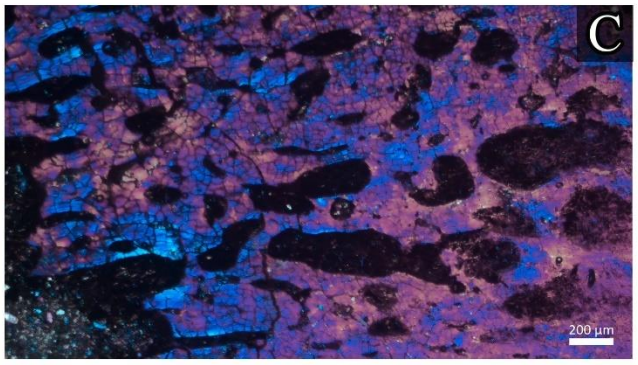
C
200 µm

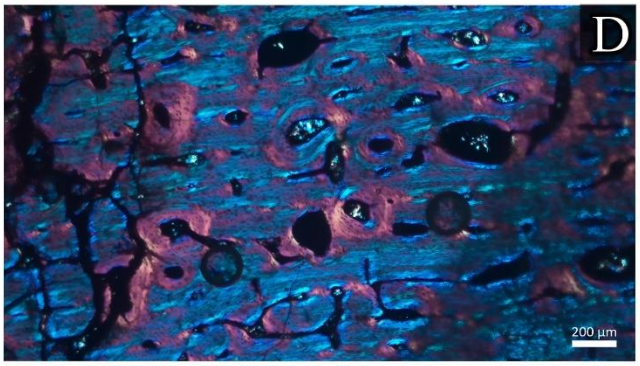
D
200 µm

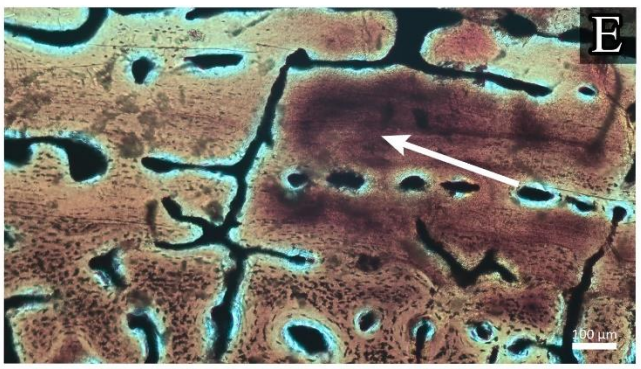
E
100 µm

Figure 3.3.1.2: Histological section of *Melanorosaurus* tibial section A2. A) Schematic of the preserved bone wall in the thin section. The black area indicates the preserved part of the bone wall. Green boxes show the location of the higher magnification photographs. B) Composite micrograph of the tibia from the perimedullary to the periphery region. White arrows indicate the growth marks. C) High magnification view of the poorly preserved secondary remodelled bone and resorption cavities in the innermost cortex. D) High magnification view of secondary osteons in the mid cortex. E) High magnification view of a LAG showing the poor surrounding osteocyte density.

3.3.1.3 Tibial section A3

The most distal section, A3 (Fig. 2.1.3B), is the best of the three thin sections as it preserves the most complete histology of the bone wall (Fig. 3.3.1.3A). General histology shows cancellous and fibrolamellar bone tissue in the inner cortex and laminar parallel-fibred bone tissue in the mid and outer cortex (Fig. 3.3.1.3B).

Inner portions of the compacta show azonal growth comprising of the woven fibrolamellar and cancellous bones tissue. In general, the bone tissue is well vascularised within the inner parts of the compacta. In these inner regions, vascular canals lack any arrangement, but are plentiful. There also appears to be a high density of osteocytes. Secondarily reconstructed bone is common throughout the perimedullary region. Secondary osteons are dispersed throughout the inner and mid-cortex, occasionally they are found in close association but do not form dense Haversian bone.

The bone tissue in the mid cortex is a mix parallel-fibred bone (Fig. 3.3.1.3C) comprising of mostly circumferential and longitudinal vascular canals and fibrolamellar bone in a plexiform arrangement. There are very few radial vascular canals present. The intrinsic fibres tend to have a higher degree of organisation in the parallel-fibred tissue and looser organisation in the fibrolamellar tissue. In this area of the compacta, the number of resorption cavities and secondary osteons become more frequent. Approaching the outer cortex, the frequency of long circumferential vascular canals increases as the deposition of zonal bone tissue begins. Secondary osteons are sometimes found overlapping each other in the possibly the early stages of dense Haversian bone (Fig. 3.3.1.3D).

The outer third of the compacta consists of highly vascularized parallel-fibred bone tissue with highly organised intrinsic fibres. The outer cortex consists predominantly of primary bone tissue with mostly circumferentially and longitudinally arranged vascular canals in a laminar arrangement. Radial vascular canals are less common but a few large radial vascular canals (Fig. 3.3.1.3E) spanning large areas of the compacta are visible. Six LAGs are present in the outer cortex.

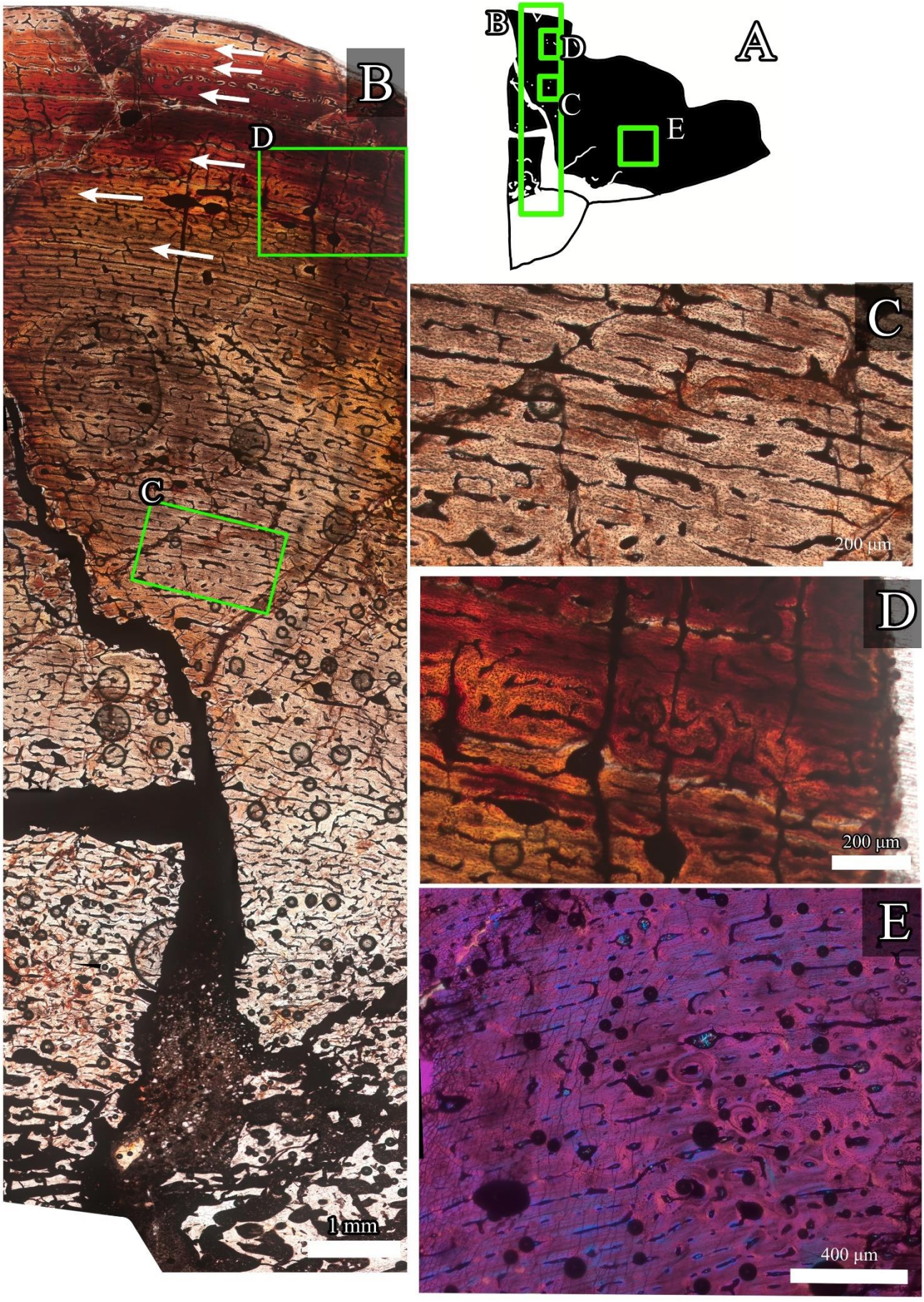
B
D
C
1 mm
B
D
C
E
A
C
200 µm
D
200 µm
E
400 µm

Figure 3.3.1.3: Histological section of *Melanorosaurus* tibial section 8B. A) Schematic of the preserved bone tissue of the thin section. The black area indicates the preserved part of the bone wall. Green boxes show the location of the higher magnification images. B) Composite micrograph of the bone wall histology from the innermost region to the outermost cortex. White arrows indicate the growth marks. C) High magnification view of large radial connections connecting several vascular canals. D) High magnification view of well vascularised parallel-fibred bone with a laminar vascular arrangement. Numerous long circumferential vascular canals are present. E) Low magnification composite view of clumped secondary osteons within the mid cortex.

3.3.2 Femoral histology of *Melanorosaurus* (NMQR-1551)

The histology of five femoral thin sections B1, B2, B3, B4 and B5 are described here. B1 and B2 are taken from the region of the fourth trochanter and B3, B4 and B5 are taken more distally from the midshaft of the femur (Figure 2.1.3A).

3.3.2.1 Femoral section B1

The general histology of the most proximal femur section, BI (Fig. 2.1.3A; Fig. 3.3.2.1A), comprised of cancellous bone in the innermost cortex, fibrolamellar bone tissue in the mid cortex and parallel-fibred bone occurs in the outer third of the compacta (Fig. 3.3.2.1B). Six LAGs are visible in the outer cortex.

The inner third of the compacta comprise of fibrolamellar bone (Fig. 3.3.2.1C) and secondarily reconstructed tissue. In the deeper regions of the compacta secondary osteons and large resorption canals are frequently seen. The intrinsic fibre arrangement is variable throughout the inner cortex. The fibrolamellar bone is well vascularised with a high density of disorganised osteocytes and a reticular arrangement of the vascular canals. The intrinsic fibre organisation of the fibrolamellar bone is highly variable.

The mid cortex comprises of predominantly highly vascularized fibrolamellar and a minor number of secondary osteons. The vascular canals of the mid cortex tend to be in laminar arrangement and is dominated by circumferentially orientated vascular canals. Longitudinal canals are present to a far lower degree and are observed between the frequent circumferential vascular canals. Intrinsic fibre arrangement of the mid-cortex tends to have a moderate degree of arrangement except the small areas of fibrolamellar tissue. The fibrolamellar bone tissue shows a low degree of intrinsic fibre arrangement. Secondary osteons and resorptive canals are present but are scattered throughout the mid compacta.

The vascularisation of the outer cortex has a more plexiform arrangement. There are predominantly short circumferential vascular canals and many branching radial vascular canals (Fig. 3.3.2.1D) spanning considerable regions of the compacta. There are small regions of fibrolamellar tissue between LAGs 2 to 3 and 4 to 5. These areas of fibrolamellar bone are visually apparent as the intrinsic fibre arrangement are

distinct from the surrounding parallel-fibred and fibrolamellar bone tissue (Fig. 3.3.2.1D). There are seven LAGs visible in region nearing the bone periphery.

A distinct layer of unusually structured bone near the periphery resembles highly vascularized reticular-plexiform fibrolamellar bone tissue (Fig. 3.3.2.1E) that appear to have been rapidly deposited. The tissue is divergent from the surrounding parallel-fibred bone tissue. The osteocyte density and size are also greater than the rest of the tissues throughout the compacta.

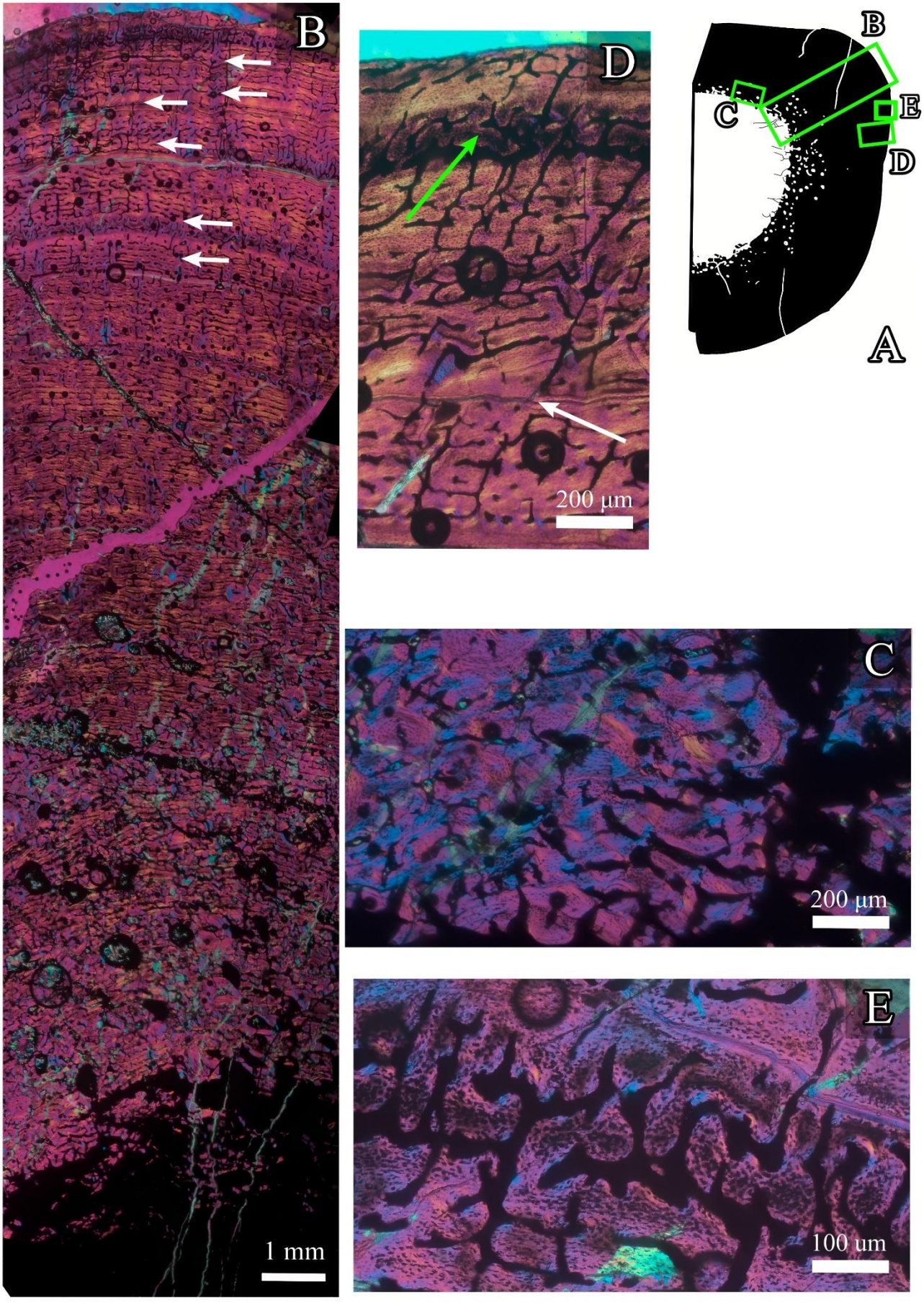
B
1 mm
D
200 µm
B
C
E
D
A
C
200 µm
E
100 um

Figure 3.3.2.1: Histological section of the most proximal *Melanorosaurus* femoral section B1. A) Schematic of the preserved bone tissue of the thin section. The black area indicates the preserved part of the bone wall. Green boxes show the location of the higher magnification photographs. B) Composite micrograph showing the histology of the femur from the medullary region to bone periphery. White arrows indicate the growth marks. C) Close up view of well vascularised fibrolamellar bone tissue in the inner cortex. D) High magnification view of the short circumferential and a few longitudinal vascular canals. Short radial anastomoses are dispersed throughout. Green arrows show the unusual fibrolamellar bone. E) High magnification view of unusually radially organised fibrolamellar tissue near the peripheral region of the bone wall.

3.3.2.2 Femoral section B2

The histology of B2 (Fig. 2.1.3A; Fig. 3.3.2.2A) preserved a good record of the histology of the compacta from the innermost cortex to the outer bone margin (Fig. 3.3.2.2B). The perimedullary region consists of mostly secondarily reconstructed bone tissue and some fibrolamellar bone tissue. The outer and mid cortex consist of primarily laminar parallel-fibred bone. Six LAGs are present within the outer cortex.

In the perimedullary region, the large number of resorptive canals gives the overall bone texture a cancellous appearance (Fig. 3.3.2.2C). The secondarily reconstructed bone is separated by the original primary fibrolamellar bone tissue. There are often secondary osteons located near these large resorptive canals. Fibrolamellar bone tissue tends to occur within the inner cortical regions and is highly vascularised (Fig. 3.3.2.2D). The vascular canals tend to be disorganised within the primary bone tissue.

The mid cortex predominantly consists of parallel-fibred bone, fibrolamellar bone and secondary reconstruction is apparent. Small resorptive canals and secondary osteons, form thin circumferential bands in the central compacta. The vascular arrangement of the laminar tissue consists of mostly long circumferentially arranged vascular canals with very few radial and longitudinal vascular canals present. The vascularity is high throughout the mid cortex (Fig. 3.3.2.2B & 3.3.2.2C).

The outer third of the compacta comprise of mostly primary bone tissue with predominantly circumferentially organised vascular canals located in the parallel-fibred bone tissue. Near the LAGs, there appears to be a decrease in vascularisation. The intrinsic fibre arrangement of the parallel-fibred bone is generally high but there is some regional variation. A distinctive, woven textured bone with abundant radially orientated vascular canals is visible near the outer bone margin. (Fig. 3.3.2.2E). This radial fibrolamellar bone is within two regions of the detached portion of the outer bone wall (Fig. 3.3.2.2F).

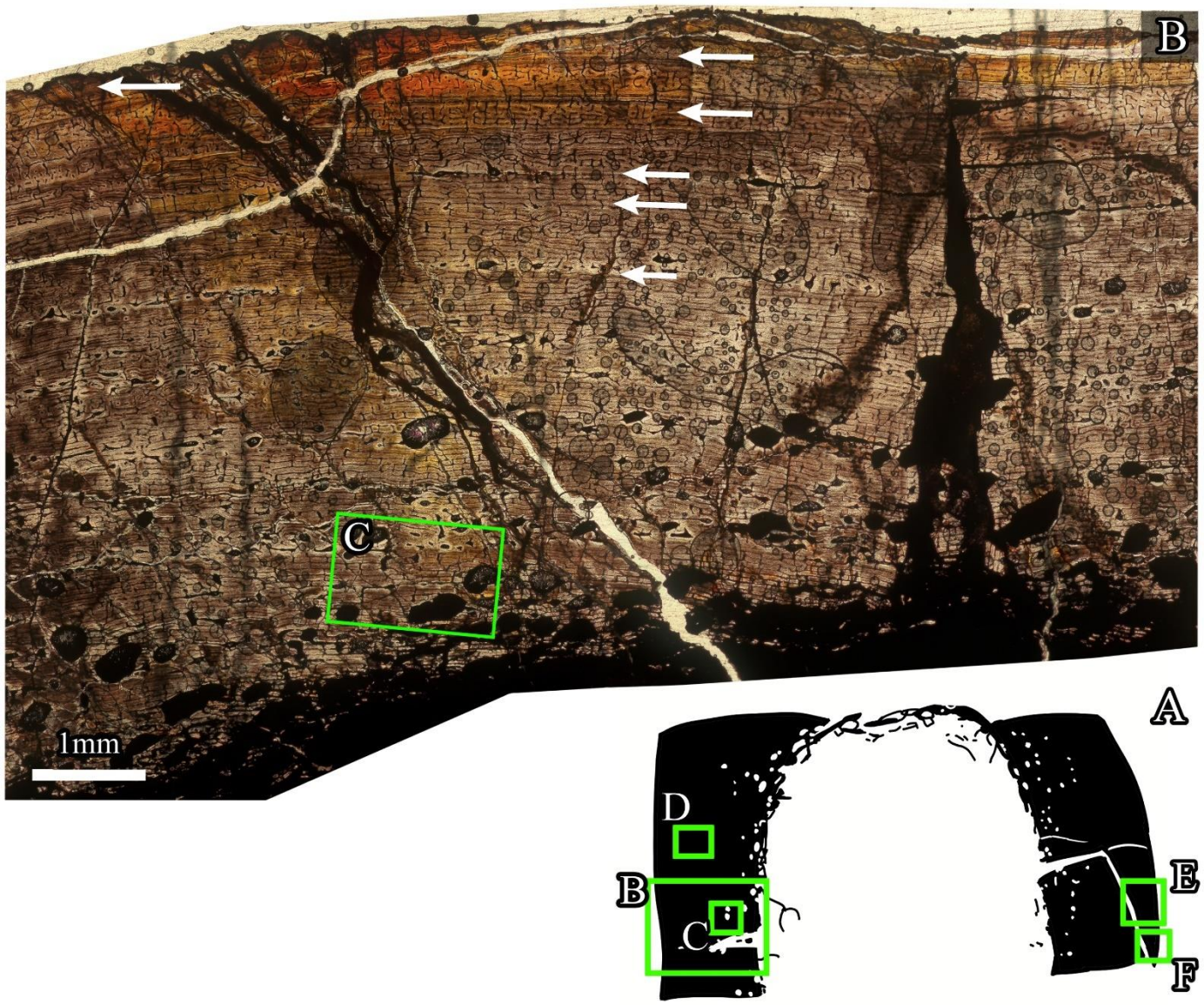
B
C
1mm
A
D
B
C
E
F
C
500 µm
D
500 µm
E
200 µm
F
200 µm

Figure 3.3.2.2: Histological section of *Melanorosaurus* femoral section B2. A) Schematic of the preserved bone tissue of the thin section. The black area indicates the preserved part of the bone wall. Green boxes show the location of the higher magnification photographs. B) Composite micrograph showing histology of the femur from the medullary region to the bone periphery. White arrows indicate the growth marks. C) Close up view of large resorptive cavities distributed throughout most of the inner and mid cortex. D) Close up view of fibrolamellar bone. E) High magnification view of the radially deposited fibrolamellar tissue between two LAGs shown by the green arrows. F) High magnification view of two instances of radially deposited fibrolamellar tissue in the outer portion of the femur.

3.3.2.3 Femoral section B3

The general histology of the thin section B3 (Fig. 2.1.3A) shows a transition from cancellous bone in the inner compacta to primary parallel-fibred bone tissue in the outer regions of the compacta (Fig. 3.3.2.3A). Five LAGs are visible in the outer cortex (Fig. 3.3.2.3B).

The perimedullary region consists of secondarily reconstructed and fibrolamellar bone tissue. The fibrolamellar bone present is generally well vascularised and the vascular canals have a reticular arrangement. However, the primary bone tissue is sporadically interrupted by the secondarily reconstructed bone tissue. Secondary osteons and large resorption cavities are common within the inner third of the cortex (Fig. 3.3.2.3C). The abundance of the resorption canals gives the perimedullary region a cancellous texture.

The mid cortex is predominantly composed of parallel-fibred bone and fibrolamellar bone. The parallel-fibred bone tissue is well vascularised and dominated by circumferential vascular canals. The fibrolamellar tissue is well vascularised and tends to be a reticular arrangement of the vascular canals. Multiple bands of secondary osteons are found circumferentially dispersed throughout many layers of growth (Fig. 3.3.2.3D). Small resorption cavities are commonly found near these circumferential bands of secondary osteons.

Well vascularised laminar parallel-fibred bone is abundant throughout the outer cortex of the bone. Radial connections are extensive within the outer cortex but are sparse within the mid-cortex. Longitudinal vascular canals are profuse within the mid and outer parts of the compacta. Five LAGs are present within the outer regions of the compacta. Bone tissue in the vicinity of LAGs show a decrease in vascularity. Secondary reconstruction in this region is minimal with some small secondary osteons occurring occasionally.

Near the bone margin, there is fibrolamellar bone with abundant radially orientated vascular canals (Fig. 3.3.2.3B & E). The vascularisation and bone texture of this tissue is distinctive from the surrounding organised parallel-fibred bone tissue.

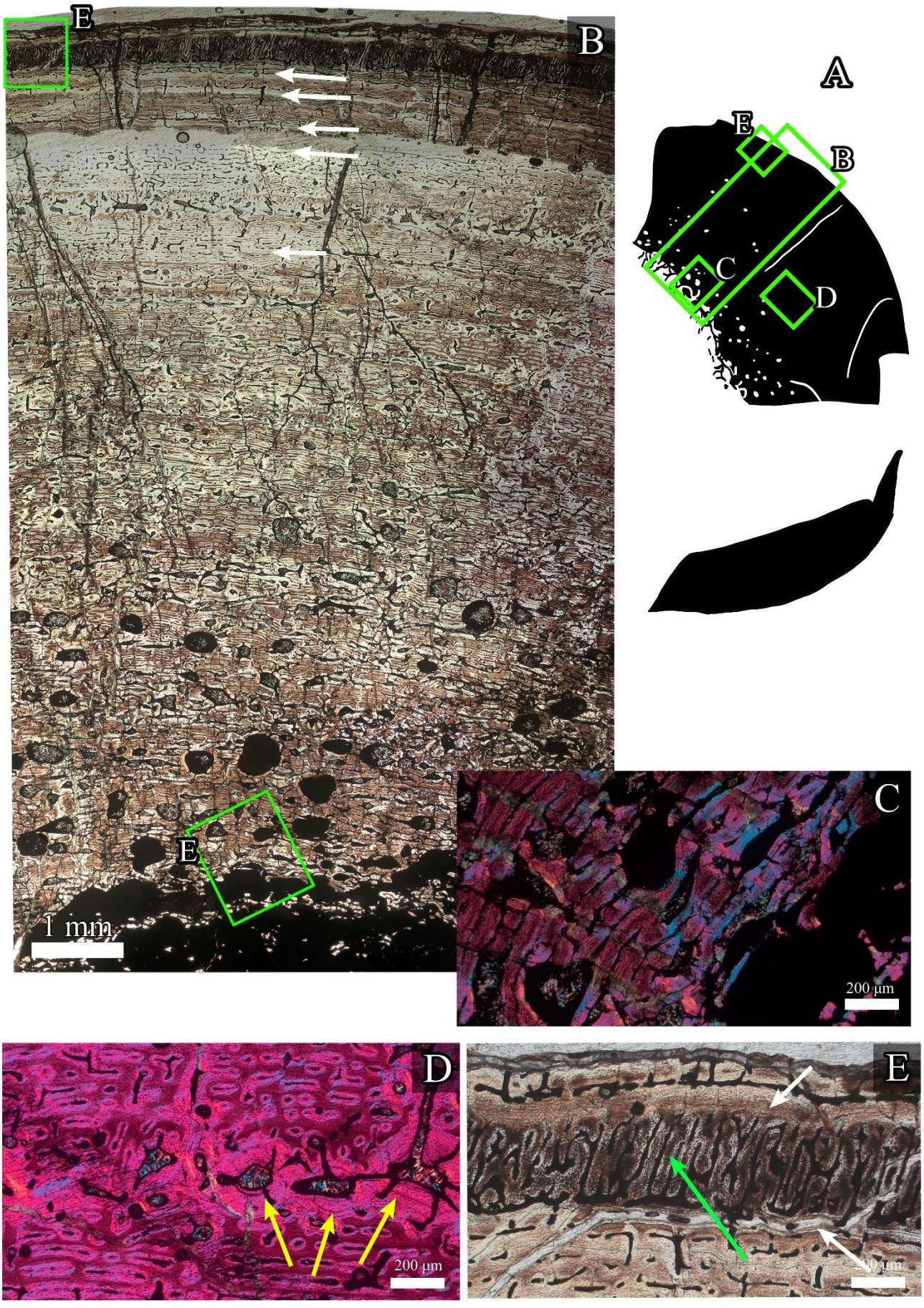
A
B
C
D
E
E
B
C
D
E
1 mm
200 µm
200 µm
200 µm

Figure 3.3.2.3: Histological section of the *Melanorosaurus* femoral section B3. A) Schematic of the preserved bone tissue of the thin section. The black area indicates the preserved part of the bone wall. Green boxes show the location of the higher magnification photographs. B) Composite micrograph showing histology of the femur from the medullary region to the outer cortex. White arrows indicate the growth marks. C) Close up of secondarily enlarged vascular cavities in the perimedullary region. D) High magnification view of well-developed secondary osteons in the mid cortex shown by the yellow arrows. E) High magnification view of the well vascularised radially organised fibrolamellar bone tissue located between two LAGs. Shown by the green arrow.

3.3.2.4 Femoral section B4

The general histology of femoral section B4 (Fig. 2.3B) was the second most distal section. The bone wall (Fig. 3.3.2.4A) presented with a transition from more cancellous textured bone in the perimedullary region to a more compacted parallel-fibred and fibrolamellar bone in the rest of the cortex. Only two LAGs can be counted due to the poor preservation of the outer cortex (Fig. 3.3.2.4B).

The innermost cortex comprised of highly reconstructed bone which gives the bone tissue a cancellous appearance (Fig. 3.3.2.4C). There are portions of fibrolamellar bone tissue between the resorption cavities. Overlying the cancellous bone, numerous vascular canals are disorganised with primary and secondary osteons present. The intrinsic fibre arrangement shows significant variation between the secondarily reconstructed bone and the fibrolamellar bone.

The mid compacta comprise of well vascularised parallel-fibred and fibrolamellar bone tissue. In the parallel-fibred bone, the arrangement of vascular canals was laminar with numerous short circumferential vascular canals. The fibrolamellar tissue showed vascular canals in reticular arrangement. The organisation of intrinsic fibres was of a higher degree in the parallel-fibred bone whereas the fibrolamellar bone show variation in the fibre organisation. The mid-cortex showed isolated secondary osteons dispersed throughout the region. Secondary reconstruction is common but not intensive within the mid cortex. Some small secondary osteons and resorptive cavities are dispersed throughout.

Although, the outer cortex is not well preserved, histological features are still visible. Near the bone periphery, the tissue is made up of predominantly primary parallel-fibred bone and fibrolamellar bone (Fig. 3.3.2.4B & D). This region is highly vascularized by mostly circumferential and longitudinal vascular canals in either a plexiform or reticular vascular arrangements. Intrinsic fibres show a moderate to high degree of arrangement in the outer third of the cortex. Primary osteons are extensive throughout the outer cortex with arrangement of vascular canals staying consistent.

A distinctive, woven textured bone with abundant radially orientated vascular canals is visible near the outer bone margin. This radial fibrolamellar bone is also visible the detached portion of the outer bone wall (Fig. 3.3.2.4E).

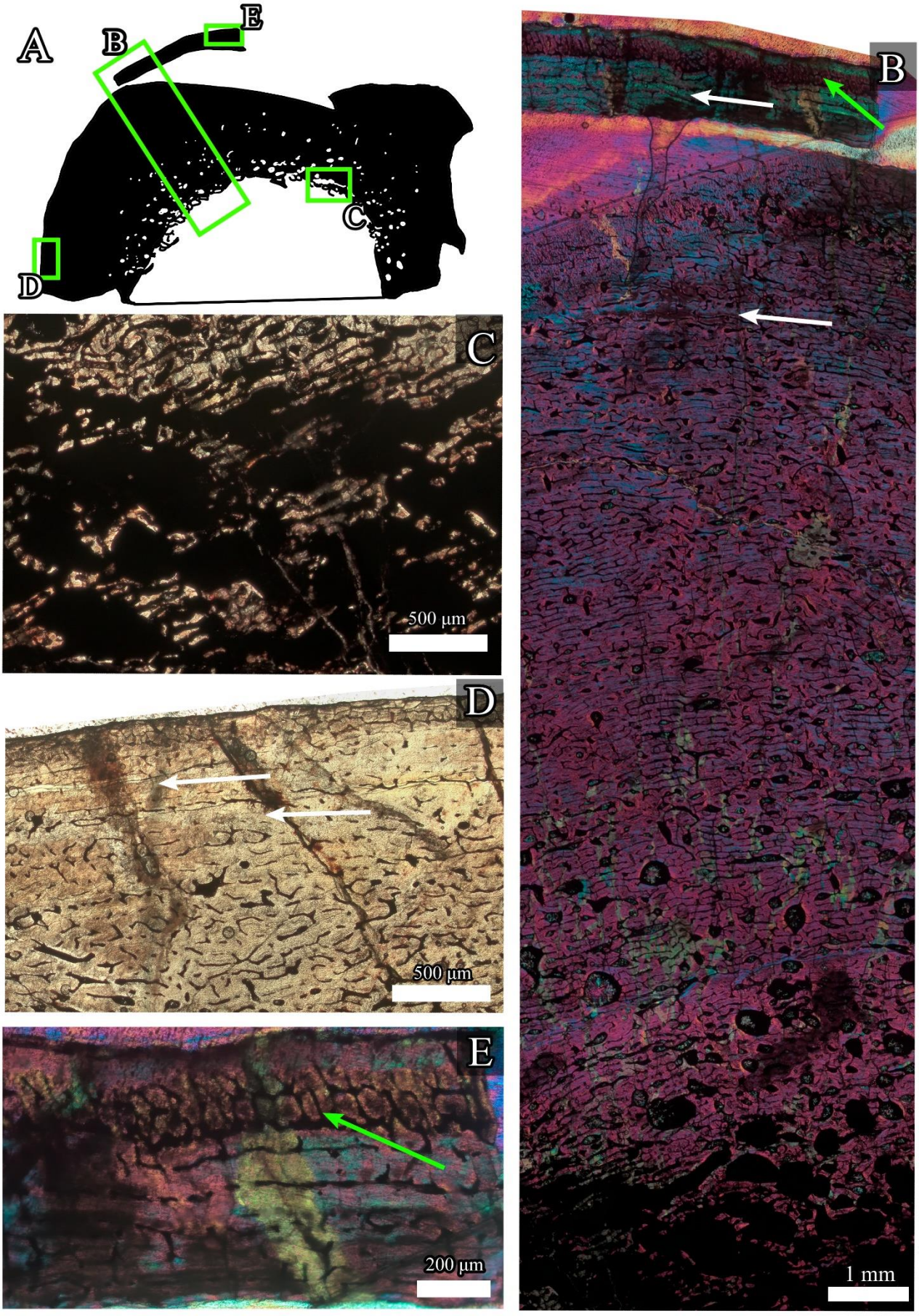
A
B
E
C
D
B
C
500 µm
D
500 µm
E
200 µm
1 mm

Figure 3.3.2.4: Histological section of the *Melanorosaurus* distal femoral section B4. A) Schematic of the preserved bone tissue of the thin section showing most of the compact bone and a detached piece of the outer bone wall. The black area indicates the preserved part of the bone wall. Green boxes show the location of the higher magnification photographs. B) Composite micrograph showing the general histology of the femur from medullary to bone periphery. White arrows indicate the growth marks. C) High magnification view of large resorptive cavities near the medullary cavity. D) High magnification view of two LAGS between loosely arranged fibrolamellar bone. E) Close up of well vascularised radial fibrolamellar bone tissue present in the detached outer cortical piece of the bone wall shown by the green arrow.

3.3.2.5 Femoral section B5

The general histology of femoral section B5 (Fig. 3.3.2.5A), the most distal section of the femur, shows cancellous bone in the perimedullary region which transitions to parallel-fibred and fibrolamellar bone in the bone periphery (Fig. 3.3.2.5B).

The perimedullary region consists of fibrolamellar bone and secondarily reconstructed bone tissue. There are numerous erosion cavities present which gives the inner bone tissue a cancellous texture (Fig. 3.3.2.5C). Remnants of the earlier deposited fibrolamellar bone are preserved between the resorptive cavities. Secondary osteons are common in the inner cortex and are often located within the fibrolamellar bone tissue. The intrinsic fibre arrangement of the inner regions tends to be variable as the secondary osteons and fibrolamellar bone tissue show differences in their fibre organisation.

The mid-cortex comprises well vascularized laminar parallel-fibred and fibrolamellar bone. Parallel-fibred tissue tended to be in a laminar vascular arrangement whereas fibrolamellar bone tissue varied between plexiform and reticular. The abundance of vascular canals is consistent throughout this portion of the compacta and only starts changing prior to LAG deposition in which there are fewer vascular canals. Secondary osteons and small resorptive cavities are dispersed throughout the mid cortex. The mid cortex shows a moderate degree in the organisation of the intrinsic fibres.

The outer cortex consists of primarily laminar parallel-fibred bone except for a band of rapidly formed fibrolamellar tissue. The frequent long circumferential canals are sometimes connected by radial vascular canals within the outer cortex. Longitudinal vascular canals are present to a lower degree. Near the bone periphery two distinctive, woven textured bands of bone tissue are located. These areas of fibrolamellar bone present with abundant radially orientated vascular canals. There is one band of radial fibrolamellar near the outer bone margin (Fig. 3.3.2.5D) and another surrounding the large circumferential crack in the bone (Fig. 3.3.2.5E).

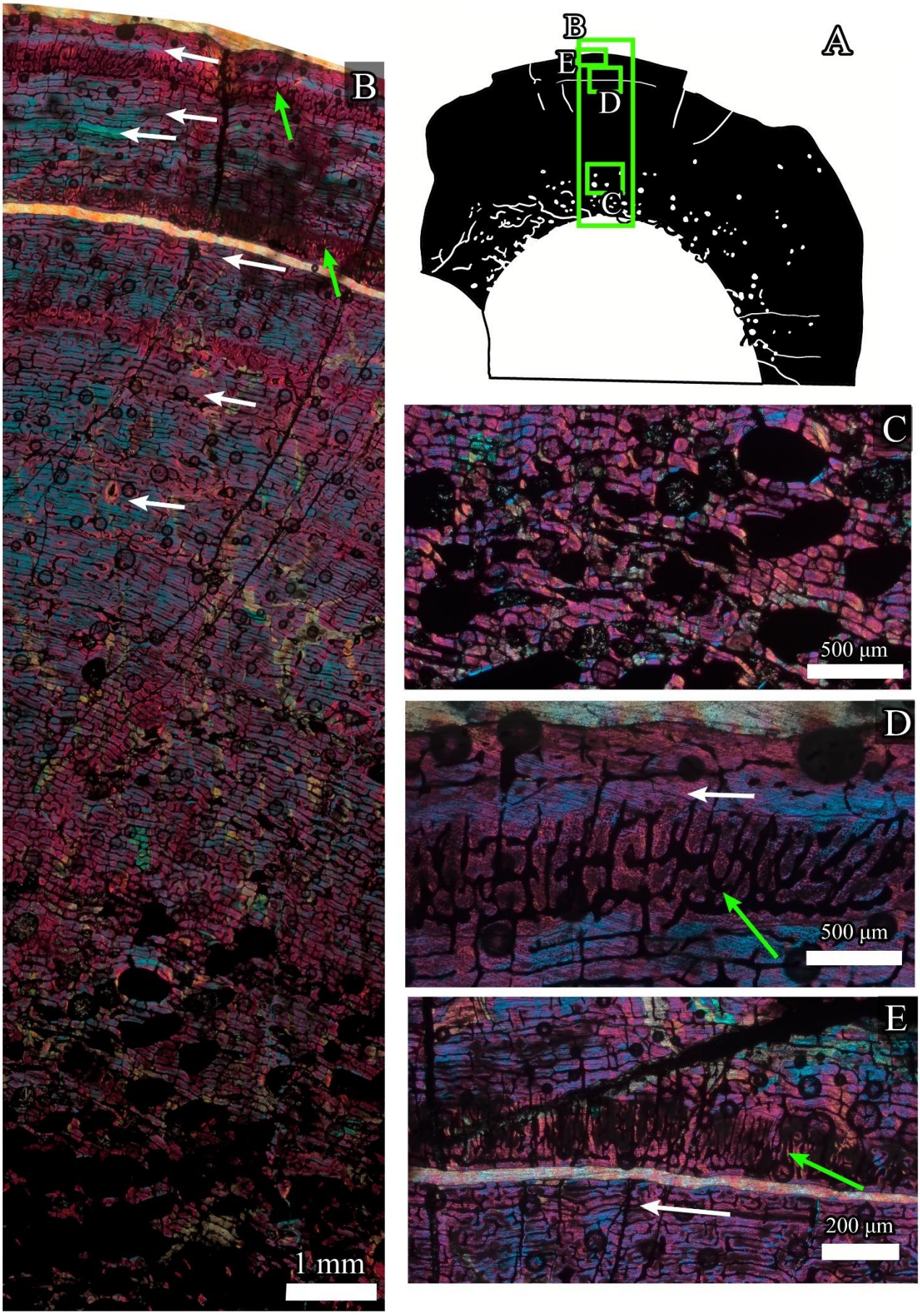
B
A
B
E
D
C
C
500 µm
D
500 µm
E
200 µm
1 mm

Figure 3.3.2.5: Histological section of the *Melanorosaurus* distal femoral section B5. A) Schematic of the preserved bone tissue of the thin section. The black area indicates the preserved part of the bone wall. Green boxes show the location of the higher magnification photographs. B) Composite micrograph showing the general histology of the femur from the medullary to the bone periphery. White arrows indicate the growth marks. Green arrows show the unusual fibrolamellar bone tissue. C) Numerous resorptive cavities and secondary osteons are visible in the inner cortex giving this region a cancellous texture. D) High magnification view of the outer portion of radially deposited fibrolamellar tissue located just prior to the outer bone margin shown by the green arrows. E) High magnification view of the inner portion of radially deposited fibrolamellar tissue located after the circumferential crack in the compacta.

3.4. Lessemsauridae indet.

Four elements of Lessemsauridae indet., a femur, left tibia, caudal vertebrae, and fibula, were sampled. One section from each of following: the femur midshaft (Fig. 2.1.4A), spinal process of caudal vertebrae (Fig. 2.1.4B), tibia midshaft (Fig. 2.1.4C) and the midshaft of the fibula (Fig. 2.1.4D). The orientation and splitting of the bone sample to fit onto petrographic slides is shown below (Fig. 3.4.4)

3.4.1 Femoral histology of Lessemsauridae indet. (SAM-PK-K382)

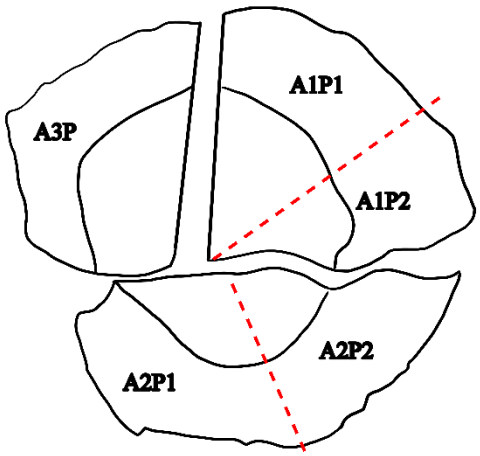

Fig. 3.4.4: Drawing of Lessemsauridae indet. femur sample indicating how the bone sample was cut for thin section analysis. A1P1 is the central anterior portion of the femora. A1P2 is the anterior portion and A2P2 is the posterior portion of the lateral half of the femora. A2P1 is lateral posterior portion and A3P is anterior medial portion of the femora. The dashed lines represent how the bone section was cut for mounting onto the petrographic slides

3.4.1.1 Anterior central section A1P1

Section A1P1 (Fig. 3.4.1.1A) represents the anterior central portion of the Lessemsauridae indet. femur (Fig. 2.1.4A; Fig. 3.4.4). The cortex presents with a transition from fibrolamellar and secondarily reconstructed bone, at the innermost cortex, to a mixture of fibrolamellar and parallel-fibred bone towards the bone periphery (Fig. 3.4.1.1B). Six LAGs are visible within the mid and poorly preserved outer cortex. Histology and LAG locations can be discerned in other portions of the thin section despite the poor preservation of the outer cortex.

The perimedullary region comprises of secondarily reconstructed bone consisting of numerous secondary osteons and resorptive canals. The inner portions of the compacta have a cancellous texture due to the presence of numerous large resorption cavities. Fibrolamellar bone tissue is found between the resorptive canals and secondary osteons are often found within larger patches of fibrolamellar bone tissue. The size and abundance of secondary osteons tends to decrease towards the mid cortex. There is a transition from woven textured fibrolamellar bone to more organised fibrolamellar and parallel-fibred bone when entering the mid cortex (Fig. 3.4.1.1C).

The mid cortex is comprised of predominantly well vascularised fibrolamellar bone (Fig. 3.4.1.1D) with minimal secondary reconstruction. The localised patches of parallel-fibred bone tissue is generally in a laminar arrangement dominated by circumferential vascular canals. Intrinsic fibres of the parallel-fibred bone present with moderate birefringence, whereas there is poor organisation in the intrinsic fibres of the fibrolamellar bone tissue. The fibrolamellar bone is well vascularised and vascular canals tend to be in a reticular arrangement and osteocytes are abundant and closely packed lacking any arrangement (Fig. 3.4.1.1E). There are a few small secondary osteons present and small resorptive cavities in the interior portions of the mid cortex. Three LAGs are counted within this central region of the compacta (Fig. 3.4.1.1E & F).

The poorly preserved outer cortex is comprised predominantly parallel-fibred bone and some fibrolamellar bone tissue. Parallel-fibred bone is well vascularised and is found in either a laminar or plexiform arrangement. Short circumferential vascular canals are abundant with numerous radial connections present.

Longitudinal vascular canals are dispersed between the stretches of circumferential vascular canals. The arrangement of the intrinsic fibres ranges from moderate to strong birefringence. The fibrolamellar tissue is well vascularised and vascular canals are in a reticular arrangement. The outer cortex generally lacks secondary reconstruction. Three LAGs are visible in the outer regions of the compacta.

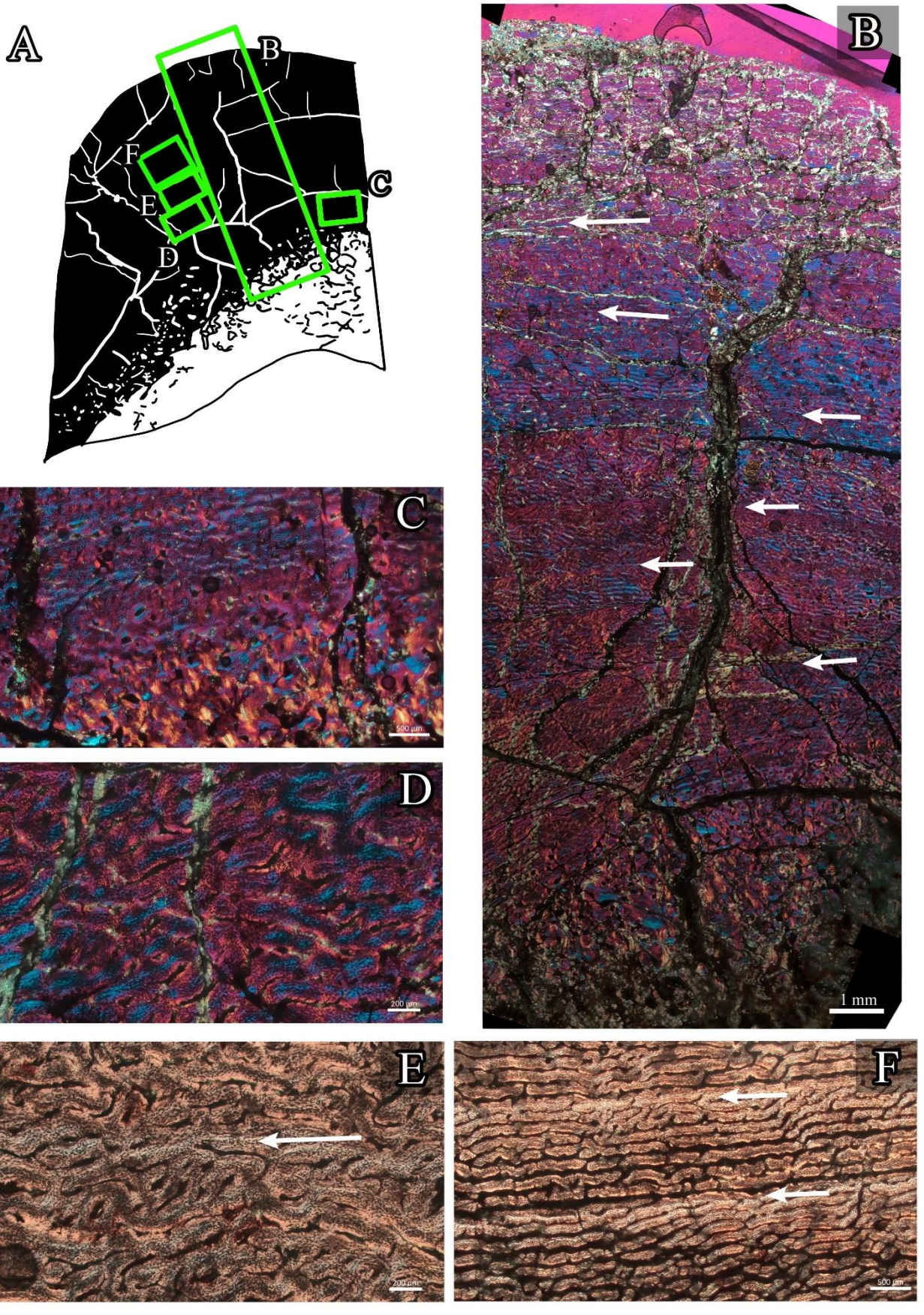
A
B
C
D
E
F
1 mm
500 µm
200 µm
200 µm
500 µm

Figure 3.4.1.1: Histological section of the central anterior portion of the Lessemsauridae indet. femur. A) Schematic of the preserved bone tissue of the thin section. The black area indicates the preserved part of the bone wall. Green boxes show the location of the higher magnification photographs. B) Composite micrograph showing the general histology of the femur from in medullary cavity to the bone periphery. White arrows indicate the growth marks. C) Lower magnification of numerous secondary osteons in the inner cortex. D) High magnification view of the typical loose intrinsic fibre organisation in the well vascularised fibrolamellar tissue. E) High magnification view of growth mark in the mid cortex. Well vascularised fibrolamellar tissue in a reticular arrangement is visible around the growth mark. F) Fibrolamellar bone tissue with vascular canals in a plexiform arrangement. Narrow bands of lamellar bone tissue (annuli) is seen associated with the two growth marks (white arrows).

3.4.1.2 Anterior lateral section A1P2

Section A1P2 (Fig. 3.4.1.2A) presents the histology of the anterior lateral portion of the femur. A transition from poorly preserved cancellous textured bone, in the inner cortex, to parallel-fibred and fibrolamellar bone, in the outer cortex, is observed (Fig. 3.4.1.2B). Seven LAGs are visible in the outer cortex.

The perimedullary region is not well preserved in this section and only bone tissue from the mid to outer cortex is fully discernible. The inner cortex cannot be completely described due to the fragmentation and poor preservation. Remnants of fibrolamellar bone tissue and secondary osteons are intermittently visible in the inner regions (Fig. 3.4.1.2C). Secondary osteons are numerous and range from moderate to large and some overlapping forms patches of dense Haversian bone tissue. The same trend is seen in the resorptive cavities. The fibrolamellar tissue, at the border of the poorly preserved inner cortex, is well vascularised and shows high variation in intrinsic fibre arrangement. The vascular canals are abundant and are seen to be in a reticular arrangement.

The mid cortex consists of a mixture of parallel-fibred bone and fibrolamellar bone tissue (Fig. 3.4.1.2D). The inner regions of the mid cortex are similar to the poorly preserved tissue which comprises the entire inner cortex (Fig. 3.4.1.2B). Vascularisation varies slightly between the different types of bone tissue. Fibrolamellar bone is well vascularised, and the vascular canals are primarily in a reticular to plexiform arrangement. Parallel-fibred bone is seen to be a laminar arrangement. Secondary remodelling is scarce in most of the mid cortex.

The outer regions of the compacta comprise predominantly primary parallel-fibred bone but there are portions of fibrolamellar and lamellar tissue associated with growth mark deposition. The parallel-fibred tissue is well vascularised with vascular canals in a circumferential arrangement, but in some areas the increase in radial connections suggest a shift to a plexiform arrangement. Intrinsic fibre organisation shows variation between moderate and mass birefringence. Variation in the arrangement of intrinsic fibres varies locally but the overall section generally has a high degree of arrangement. Fibrolamellar bone tissue is seen prior to the deposition of lamellar bone which forms an annulus containing the associated LAG (Fig. 3.4.1.2E). The combination of

digenic alteration and secondary reconstruction obscures most of the mid cortex LAGs but seven can be counted in outer cortex (Fig. 3.4.1.2B).

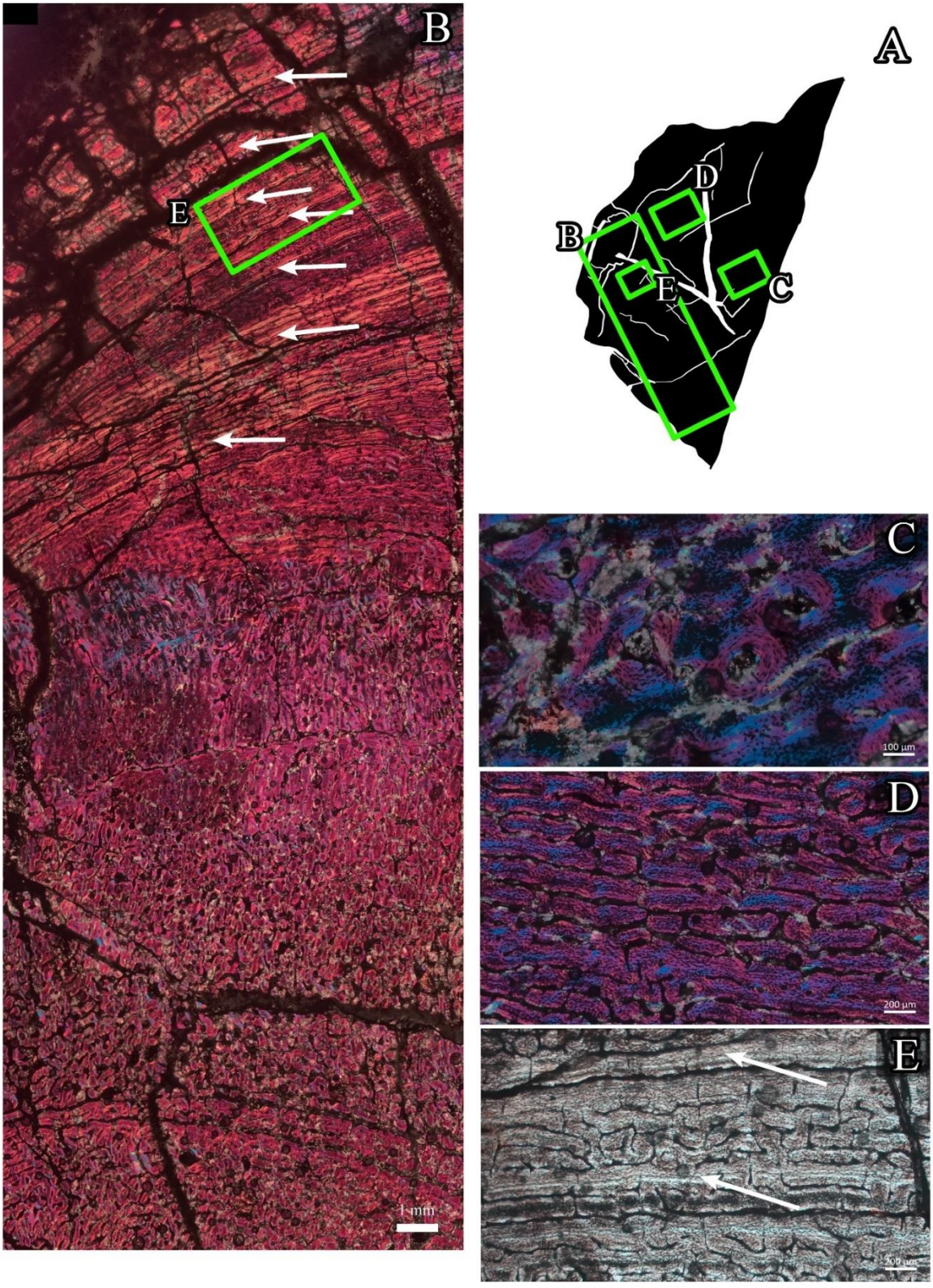

Figure 3.4.1.2: Histological section of the lateral anterior portion of the Lessemsauridae indet. femur. A) Schematic of the preserved bone tissue of the thin section. The black area indicates the preserved part of the bone wall. Green boxes show the location of the higher magnification photographs. B) Composite micrograph showing the general histology of the femur from in medullary cavity to the bone periphery. White arrows indicate the growth marks. C) High magnification view of small fully formed secondary osteons in the mid cortex. D) The typical loosely organised fibrolamellar bone tissue observed throughout the mid and outer cortex. E) High magnification view of plexiform fibrolamellar bone tissue between two growth marks in relatively close succession. The growth marks (white arrows) are embedded within a layer of lamellar bone tissue (annuli).

3.4.1.3 Posterior medial section A2P1

Section A2P1 shows the medial portion of the anterior side of the femur. The general histology of this section is quite fragmented but most of mid and outer cortex are preserved (Fig. 3.4.1.3A). The compacta presents with a transition from cancellous bone in the innermost cortex towards parallel-fibred bone and fibrolamellar bone in the bone periphery. Four LAGs are present in the mid cortex and five are located within the outer cortex (Fig. 3.4.1.3B).

What is visible of the inner cortex consists primarily of fragmented secondarily reconstructed bone tissue and woven textured bone tissue. Fragmented secondary cancellous tissue (Fig. 3.4.1.3C) is present in the perimedullary region. Numerous fragmented secondary osteons (Fig. 3.4.1.3D) and resorptive cavities with lamellar bone deposits make up the perimedullary region. The abundance of resorption cavities gives the bone a cancellous texture (Fig. 3.4.1.3B). Well vascularised fibrolamellar bone is present with a lower degree of birefringence throughout the inner cortex. Nearing the mid cortex, the intrinsic fibres start to increase in the degree of arrangement and bone deposition becomes more organised.

The mid cortex shows the transition from fibrolamellar bone to parallel-fibred bone. Vascular canals are primarily in plexiform to laminar arrangement (Fig. 3.4.1.3E) with some portions of plexiform arrangement. Within the inner portion of the mid cortex, secondary reconstruction is common as several fully formed secondary osteons are observed in addition to numerous resorption cavities. This large array of secondary osteons present prior to the parallel-fibred bone transition is also seen in the other femur sections. The amount of secondary remodelling decreases significantly in the parallel-fibred portion of the mid cortex. Thin bands of lamellar bone tissue surround the growth marks forming annuli which alternate with zones of fibrolamellar bone tissue (Fig. 3.4.1.3B).

Most of the outer portion is well vascularised, primary parallel-fibred and fibrolamellar bone tissue (Fig. 3.4.1.3F). There is a decrease in vascular canal abundance when approaching the outer bone margin but an OCL does not appear to be present, although distance between growth marks tend to decrease (Fig. 3.4.1.3B). Vascular canals are mostly in a laminar arrangement but there are small portions of reticular and plexiform dispersed throughout. Intrinsic fibres show moderate birefringence and osteocyte lacunae are generally well

organised. Secondary reconstruction is minimal in the outer third of the compacta but occasionally there are a small fully formed secondary osteons are present. Additionally, resorption cavities are scarce and small when found.

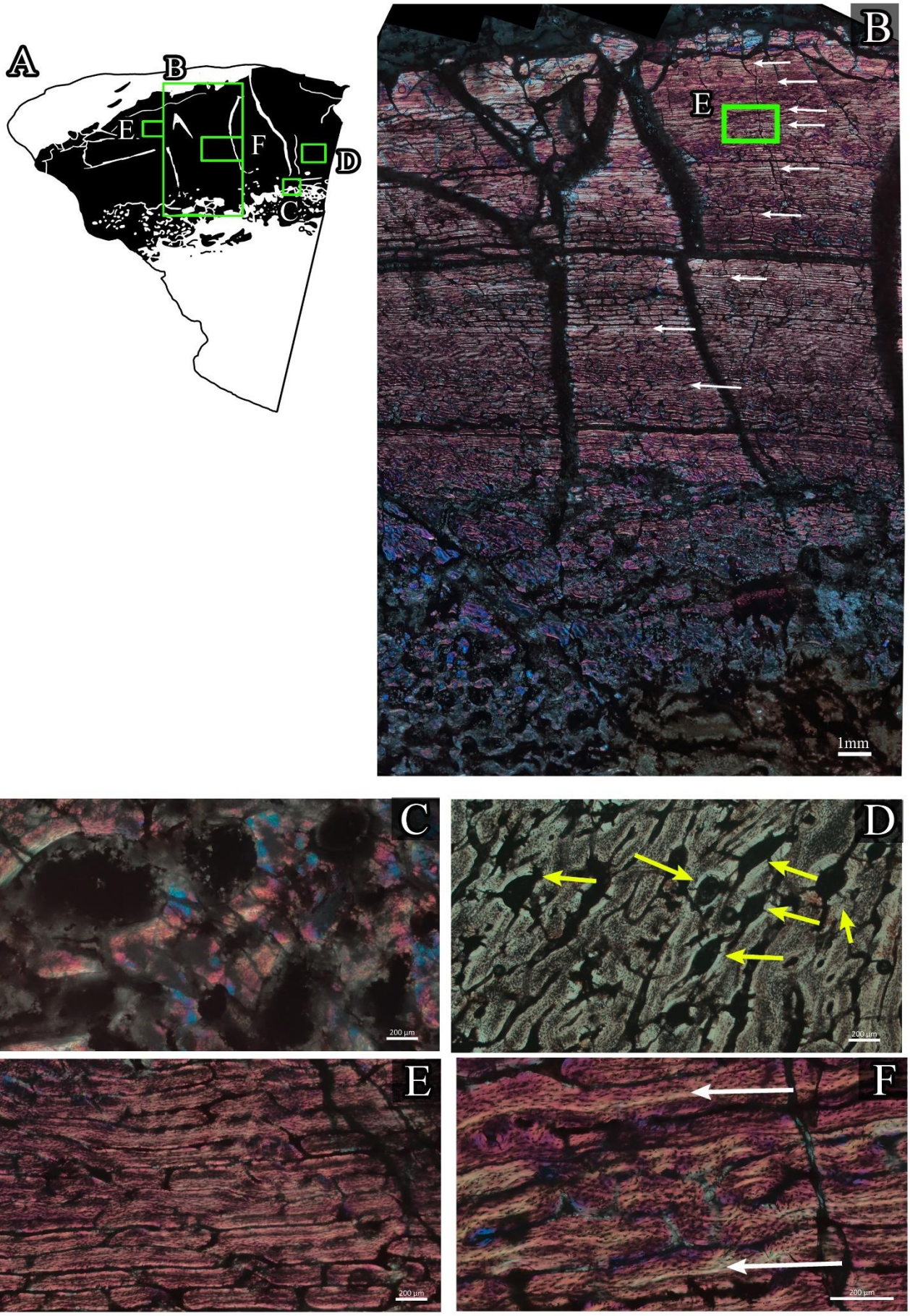
A
B
E
F
D
C
B
E
1mm
C
200 µm
D
200 µm
E
200 µm
F
200 µm

Figure 3.4.1.3: Histological section of the posterior medial portion of the Lessemsauridae indet. femur. A) Schematic of the preserved bone tissue of the thin section. The black area indicates the preserved part of the bone wall. Green boxes show the location of the higher magnification photographs. B) Composite micrograph showing the general histology of the femur from in medullary cavity to the bone periphery. White arrows indicate the growth marks. C) Fragmented secondary bone tissue in the perimedullary region. The numerous resorptive cavities give the inner regions a cancellous texture. D) High magnification view of secondary osteons (yellow arrows) being infilled with lamellar bone tissue. E) Plexiform to laminar arranged vascular canals present in the well vascularised fibrolamellar bone tissue. F) High magnification view of two growth marks (white arrows) within the fibrolamellar bone tissue in a plexiform arrangement.

3.4.1.4 Posterior lateral section A2P2

The posterior lateral section of the femur is represented by section A2P2 and the general preservation of the bone tissue is extremely poor with large cracks throughout the compacta (Fig. 3.4.1.4A). The histology of the compacta consists of cancellous inner cortex and parallel-fibred dominated mid to outer cortex (Fig. 3.4.1.4B). The fragmented compacta does not preserve the continuation of growth marks however, four to five are visible in the mid and outer cortex (Fig. 3.4.1.4A).

The fragmented inner cortex is comprised of fibrolamellar and cancellous textured bone tissue. Resorption cavities are common throughout the perimedullary region (Fig. 3.4.1.4C). Well vascularised fibrolamellar bone is found surrounded by secondarily reconstructed bone tissue made up of numerous large secondary osteons (Fig. 3.4.1.4D) and resorptive cavities. Haphazardly arranged osteocytes and vascular canals are common in the less fragmented portions of the inner cortex.

The central area of the compacta is comprised of predominantly parallel-fibred issue and fibrolamellar bone tissue (Fig. 3.4.1.4D), although there are dispersed portions of secondarily reconstructed bone throughout the mid cortex. Vascular canals tend to be in a laminar arrangement apart from the areas of reticular and sub-plexiform vascular canals within the fibrolamellar bone. The well vascularised fibrolamellar bone is present throughout and consists of a loose organisation within the intrinsic fibres. Secondarily reconstructed bone occurs sparsely in the mid cortex with fully formed secondary osteons and resorptive cavities more common in the inner portion of the mid cortex. In the complete portions of the mid cortex, two LAGs are located close to each other (Fig. 3.4.1.4E). Poorly vascularised lamellar tissue is present near growth marks forming an annulus which is sometimes surrounded by fibrolamellar bone (Fig. 3.4.1.4F).

Most of the outer cortical regions comprise of primary parallel-fibred bone with small portions of secondarily reconstructed bone present. Vascularisation decreases towards the outer bone wall. The primary vascular canal arrangement tends to be laminar consisting of mostly short circumferential and small longitudinal vascular canals. Intrinsic fibres are generally of a higher degree of organisation in the outer regions of the compacta. Three LAGs are visible throughout the fragmented portions of bone peripheral tissue totalling five throughout the compacta (Fig. 3.4.1.4B).

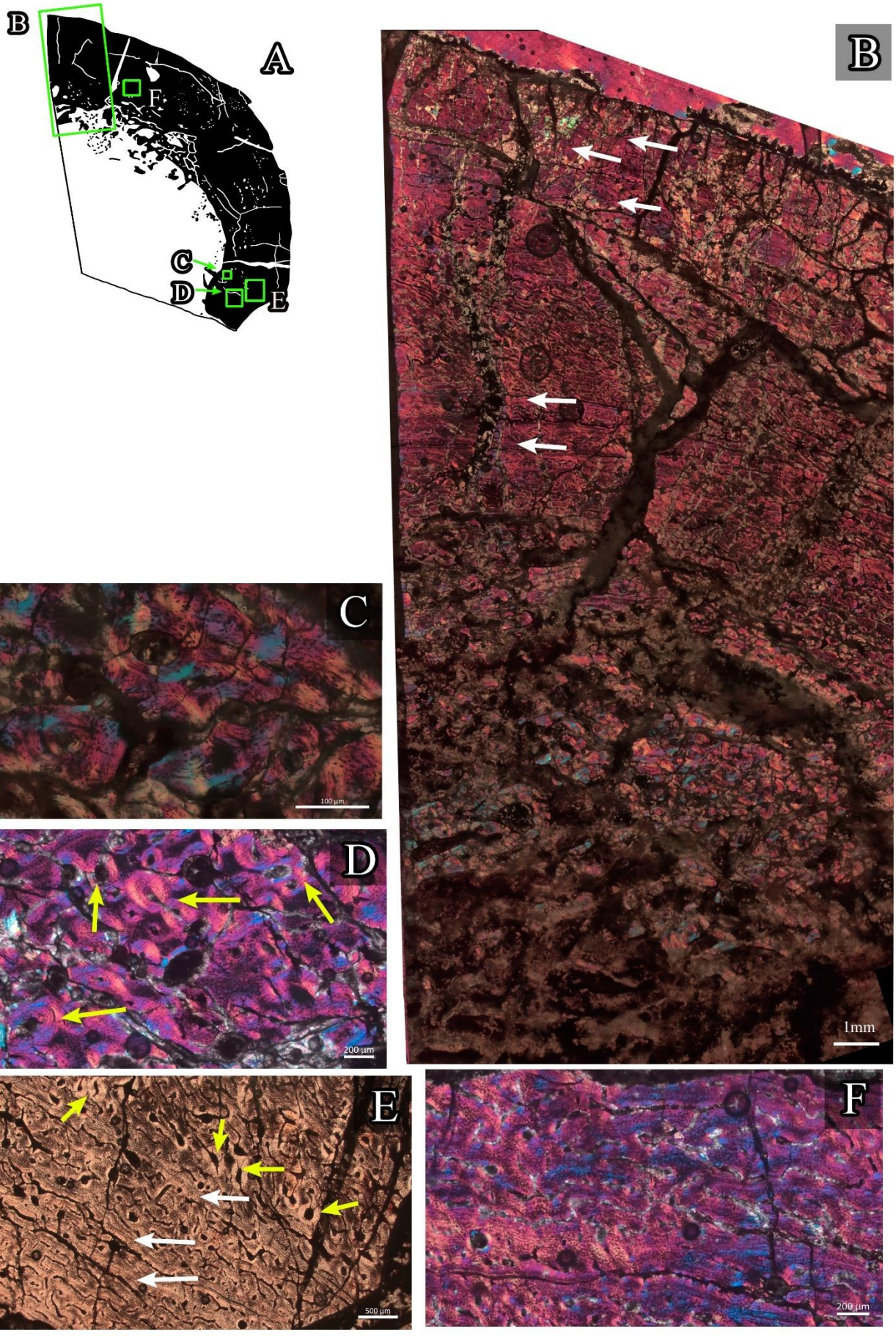
A
B
C
D
E
F
1mm
100 µm
200 µm
500 µm
200 µm

Figure 3.4.1.4: Histological section of the posterior lateral portion of the Lessemsauridae indet. femur. A) Schematic of the preserved bone tissue of the thin section. The black area indicates the preserved part of the bone wall. Green boxes show the location of the higher magnification photographs. B) Composite micrograph showing the general histology of the femur from in medullary cavity to the bone periphery. White arrows indicate the growth marks. C) The infilling of resorptive canals in the innermost regions of the cortex. D) High magnification view of fully formed small secondary osteons (yellow arrow). A high density of osteocytes can be seen in the primary tissue separating the secondary osteons. E) Fibrolamellar bone tissue in between the intensively secondary reconstruction in the inner cortex. Fully formed secondary osteons are visible (yellow arrows). Thin bands of lamellar tissue are seen around the growth marks forming annuli. F) Close up view of fibrolamellar bone in the inner cortex. Intrinsic fibres show some degree of organisation but osteocytes are irregular shaped and deposited.

3.4.1.5 Anterior medial section A3P1

Section A3P1 shows the histology of the anterior medial portion of the femur. The compacta is partially fragmented and numerous cracks obscure a complete histology but the features of each region are visible. The cortex comprises of cancellous textured tissue and fibrolamellar bone in the inner regions and transitions towards parallel-fibred and fibrolamellar bone in the mid and outer cortex. While major areas have been fragmented due to diagenesis, the overall histology can still be observed from the medullary regions to the bone periphery. Additionally, most growth marks are well preserved showing ten growth marks spanning the mid and outer cortex, although it is likely that several more growth marks may have occurred in the outermost compacta that is damaged by intense mineral infiltration and fragmentation of the bone wall (Fig. 3.4.1.5B).

The inner cortex has undergone intensive secondary reconstruction to form patches of dense Haversian bone tissue but occasionally dispersed patches of woven fibrolamellar bone tissue can be observed within the secondary tissue (Fig. 3.4.1.5C). Most of the perimedullary region consists of large secondary osteons being endosteally infilled with lamellar bone (Fig. 3.4.1.5D) and many resorptive cavities. Cancellous trabeculae are present bordering the medullary-compacta barrier. A poorly preserved transition from more woven texture bone to more organised fibrolamellar bone tissue is visible approaching the mid cortex (Fig. 3.4.1.5E).

The mid cortex is comprised of predominantly primary parallel-fibred bone and some secondary bone dispersed throughout the compacta. Vascularity varies throughout with most portions presenting with numerous vascular canals in reticular arrangement. Plexiform and laminar vascular arrangement is present to a lesser degree. The intrinsic fibre arrangement is of a high to moderate degree throughout the region. Small secondary osteons are present throughout with dense haversian bone present in the most medial portion of the section. Moderately sized resorptive cavities are abundant near secondary osteons and around haversian bone. There is poor continuity of LAGs as there frequent remodelling but remnants of three to four LAGs (Fig. 3.4.1.5B) are seen in the mid cortex. A small portion of lamellar bone tissue is seen containing these growth marks and often these annuli are surrounded by fibrolamellar bone tissue (Fig, 3.4.1.5F).

The poorly preserved and cracked outer cortex consists of mostly parallel-fibred bone and some secondarily reconstructed bone tissue. Vascular canals are primarily in plexiform arrangement. Short circumferential and

radial vascular canals are abundant whereas longitudinal vascular canals are dispersed and scarce. Intrinsic fibres are moderately arranged with variations in birefringence seen between distant areas of the bone periphery. Secondary osteons are dispersed and often in early stages in most of the section except the most medial portion. Some fully formed secondary osteons and small resorptive cavities are present near the mid cortex but not near the bone periphery. Approximately four growth marks are present and are almost equidistant (Fig. 3.4.1.5B). The same pattern of lamellar bone containing the growth mark is observed in the outer cortex.

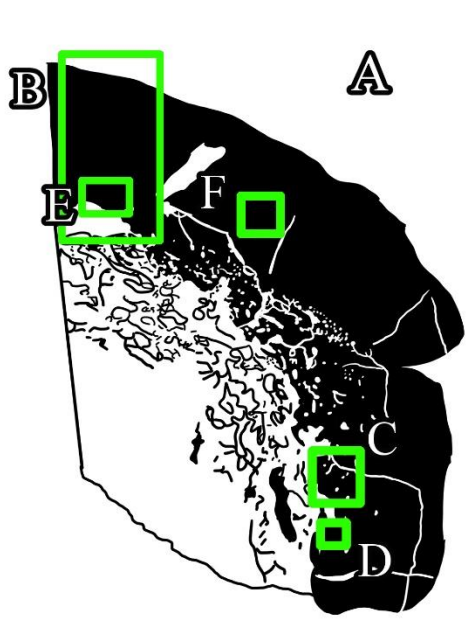
A
B
E
F
C
D

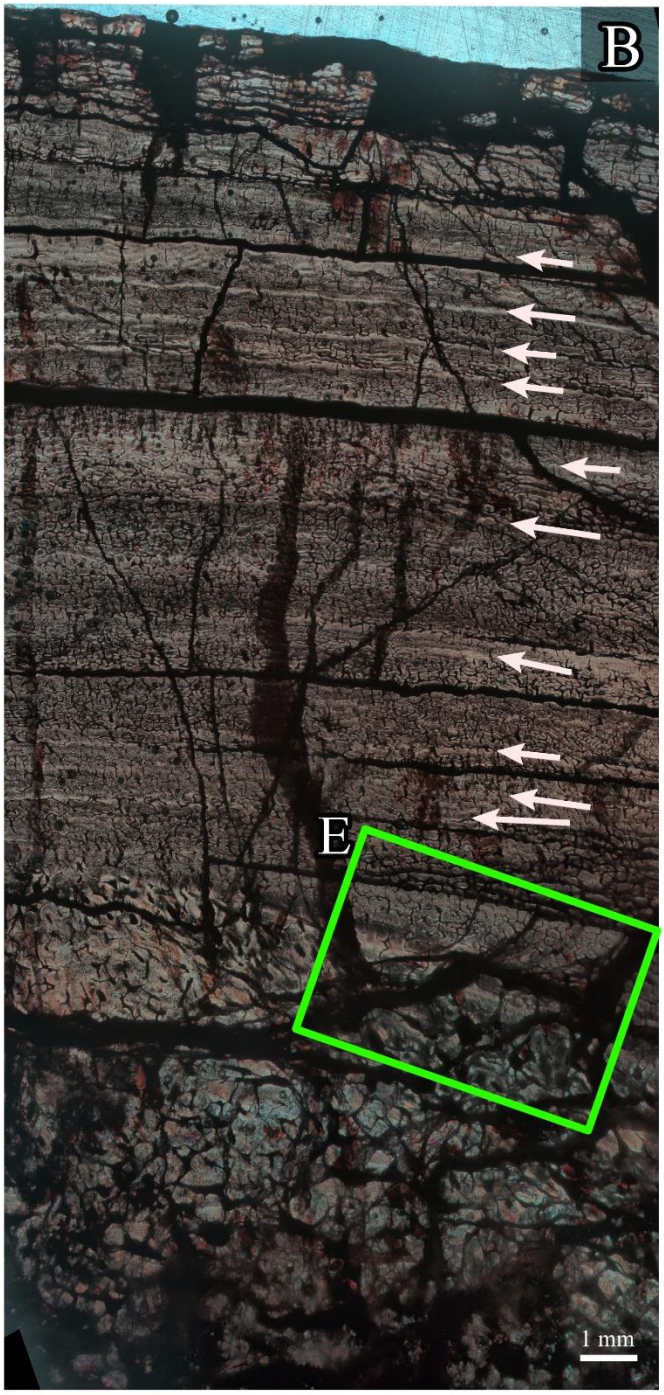
B
E
1 mm

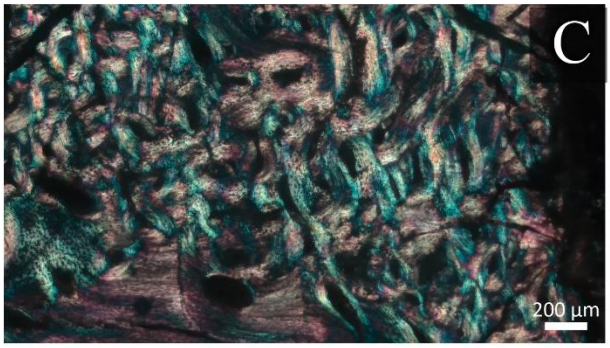
C
200 µm

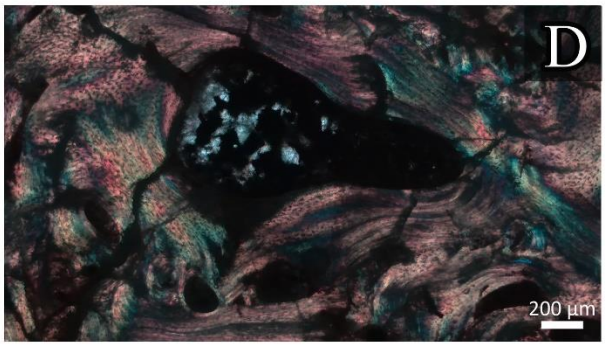
D
200 µm

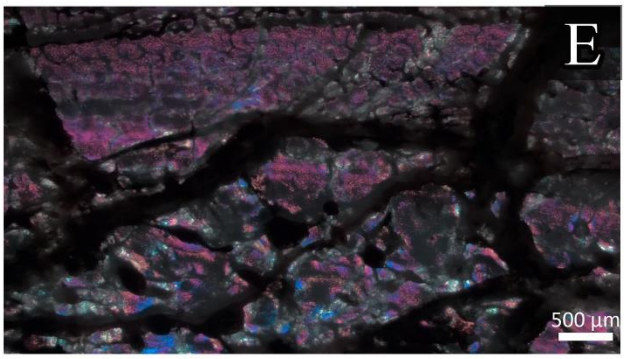
E
500 µm

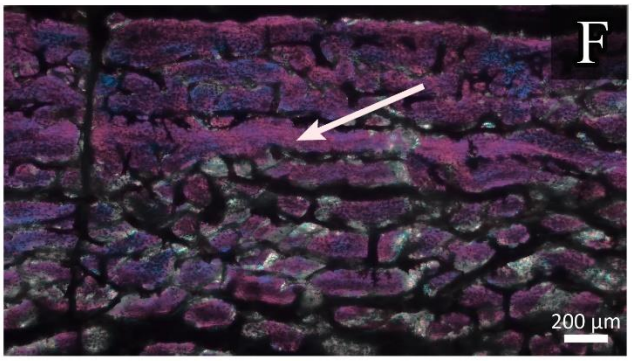
F
200 µm

Figure 3.4.1.5: Histological section of the anterior medial portion of the Lessemsauridae indet. femur. A) Schematic of the preserved bone tissue of the thin section. The black area indicates the preserved part of the bone wall. Green boxes show the location of the higher magnification photographs. B) Composite micrograph showing the general histology of the femur from in medullary cavity to the bone periphery. White arrows indicate the growth marks. C) Fibrolamellar bone tissue in between fully formed secondary osteons in the inner cortex. Some secondary osteons start to overlap forming incipient haversian bone. D) High magnification view of a secondary osteon with a large resorptive canal being endosteally infilled with lamellar bone tissue in the same region as D E) Poorly preserved transition from mostly secondary reconstruction to primary fibrolamellar bone tissue bordering the inner and mid cortex. The change in bone texture is still apparent through the poor preservation. F) Fibrolamellar bone tissue with vascular canals in a plexiform arrangement. A thin band of lamellar tissue is visible around the growth mark.

3.4.2 Tibial histology of Lessemsauridae indet. (SAM-PK-K382)

Two thin sections were made from the tibia of Lessemsauridae indet. as shown below in figure 3.4.2.

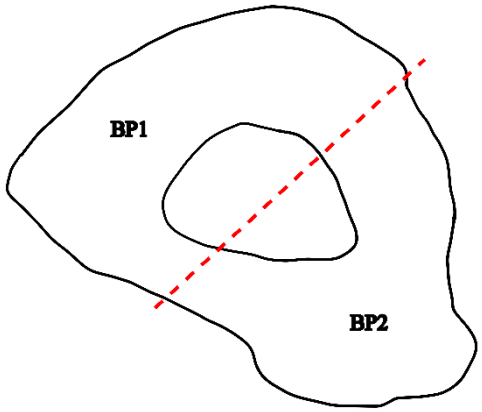

Figure 3.4.2: Drawing of Lessemsauridae indet. tibia indicating how the bone sample was cut for thin section analysis. BP1 is the medial half and BP2 is the lateral half of the tibia thin section. The dashed lines represent how the bone section was cut for mounting onto the petrographic slides.

3.4.2.1 Tibial section BP1

Section BP1 represents the medial half of the left tibia (Fig. 3.4.2.1A). The tibia is badly fragmented and large cracks obstruct the histology of the compacta. The preserved portions show the transition from fibrolamellar and secondary bone tissues, in the inner half of the cortex, to the well vascularised parallel-fibred and fibrolamellar bone in the outer cortex (Fig. 3.4.2.1B).

The inner cortex consists of some cancellous textured bone but mostly fibrolamellar and secondarily reconstructed bone tissue. A change in bone texture towards more fibrolamellar tissue is observed as the amount of secondary tissue decreases towards the middle region of the compacta (Fig. 3.4.2.1C). The inner regions of the compacta are comprised of mostly secondary osteons and resorptive cavities. The fibrolamellar tissue is the only primary bone tissue present in this region between the areas of intensive secondary reconstruction. Dense haversian bone tissue is found within the inner regions and continues towards the mid cortex.

The mid portion of the compacta consists of well vascularised fibrolamellar, parallel-fibred (Fig. 3.4.2.1D) and patches of secondarily reconstructed bone tissue. The vascular canals are either in a laminar arrangement in the parallel-fibred bone or a reticular arrangement in the fibrolamellar bone tissue. The arrangement of intrinsic fibres is variable as the fibrolamellar and secondary remodelling present as patches of high birefringence in the mid cortex. Within the mid-cortex, the vascular arrangement is dominated by circumferential canals with a significant number of longitudinal canals. The radial vascular canals are scarce. Regions of moderate vascularity are observed near areas of intensive secondary reconstruction (Fig. 3.4.2.1E) and within the vicinity of LAGs. There are regions of dense Haversian bone dispersed throughout the mid cortex (Fig. 3.4.2.1F) but are generally localised as there is still primary bone present in most of the mid cortex. The first LAG is seen approximately midway in the compacta.

Parallel-fibred bone is the predominant bone tissue near the bone periphery. The vascular canals are arranged in a laminar arrangement throughout the outer regions of the compacta but a decrease of the abundance of

vascular canals is also observed. The decrease in vasculature is evident when approaching the vicinity of LAGs. There is a small amount of secondary reconstruction in the outer cortex. There five LAGs in the outer cortex totalling six throughout the compacta but due to diagenesis and secondary reconstruction, there is likely to be more growth marks within the mid cortex.

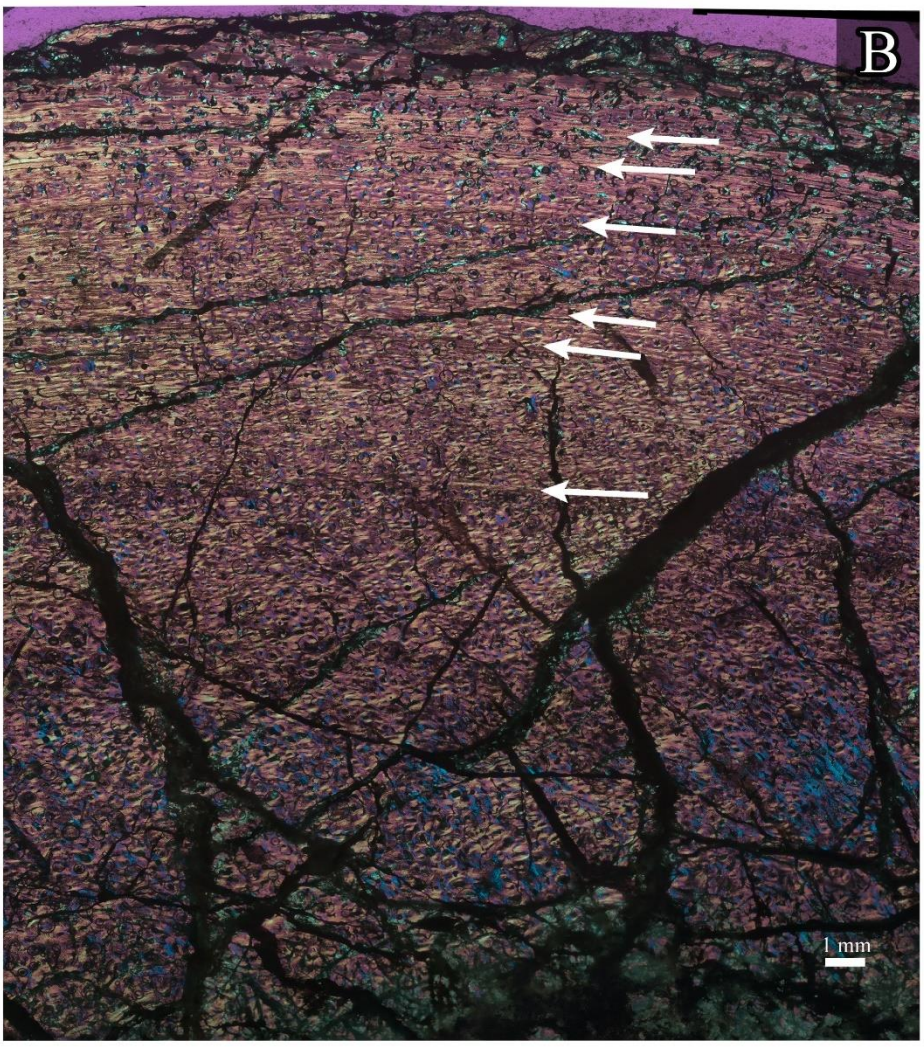
B
1 mm

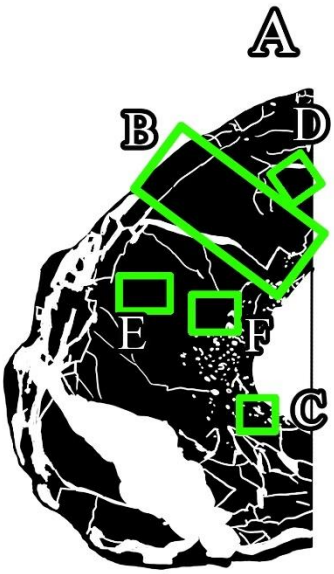
A
B
D
E
F
C

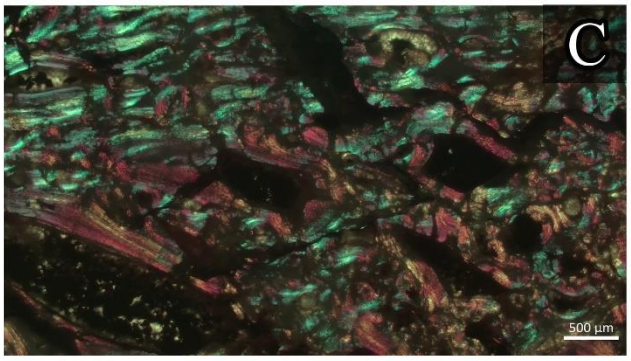
C
500 µm

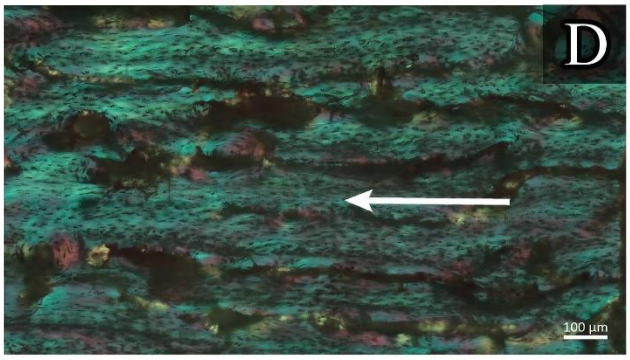
D
100 µm

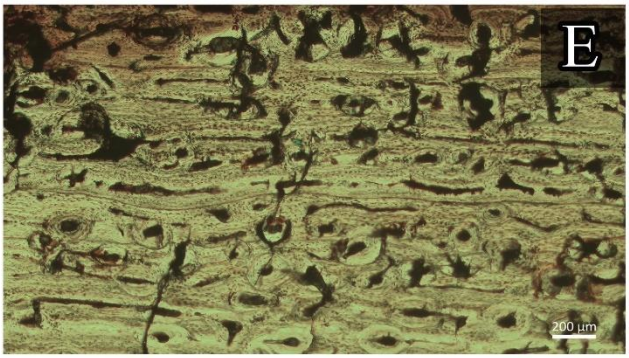
E
200 µm

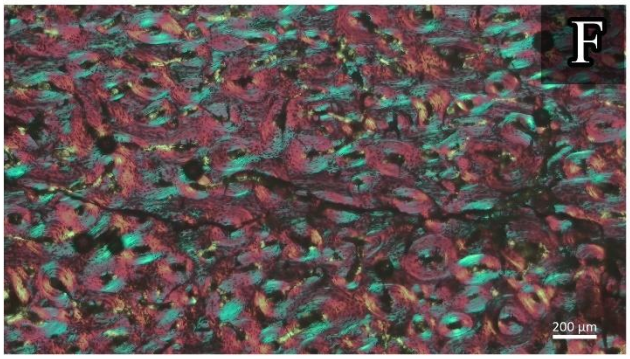
F
200 µm

Figure 3.4.2.1: Histological section of the medial half of Lessemsauridae indet. tibia. A) Schematic of the preserved bone tissue of the thin section. The black area indicates the preserved part of the bone wall. Green boxes show the location of the higher magnification photographs. B) Composite micrograph showing the general histology of the tibia from the medullary cavity to the bone periphery. White arrows indicate the growth marks. C) Enlarged erosion cavities being infilled with secondary lamellar bone tissue. D) Parallel-fibred bone with numerous secondary osteons. E) Fully formed secondary osteons in the mid cortex approaching the bone periphery. F) Concentration of secondary osteons forming dense Haversian bone tissue in the inner compacta.

3.4.2.2 Tibial section BP2

Section BP2 shows the histology of the lateral half of the left tibia. The bone tissue has several cracks which have been infilled, but the histology of the preserved portions is visible (Fig. 3.4.2.2A). The general histology shows a transition from cancellous bone to fibrolamellar and parallel-fibred bone (Fig. 3.4.2.2B). The lateral half shows less overall bone tissue as most of the medullary cavity has expanded in this half.

The inner cortex consists of well vascularised fibrolamellar and cancellous textured bone tissue (Fig. 3.4.2.2C). Secondary osteons and large resorption cavities are very common throughout the perimedullary region. The original fibrolamellar bone tissue is visible between the secondary reconstructed bone tissue. Intrinsic fibres of this region show great variability with low degree of organisation. Nearing the middle area of the compacta, overlapping of secondary osteons start becoming more prevalent and dense haversian bone is observed.

The mid-cortex consists of predominantly parallel-fibred and fibrolamellar bone with some portions of secondarily reconstructed bone tissue. Most of the vascular canals are in a laminar arrangement with many circumferential and longitudinal vascular canals but few radial connections. The mid cortex is well vascularised but a decrease in the abundance of vascular canals is seen in the vicinity of LAGs as lamellar bone tissue is deposited forming an annulus. The arrangement of intrinsic fibres is haphazard in the plexiform arranged fibrolamellar tissue (Fig. 3.4.2.2D) but more organised in the parallel-fibred bones. Four LAGs are visible in the mid cortex (Fig. 3.4.2.2B & D). The posterior-lateral area of the mid cortex shows considerably more secondary reconstruction than the rest of the bone tissue evident by the large erosion cavities (Fig. 3.4.2.2A). Intrinsic fibre arrangement is variable throughout the mid cortex as secondary bone shows local variation of fibre organisation but the parallel-fibred bone in the mid cortex presents with moderate birefringence.

The outer cortex is made of up of primary parallel-fibred and fibrolamellar tissue which are separated by annulus formed by lamellar bone (Fig. 3.4.2.2E). Laminar arrangement of vascular canals is still common but circumferential vascular canals shorten and the number of longitudinal canals increase. Four to five LAGs are visible in the disjointed outer cortex. Annuli are visible as lamellar bone tissue is visible around the LAGs. A

few small secondary osteons are observed in the outer cortex. Intrinsic fibre arrangement of the outer cortex is of high birefringence generally as bone growth slows down in late ontogeny.

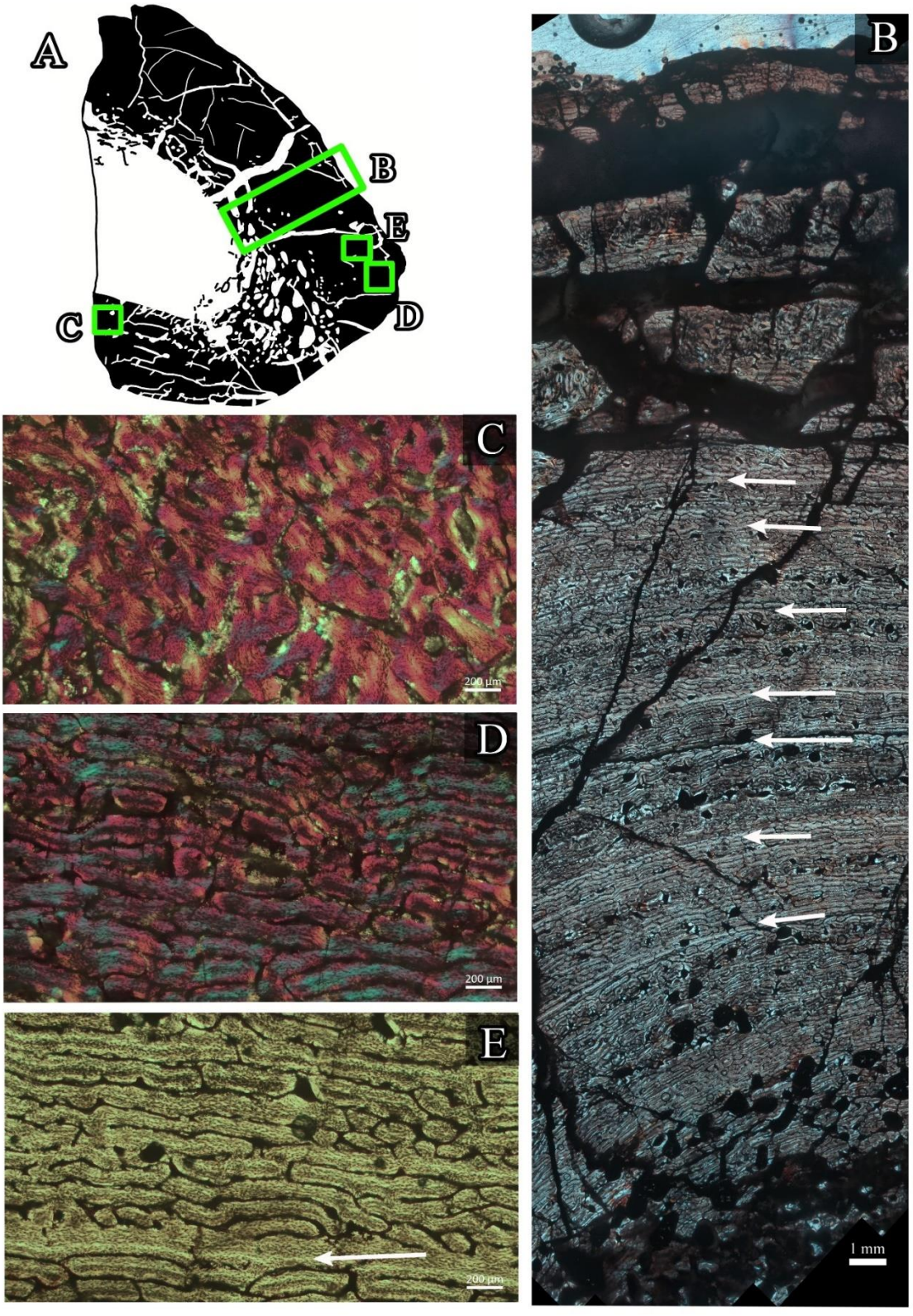

Figure 3.4.2.2: Histological section of medial half of Lessemsauridae indet. left tibia. A) Schematic of the preserved bone tissue of the thin section. The black area indicates the preserved part of the bone wall. Green boxes show the location of the higher magnification photographs. B) Composite micrograph showing the general histology of the tibia from in medullary cavity to the bone periphery. White arrows indicate the growth marks. C) A concentration of numerous secondary osteons forming dense Haversian bone. D) Close up of view of the poor birefringence of intrinsic fibres seen in the fibrolamellar bone. E) Fibrolamellar bone tissue with vascular canals in a laminar to plexiform arrangement. One growth mark in visible within a small band of lamellar bone tissue.

3.4.3 Histology of caudal vertebrae of Lessemsauridae indet. (SAM-PK-K382)

The thin section (Fig. 3.4.3A) of the spinous process of the caudal vertebrae consists of a large amount of secondarily reconstructed bone tissue in the form of large erosion cavities (Fig. 3.4.3B). Cancellous trabeculae are common throughout the inner regions of the spinous process (Fig. 3.4.3C). Some of the erosion cavities have narrow bands of lamellar bone tissue but there are no fully formed secondary osteons visible (Fig. 3.4.3D). The peripheral bone tissue consists of poorly vascularised lamellar bone with several incompletely formed secondary osteons and many small resorptive canals (Fig. 3.4.3D). Organisation of intrinsic fibres are uniform apart from some small variations presented by later deposited secondary bone tissue. Two closely associated growth marks are visible in the poorly vascularised bone periphery (Fig. 3.4.3D & E).

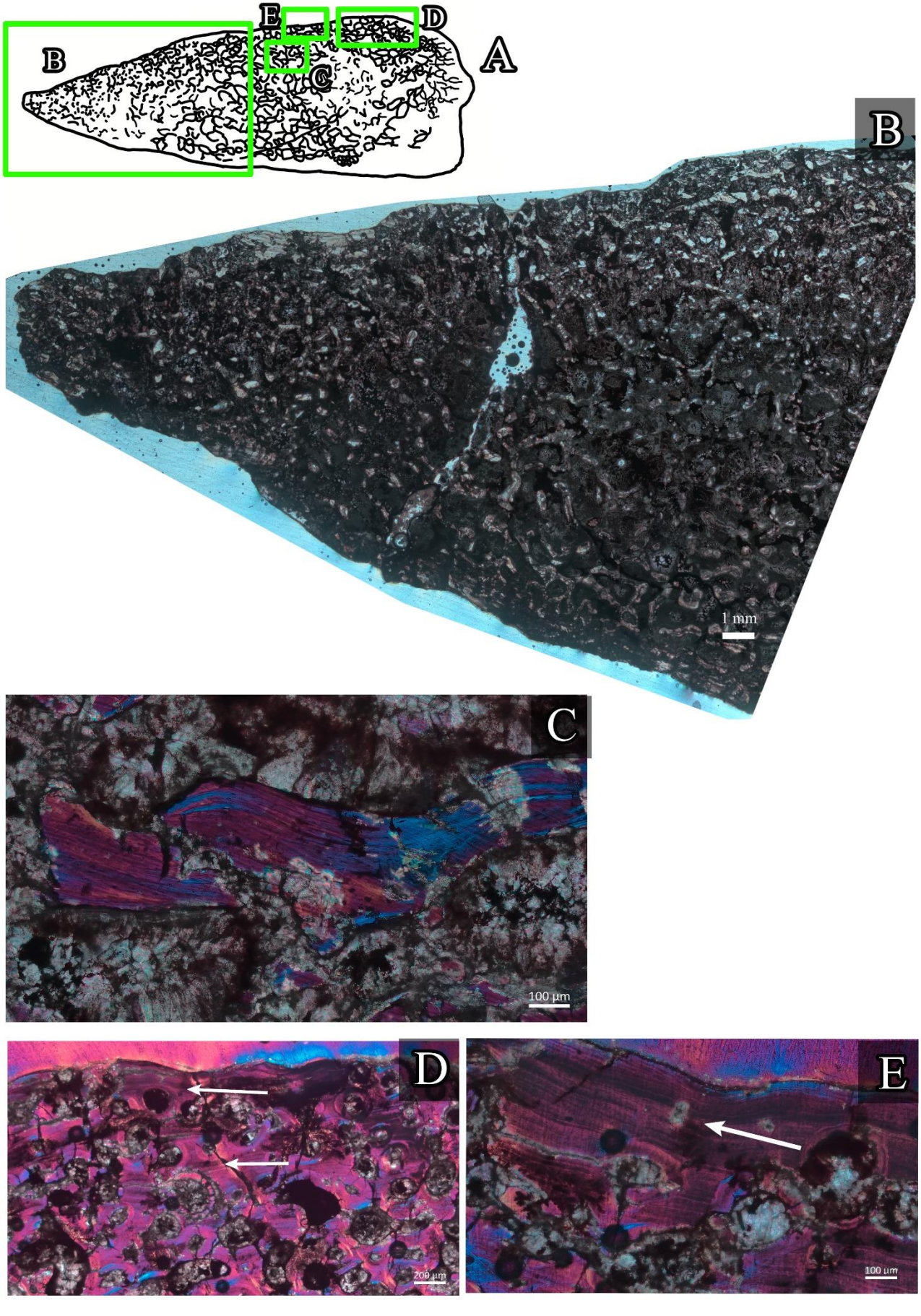
A
B
C
D
E
B
1 mm
C
100 µm
D
200 µm
E
100 µm

Figure 3.4.3: Histological section of the spinous process of the Lessemsauridae indet. caudal vertebra. A) Schematic of the preserved bone tissue of the thin section. The black area indicates the preserved part of the bone wall. Green boxes show the location of the higher magnification photographs. B) Composite micrograph showing the general histology of the spinous process showing the overall cancellous texture of the compacta. C) A poorly vascularised cancellous trabecula within the inner cortex. D) Many erosion cavities are visible within the small amount of the primary lamellar bone remaining. Two closely spaced growth marks (white arrows) are visible in the outer regions. E) Close up view of the peripheral region showing the poorly vascularised lamellar bone tissue and a growth mark (white arrow).

3.4.4 Fibular histology of Lessemsauridae indet. (SAM-PK-K382)

Two sections were prepared from the sample from the fibula mid shaft of Lessamsauridae indet. show below in figure 3.4.4.

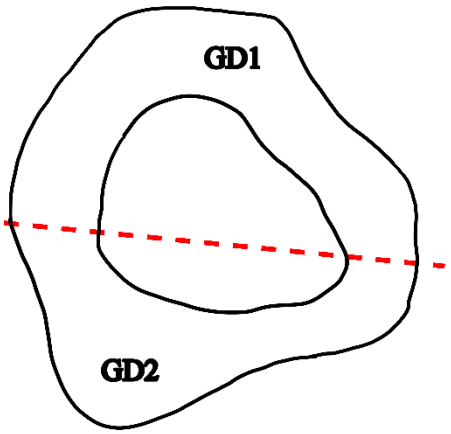

Fig. 3.4.4: Drawing of Lessemsauridae indet. fibula indicating how the bone sample was cut for thin section analysis. The dashed line represent how the bone section was cut for mounting onto the petrographic slides.

3.4.4.1 Lateral fibula section GD1

Section GD1 (Fig. 3.4.4.1A) represents the lateral half of the Lessemsauridae indet. fibula. The compacta is very fragmented and only small portions of compact bone are preserved (Fig. 3.4.4.1A). The general histology of the preserved fragments consists of cancellous bone and fibrolamellar tissues in the supposed inner regions and transitions to parallel-fibred and fibrolamellar bone tissue in the outer cortex.

The perimedullary region consists of mostly secondarily reconstructed bone tissue (Fig. 3.4.4.1D) which gives the bone an overall cancellous texture. Well vascularised fibrolamellar bone is common within the fragmented pieces of the inner cortex. Numerous secondary osteons overlap in the anterior portion of the section but do not reach the dense Haversian proportions (Fig. 3.4.4.1E).

The mid cortex is predominantly moderately vascularised parallel-fibred bone tissue (Fig. 3.4.4.1C). Enlarged resorptive cavities and secondary osteons are also semi-common within the mid cortex. The predominant circumferential and longitudinal vascular canals are found in a laminar arrangement. The intrinsic fibre arrangement is of a higher degree with some variation between the posterior and anterior ends of the compacta. No LAGs are visible in the mid cortex due to the poor preservation. Small secondary osteons and resorptive cavities, in the early stages of infilling, are dispersed throughout the middle portions of the compacta.

The outer cortex consists of parallel-fibred bone and isolated portions of secondarily reconstructed bone tissue (Fig. 3.4.4.1B). Vascular canal abundance is generally moderate or low throughout the outer cortex as distance between consecutive LAGs decrease. The arrangement of vascular canals is laminar and consists of long circumferential vascular canals and longitudinal vascular canals. A few secondary osteons and resorptive occur in outer cortex. Five LAGs, visible in outer cortex, are the only LAGs present in the cortex.

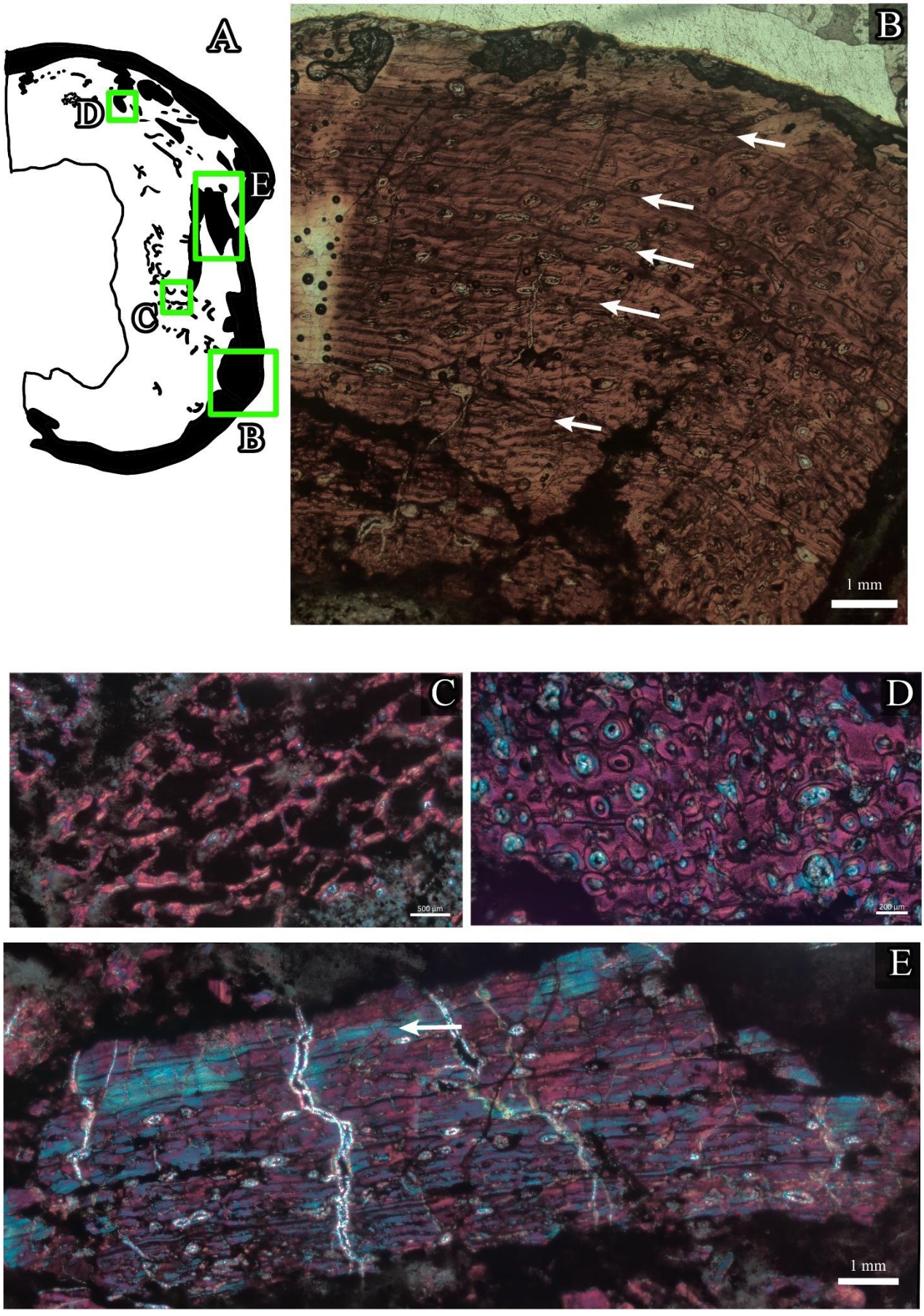
A
D
E
C
B
B
1 mm
C
500 µm
D
200 µm
E
1 mm

Figure 3.4.4.1: Histological section of the lateral half of the Lessamsauridae indet. fibula. A) Schematic of the preserved bone tissue of the thin section. The black area indicates the preserved part of the bone wall. Green boxes show the location of the higher magnification photographs. B) Composite micrograph of the anterior end of the fibula. Osteocytes are poorly preserved and bone texture resembles a fibrolamellar-parallel-fibred complex. White arrows indicate the growth marks. C) Lower magnification photograph of cancellous bone near the medullary cavity. D) Close up view of dense Haversian bone in the middle cortex. E) Composite micrograph of the fragmented portion of the compacta showing some birefringence in the parallel-fibred and fibrolamellar bone tissue.

3.4.4.2 Medial fibula section GD2

Section GD2 presents the histology of the medial half of the fibula. The bone wall is not well preserved but the histology of the mid and outer cortex can be discerned (Fig. 3.4.4.2A). The section presents with a transition from cancellous bone to parallel-fibred bone (Fig. 3.4.4.2B). Since the bone is poorly preserved, only three LAGs are visible, but cannot be followed due to the intensive fragmentation of the compacta.

The inner cortex consists of secondarily reconstructed and well vascularised fibrolamellar bone tissue. Fully formed secondary osteons can be observed within the inner cortex in addition to the numerous erosion cavities (Fig. 3.4.4.2C) which gives the section an overall cancellous texture. Intrinsic fibres within the inner cortex show a moderate degree of arrangement as the fibrolamellar bone is haphazardly deposited.

The mid-cortex comprises of predominantly well vascularised fibrolamellar and parallel-fibred bone tissue (Fig. 3.4.4.2D) but there are also portions of secondary reconstruction present. Vascular canal arrangement is laminar throughout as circumferential and longitudinal vascular canals dominate the mid cortex. Moderate secondary construction is observed as secondary osteons and resorptive canals are present but most secondary osteons are still being infilled. Growth marks throughout are poorly preserved due to the fragmentation and overall poor tissue quality, but one is visible (Fig. 3.4.4.2E)

The outer cortex consists of predominantly fragmented parallel-fibred and fibrolamellar bone tissue. Lamellar bone tissue is also visible in the vicinity of LAGs. The preserved portions of the periphery show vascular canals to be a laminar arrangement. The arrangement of intrinsic fibres tends to be of a moderate degree of arrangement with some birefringence. There are a few small secondary osteons and resorptive cavities are present. Disjointed patches of dense haversian bone are visible in outer cortex but cannot be reliably placed due to fragmentation. One growth mark can be seen in outer cortex (Fig. 3.4.4.2B).

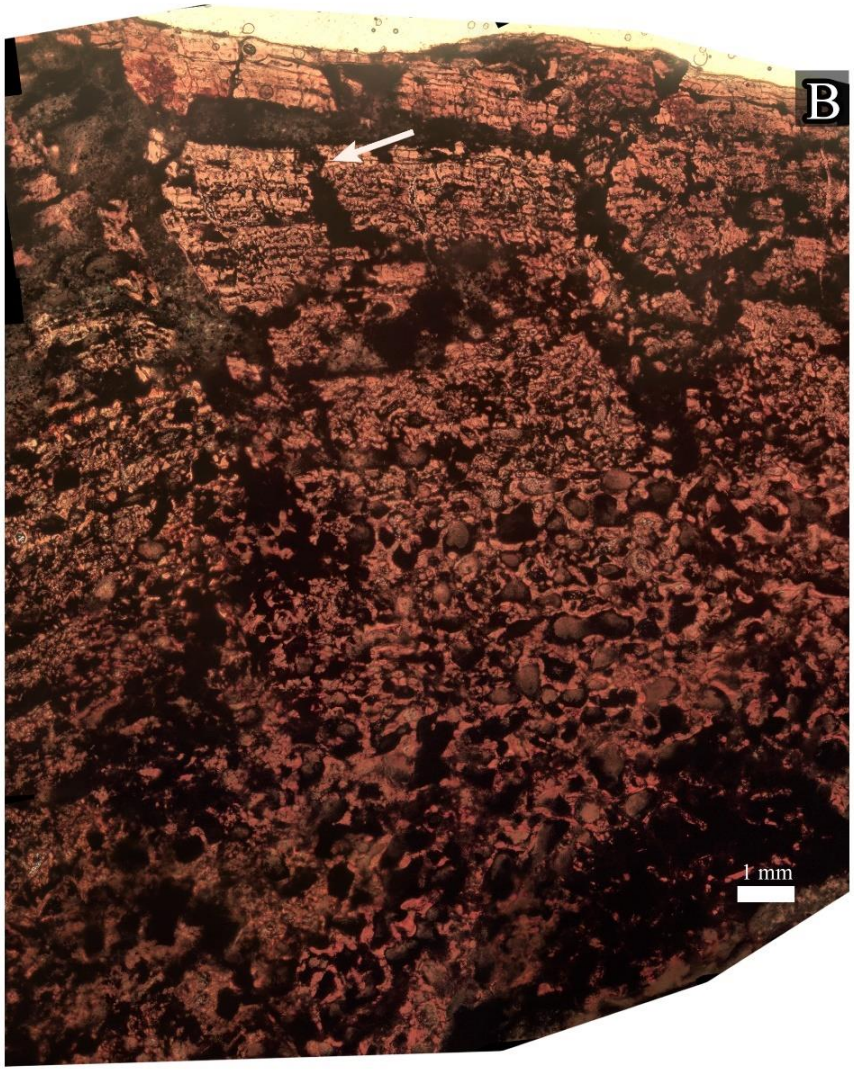
B
1 mm

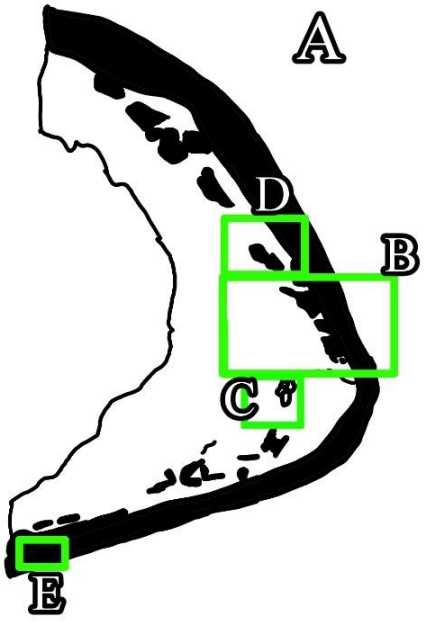
A
D
B
C
E

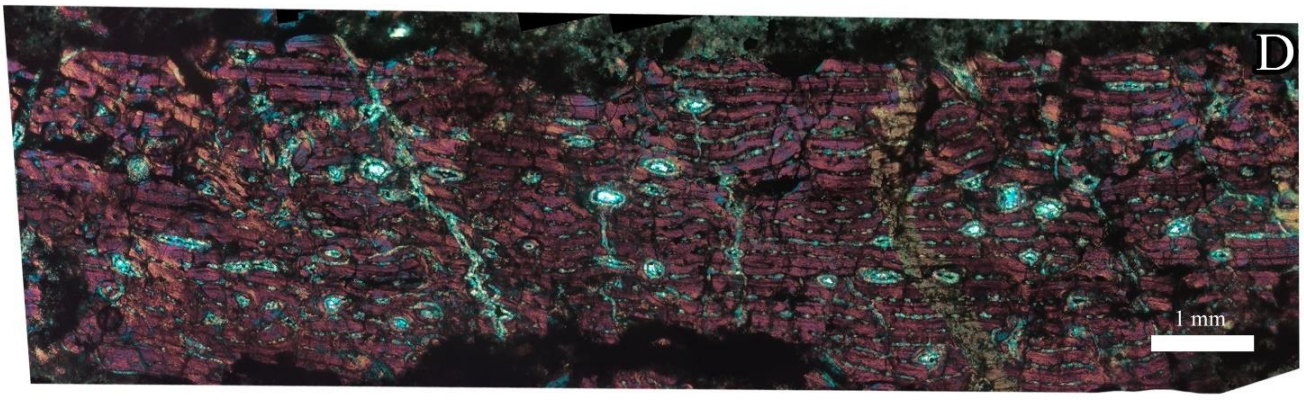
D
1 mm

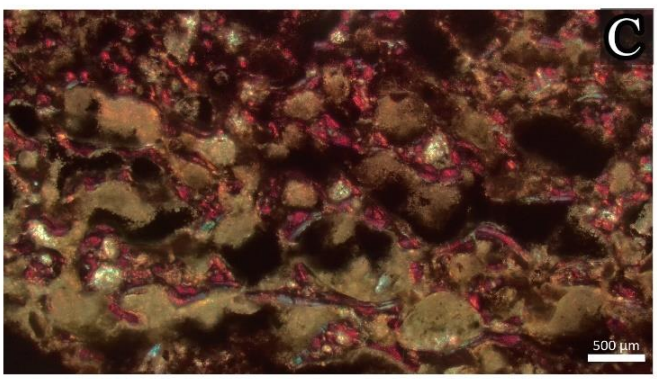
C
500 µm

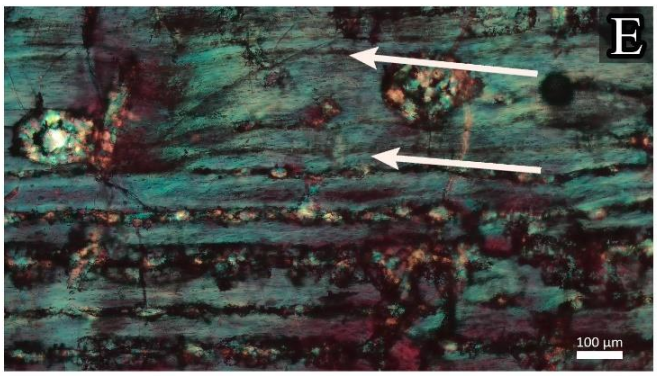
E
100 µm

Figure 3.4.4.2: Histological section of the medial half of the Lessemsauridae indet. fibula. A) Schematic of the preserved bone tissue of the thin section. The black area indicates the preserved part of the bone wall. Green boxes show the location of the higher magnification photographs. B) Composite micrograph of the anterior end of the fibula. White arrows indicate the growth marks. Note the overall poor preservation of the compacta. C) Low magnification view of the cancellous bone which surrounds the medullary cavity. D) Composite micrograph of the fragmented portion of the compacta showing numerous small resorptive cavities in the parallel-fibred fibrolamellar complex. E) High magnification view of laminar parallel-fibred bone and two possible growth marks (white arrows).

Chapter 4 Discussion

The changes in the growth dynamics in the transition from basal Sauropodomorpha to Sauropodiformes to derived Sauropoda are significant. These changes directly relate to the shifts in the rate of growth which impacts on the body sizes that these dinosaurs were able to attain. The development of their growth dynamics is evident in the microstructure of their bones i.e., their osteohistology. Early studies into the osteohistology of Sauropodomorpha showed stark differences in growth patterns and the subsequent variation in body sizes of the basal Sauropodomorpha and derived Sauropoda. The initial hypotheses into how sauropodomorph dinosaurs grew (Sander *et al*., 2004;2011) were based on smaller sample sizes of histological material and was compared to the more extensive studies of the Sauropoda. These studies suggested a dichotomy in growth dynamics between basal and derived Sauropodomorpha (Sander *et al*., 2004; Sander *et al*., 2011; Sander, 2013). These earlier studies into the palaeohistology of sauropodomorph dinosaurs suggested that non-sauropod Sauropodomorpha, i.e., basal Sauropodomorpha and Sauropodiformes, generally underwent zonal growth throughout their ontogeny (Sander *et al*., 2004; 2007; 2011). Well studied basal Sauropodomorpha such as *Massospondylus* (Chinsamy 1993; 1994; Cerda *et al*., 2017; Chapelle *et al*., 2021;2022) and *Plateosaurus* (Sander & Klein; 2005; 2008) primarily show zonal growth strategies. However, more recent studies that have examined a wider range of transitionary Sauripodiformes and basal Sauropoda show significant variation in terms of growth dynamics. Primarily *Mussaurus* presents with multiple different types of growth strategies including the so called 'typical' basal sauropodomorph zonal growth as well as the 'typical' sauropod azonal growth (Cerda *et al*., 2017; 2022). *Aardonyx* and *Sefapanosaurus* both show a mix of zonal and azonal growth with growth marks in late ontogeny and varying rates of bone growth (Yates *et al*., 2010; *Botha et al*., 2022). Similarly, *Ingentia* shows growth marks throughout its cortex but exhibits rapid growth through the deposition of fibrolamellar bone throughout its ontogeny (Apaldetti *et al*., 2018). Numerous other Sauropodomorpha examined by Cerda and colleagues (2017) also add an abundance of vital information into how these dinosaurs grew and clearly shows the variation in growth dynamics of the Sauropodomorpha clade. These key studies among others give evidence to suggest that there is no dichotomy in the growth of sauropodomorph dinosaurs. The variation in growth rates and dynamics of basal Sauropodomorpha and Sauropodiformes are better known today since recent studies have expanded the

number of taxa evaluated (Cerda *et al*., 2017; Krupandan *et al*., 2018; Apaldetti *et al*., 2018; Chapelle *et al*., 2021; de Cerff *et al*., 2021; Botha *et al*., 2022; Cerda *et al*., 2022).

The current study investigates the osteohistology and growth dynamics of four Sauropodomorpha: *Plateosauravus cullingworthi*, an indeterminate Sauropodiforme, *Melanorosaurus readi* and an indeterminate Lessemsaurid. This research into the osteohistology of one basal sauropodomorph dinosaur and three sauropodiform dinosaurs greatly improves our understanding of sauropodomorph growth dynamics. Firstly, through an analysis of *Plateosauravus,* I provide new information about the growth of the basal Sauropodomorpha. Secondly, through the assessment of the osteohistology of *Melanorosaurus*, Sauropodiforme indet. and Lessemsauridae indet., I contribute to our understanding of the growth dynamics evident among the more derived, Sauropodiformes clade.

4.1 Intraskeletal variation and general histology of each of the taxa studied

4.1.1 *Plateosauravus*

Plateosauravus was represented by a rib and two femora, one of which was partial distal end of a femur. The deposition of fibrolamellar bone tissue during the early and mid-ontogeny suggest rapid yet interrupted growth during the early stages of growth. However, during late ontogeny, parallel-fibred bone was deposited and is associated with a moderate rate of deposition which is expected in late ontogeny (Chinsamy-Turan. 2005; Cerda *et al*., 2017; Chinsamy, 2023). The shift towards parallel-fibred bone suggest that *Plateosauravus* had passed its stage of rapid growth and was close to skeletal maturity as growth marks are more closely associated in the bone periphery (Chinsamy-Turan, 2005; Cerda *et al*., 2022). It should be noted that growth marks are not abrupt but consist of small depositions of lamellar bone (which form an annulus) as well as a LAG (Reid, 1990; Chinsamy-Turan, 2005). After the deposition of the annuli, the rapid growth resumes via the deposition of well vascularised fibrolamellar bone tissue.

Growth marks are present throughout the compacta signifying interrupted growth throughout ontogeny. The zonal growth observed is a ‘typical basal’ sauropodomorph trait which is shared by several other sauropodomorph dinosaurs such as *Massospondylus* (Chinsamy, 1993;1994; Cerda *et al*., 2017; Chapelle *et al*., 2021), *Plateosaurus* (Klein & Sander 2007), *Ngwevu* (Chapelle *et al*., 2019), *Leyersaurus* (Cerda *et al*.,

2017) and *Leonerasaurus* (Pol *et al*., 2011; Cerda *et al*., 2017). *Plateosauravus* shows very similar growth dynamics to that of *Ingentia* (Apaldetti *et al*., 2018; 2022) which presents with fibrolamellar dominated zonal growth. Alternating bands of reticular-plexiform and circumferential vascular canal arrangements in fibrolamellar tissue is observed in *Plateosauravus.* This type of zonal bone is similar to the alternating fibrolamellar bands of tissue seen in the polar hadrosaurids *Edmontosaurus* which were considered to be a consequence of seasonal environmental pressures (Chinsamy *et al*., 2012). *Plateosauravus* did not live in the arctic but the alternation of vascular arrangements in the fibrolamellar bone suggests high rates of growth with just subtle changes in organisation of the vascularisation which may be related to some environmental pressures such drought or food unavailability. Similar alternating vascular arrangements are present in *Antetonitrus* (Krupandan *et al*., 2018) and other lessemsaurids (Cerda *et al*., 2017; McPhee *et al*., 2018) which suggest that the trait is less coupled to phylogenetic placement and is likely more related to environmental conditions.

The rib preserves eight growth marks and its bone tissue agrees with the overall slowing down of growth seen in the outer cortex of the two femora. These findings, in addition to the lack of an OCL, suggest that the overall growth of this individual was slowing down, but has not yet reached skeletal maturity. The fewer LAGs observed in the femora when compared to the rib directly indicates that the earlier growth marks may have been removed due to endosteal remodelling.

Furthermore, these findings suggest that in terms of age assessment, the rib is a better element to utilise in *Plateosauravus* as the rib preserved growth marks more reliably than the femora. This agrees with findings of other researchers in terms of rib histology (Erickson *et al*., 2007; Waskow & Sander, 2014; Waskow & Mateus, 2017). Aside from the growth dynamics, histology of the femora provides more information pertaining to the biology of this dinosaur.

Secondary reconstruction

The two femora show considerable amounts of secondary reconstruction primarily in the inner regions of the cortex. Considering the femora bears most of the weight during locomotion and it is likely that they would suffer more microdamage which leads to resorption of bone tissue (McFarlin *et al*., 2016). However, the rib is not involved in weight bearing and yet almost the entire compacta underwent secondary reconstruction and

led to the development of dense Haversian tissue. Similar observations have been made in other sauropodomorph dinosaurs (Cerda *et al*., 2017; Ibiricu *et al*., 2017; Lambertz *et al*., 2018). Nevertheless, despite intensive secondary reconstruction in the rib, the preservation of growth marks is barely impacted making it ideal for skeletochronology.

4.1.2 Sauropodiforme indet.

The well-preserved tibia that was studied shows the complete histological record of growth. This contrasts with the poor preservation evident in the highly fragmented fibula. Despite these differences, it is evident that the tibia and fibula have rather similar bone histology, although they vary slightly in terms of the extent of the development of secondary remodelling.

The abundance of fibrolamellar tissue in the compacta would suggest this sauropodiform dinosaur had experienced rapid early growth (Chinsamy-Turan 2005; Erickson 2007) and had sustained this rapid growth for much of its life. It is apparent that the animal experienced a decrease in growth rate during later stages of ontogeny as parallel-fibred tissue is evident in the outer parts of the compacta. The tibial histology shows very sauropod-like growth dynamics as most of the growth is uninterrupted in addition to either rapid or moderate rate of bone deposition. The fragmented fibula shows similar growth patterns as the compacta is primarily fibrolamellar bone tissue with parallel-fibred bone late into the ontogeny and in both elements growth marks only form late in ontogeny. The dominance of fibrolamellar bone tissue and delayed deposition of LAGs is similar to *Antetonitrus* (Krupandan *et al*., 2018) and *Mussaurus* (Cerda *et al*., 2022; Chinsamy, 2023).

Secondary reconstruction

Secondary reconstruction has numerous causes such as the repair of microcracks caused by biomechanical stress (Enlow, 1962b; McFarlin *et al*., 2016; Chinsamy *et al*., 2021) or for the phosphocalcic metabolism (Chinsamy, 1994; Cubo & Huttenlocker, 2020). In terms of weight bearing, both are elements of the lower hindlimb and would have probably experienced similar biomechanical stressors (Montoya-Sanhueza & Chinsamy, 2018). The associated secondary reconstruction for muscle attachment would change over time as this animal get older and larger (McFarlin *et al*., 2016). However, this specimen was relatively young shown by the three to four LAGs in the compacta. Generally older individuals tend to show more reconstruction and

thus it is unexpected to find highly reconstructed tissue in a young individual (Klein & Sander, 2008). The moderate amount of secondary reconstruction is likely a combination of resorption for the repair of damage caused by biomechanical stressors and for the phosphocalcic metabolism.

4.1.3 *Melanorosaurus*

The histology of multiple sections of the femur and tibia of *Melanorosaurus* all present with similar bone tissue types and growth dynamics. Both elements show rapid deposition of fibrolamellar bone tissue during early stages of ontogeny, which is shared trait among the Sauropodomorpha clade (Table 2), which later transitions to a more moderate rate of deposition leading to parallel-fibred tissue in late ontogeny. The growth during early and mid-stages of ontogeny in *Melanorosaurus* primarily comprised of azonal growth and only much later is the deposition of growth marks in the outer cortex (Chinsamy-Turan, 2005; Cerda *et al*., 2017; Krupandan *et al*., 2018). The rapid growth followed by a slight decrease in growth is like that of other basal Sauropodiformes primarily, some specimens of *Mussaurus* (Cerda *et al*., 2017; Cerda *et al*., 2022), *Aardonyx* (Yates *et al*., 2010) and *Sefapanosaurus* (Botha *et al*., 2022). However, *Aardonyx* and *Sefapanosaurus* both show rapid growth in conjunction with zonal growth. The late deposition of LAGs is associated with the derived Sauropoda (Sander, Christian, *et al*., 2011; Cerda *et al*., 2017; González *et al*., 2020). *Melanorosaurus* is suggested to be the immediate outgroup to the Sauropoda (Fig. 1) but does not show the sustained rapid growth like other more derived sauropodiforms such as *Patagosaurus* or *Volkheimeria* (Cerda *et al*., 2017) which resemble the ‘typical’ sauropod-like growth. Instead, *Melanorosaurus* shows more moderate growth during the mid- and late stages of ontogeny via the deposition of parallel-fibred tissue which is like many basal Sauropodomorpha (Table 2).

In *Melanorosaurus*, the growths marks of both the femur and tibia occur only within the outer third of the cortex and indicates that it grew uninterruptedly throughout most of its ontogeny which resembles the growth pattern of derived Sauropoda (Rogers *et al*., 2005; Cerda *et al*., 2017; Gonzalez *et al*., 2020). The number of growth marks observed are variable since there is diagenesis and secondary reconstruction but most of the sections show six or seven LAGs. The rate of growth during the azonal growth period does vary as the abundance of fibrolamellar tissue decreases later into ontogeny when parallel-fibred bone becomes more

common. It is expected that the termination of characteristic early rapid bone growth (indicated by fibrolamellar bone tissue) and that the onset of growth marks likely indicate sexual maturity (Sander, 2000; Erickson *et al*., 2007; Griebeler, Klein & Sander, 2013). In *Melanorosaurus*, there are no LAGs located within the inner cortex thus the late deposition of the LAGs suggests that sexual maturity was obtained much later in its ontogeny. In terms of skeletal maturity, there is a notable accumulation of LAGs towards the bone periphery but there is no observable OCL suggesting that this individual was still growly albeit slowly and that OCL would likely have formed soon.

Secondary reconstruction

Secondary remodelling was far more abundant in the femur than in the tibia. *Melanorosaurus* is suggested to have been either fully quadrupedal or an obligate quadruped and thus would spend a significant portion of its time on all four limbs. This would suggest that the *Melanorosaurus* femur would have likely experienced more biomechanical stress than the tibia which in turn would require secondary reconstruction for recruitment of bone tissue for repairing fatigued bone (McPhee *et al*., 2014). The femur having more secondary reconstruction than other long bones has been consistently observed in all *Mussaurus* specimens with secondary reconstruction also present (Cerda *et al*., 2022). It is likely that *Melanorosaurus* and *Mussaurus* employed similar locomotory methods. In *Melanorosaurus*, there were closely associated patches of secondary osteons but no dense Haversian bone was observed even though growth was slowing down.

Radial fibrolamellar bone

The most significant difference between the histology of the femur and the tibia of *Melanorosaurus* is the development of radially oriented fibrolamellar bone tissue in the peripheral region of the femora. Most of the outer bone tissue of the femur comprised of parallel-fibred bone tissue, but the most recently formed tissue was distinct from the surrounding as it consisted of radial fibrolamellar bone. The radial spiculate, sunburst pattern or hair-on-end fibrolamellar tissue has been identified as a pathology in modern relatives of dinosaurs (Lehrer *et al*., 1970; Lorigan *et al*., 1989; Chinsamy & Tumarkin-Deratzian, 2009). The resemblance of the abnormal bone tissue in *Melanorosaurus*, and the radial fibrolamellar pathology seen in other dinosaurs (Chinsamy & Tumarkin-Deratzian, 2009; Jentgen-Ceschino *et al*., 2020) strongly suggests that this tissue is

pathological in *Melanorosaurus* as well. The pathological tissue tends to be localised in only part of the femoral thin sections. Similar distribution of pathological bone tissue has been observed in other Sauropodomorpha (Krupandan *et al*., 2018; Jentgen-Ceschino *et al*., 2020; de Cerff *et al*., 2021) The actual cause of the pathology in the femur of *Melanorosaurus* is uncertain but could have been the result of infection or disease. De Cerff and colleagues (2021) found a similar pathology in a basal sauropodomorph dinosaur from the EF of South Africa and concluded that it was likely due to infection of an injury which may be the case for this *Melanorosaurus* specimen. In the more distally located sections, two instances of the pathology are present which would suggest an initial infection then recovery (indicated by the normal bone tissue) but then followed by a subsequent reinfection later in ontogeny.

4.1.4 Lessemsauridae indet.

The Lessemsauridae indet, specimen is represented by a large femur, a tibia, a fibula, and a caudal vertebra. The long bones are relatively homogenous in their histology with slight differences, but as expected the caudal vertebra had a rather distinctive histology from the long bones.

Among all the long bones, the early stages of bone deposition are characterised by the uninterrupted deposition of fibrolamellar bone tissue. These rapid rates of bones deposition continue throughout most of the compacta but becomes interrupted by deposits of growth marks during late ontogeny. Such rapid rates of early growth to mid-ontogeny observed in Lessemsauridae indet., is shared by both the other sauropodiforms in this study, as well as numerous other derived Sauropodomorpha such as *Antetonitrus*, *Ingentia*, *Lessemsaurus* and *Volkheimeria*. Growth does slow down in areas of the mid and outer cortex leading to the deposition of growth marks surrounded by lamellar tissue in turn forming an annulus. These annuli containing a LAG is seen both Sauropodiforme indet. and *Plateosauravus* but is absent in *Melanorosaurus*.

The number of growth marks visible in the compacta is somewhat variable among the long bones. The femora had at most ten LAGs starting from approximately halfway into the compacta, the tibia had about seven, whereas the fragmented compactum of the fibula only had four. The late deposition of growth marks shows that this lessemsaurid underwent a large amount of uninterrupted growth prior to the deposition of its first LAG. It may be that this LAG also marked the onset of sexual maturity (Sander, 2000; Erickson *et al*., 2007;

Griebeler *et al*., 2013). The delayed deposition of the growth marks and primarily azonal growth are traits commonly observed in the osteohistology of Sauropoda (Sander *et al*., 2011; Cerda *et al*., 2017; Gonzalez *et al*., 2020). However, the overall characteristics of the osteohistology of the lessemsaurid studied here is more like sauropodiform dinosaurs, such as *Antetonitrus* (Krupandan *et al*., 2018) and some *Mussaurus* specimens (Cerda *et al*., 2022). During times of slowed growth, thin bands of lamellar tissue are deposited and suggest that the animal might have experienced some environmental pressure (such as temperature, nutrient availability etc.) (Chinsamy, 1990; Horner *et al*., 2009; Chinsamy, 2023). Once the unfavourable period is over, the deposition of fibrolamellar tissue resumes. The distance between growth marks is clearly decreasing towards the bone periphery suggesting that growth is slowing down, and that skeletal maturity is approaching. The caudal vertebrae, like the rib of *Melanorosaurus*, does not preserve significant features related to growth dynamics of the Lessemsauridae indet.. Most of the cortex is cancellous due to numerous resorptive cavities and trabeculae. It is noteworthy that the spinous process does not resemble the histology of the supraspinous or supraspinous rod observed on some Sauropoda which both consist of highly reconstructed bone tissue (Cerda *et al*., 2015; Cerda *et al*., 2022).

Secondary reconstruction

Secondary reconstruction is common among all the elements studied of this lessemsaurid. The amount of reconstruction within the outer half of these elements are minimal as most secondary bone is found in the inner third. Portions of Haversian bone are in the inner cortex of the tibia and fully developed dense Haversian bone is seen in fibula inner cortex. As this Lessemsauridae indet. is from a sample of two dinosaurs, it is likely that the fibula was not the same individual as the tibia and femur when comparing the bone growth as well as the texture of preserved tissue. Significant portions of dense Haversian bone are present in addition to poorly vascularised parallel bone in the outer cortex of the fibula, both of which are absent in the other elements. The absence of the distinct Haversian bone in the primary elements of muscles attachment suggests that this could separate the two individuals. Coupled with the numerous LAGs present, the femur and tibia likely belonged to the older individual with the fibula belonged to the supposed younger individual. The age of this individual in conjunction with the size suggests that most of the secondary reconstruction would be attributed to

biomechanical stress over long periods of time (McFarlin *et al*., 2016). The intensive secondary reconstruction in the tibia when compared to femur is unexpected as the femur usually undergoes more biomechanical stress and muscle attachment throughout life (Mcphee *et al*., 2014; McFarlin *et al*., 2016). The intensive secondary reconstruction could be attributed to the need for calcium for the phosphocalcic metabolism or other life history events such as egg laying (Chinsamy, 1994; Montoya-Sanhueza & Chinsamy, 2018; Cubo & Huttenlocker, 2020)

4.2 Interskeletal variation

The most common and distinguishable shared characteristics of our sampled sauropodomorph dinosaurs is the presence and abundance of fibrolamellar bone tissue in early ontogeny as well as the continued deposition of fibrolamellar tissue later in their ontogeny. Although, secondary reconstruction often remodels much of inner cortex, it is still evident that the primary tissue was fibrolamellar bone. The deposition of fibrolamellar bone is common throughout basal Sauropodomorpha, and Sauropodiformes and basal Sauropoda in general (Table 2; Sander *et al*., 2011; Cerda *et al*., 2017). The addition of four more sauropodomorph dinosaurs with these characteristics supports the hypothesis that fibrolamellar bone and rapid early growth are key traits in the eventual evolution of gigantism. In all four dinosaurs studied, there are varying amounts of fibrolamellar bone deposited during the mid and later parts of their ontogeny, but generally the more derived taxa show more fibrolamellar bone tissue throughout their respective compacta. In our study, *Plateosauravus* shows a decrease in abundance of fibrolamellar tissue in the late stages of its ontogeny whereas Lessemsauridae indet. shows abundant fibrolamellar bone in late stages of its ontogeny. Lessemsauridae indet. and *Melanorosaurus* both show the most fibrolamellar tissue and they had the largest femora studied here, suggesting that they needed to grow to reach large body sizes. The increase in the relative abundance of fibrolamellar bone tissue in the more derived taxa is predictable since sauropods effectively deposit fibrolamellar bone until the very late stages in their ontogeny (when growth marks occur and lamellar tissue is deposited) (Curry Rogers & Kulik, in press; Sander & Clauss, 2008; Cerda *et al*., 2017; González *et al*., 2020).

Cerda and colleagues (2017) present a comprehensive overview of twelve taxa of Sauropodomorpha. Eight of the twelve taxa show majority deposition of parallel-fibred bone in their cortices but compared to the

Sauropodomorpha in this study, fibrolamellar tissue starts becoming more abundant in the outgroups to Sauropoda. Parallel-fibred tissue is observed in the sampled dinosaurs of this study, but it is not abundant and usually occurs in the outermost regions of the cortices as growth starts to slow down.

Lamellar bone is uncommon in our sampled sauropodomorphs except for thin bands of lamellar tissue (forming an annulus), often associated with a LAG observed, in the Lessemsauridae specimen and *Plateosauravus*. These alternating periods of fast and slow depositional cycles is seen in both the most basal and derived taxon of this study. These findings suggest cyclical events (likely seasonal changes) that affect their growth dynamics (Horner *et al*., 2000; Chinsamy *et al*., 2012). While the Sauropodiforme indet. growth marks were poorly preserved, *Melanorosaurus* clearly shows LAGS without any associated lamellar tissue suggesting that there was an abrupt stop in growth unlike the other dinosaurs where growth had slowed down (as indicated by the lamellar bone deposits) prior to an arrest in growth. It is noteworthy that besides these thin bands, lamellar bone is not regularly observed as parallel-fibred is the late ontogenetic bone tissue in the four dinosaurs sampled.

Ontogenetic status

The OCL in all four taxa is not present as bone appears to still be deposited subperiosteally. *Plateosauravus*, *Melanorosaurus* and Lessemsauridae indet. show closely spaced LAGs in the outer cortices of their bones. This would suggest that these dinosaurs were nearing skeletal maturity, but growth had not stopped yet (Enlow, 1962a; Chinsamy-Turan, 2005; Cerda *et al*., 2022; Chinsamy 2023). The poor preservation of Sauropodiforme indet. makes it difficult to determine how close it was to forming an OCL but from the few growth marks that are evident, it is likely that it was a younger individual when compared to the other three dinosaurs studied.

The inner circumferential layer was not observed in these dinosaurs studied, (Enlow, 1962a; Chinsamy-Turan, 2005) since cancellous bone is consistently found in the perimedullary regions of all long bones sampled. In the Sauropodiforme indet. femur, there is a small band of lamellar bone surrounding the medullary, which resembles the bone texture of an ICL but cancellous textured bone is evident in the other perimedullary regions of the Sauropodiforme indet. femur.

Klein and Sander (2008) proposed the concept of histological ontogenic stages (HOS) to better compare life histories of Sauropoda. In our study the ontogenetic stages using the HOS method would range from HOS-10 to HOS-12. HOS-10 consists of primarily fibrolamellar tissue in primary cortex with the inner cortex consisting of a few secondary osteons as well as a few secondary osteons in the outer cortex. HOS-10 describes the histological stage of *Plateosauravus* which is a young individual with not many LAGs visible and most of the reconstruction occurring in the innermost cortex. The cortex of Sauropodiforme indet. resembles either HOS-10 in the lesser reconstructed portions or HOS-11 where secondary reconstruction becomes more prevalent. The number of LAGs does not suggest such a late HOS but the poor preservation prevents a full account of all LAGs in Sauropodiforme indet. The two larger body size specimens, Lessemsauridae indet. and *Melanorosaurus*, are HOS-12 due to the prevalence of fibrolamellar tissue, considerable secondary reconstruction of inner cortex as well as the lamellar deposits forming annuli containing LAGs. The only feature preventing the classification of HOS-13 is the lack of the OCL. When comparing the ages of our dinosaurs using HOS classification system, it was accurate in determining that Lessemsauridae indet. and *Melanorosaurus* are older individuals but suggested an earlier ontogenetic stage for *Plateosauravus* which had the same number of LAGs as *Melanorosaurus*. As the HOS concept was based on neosauropod dinosaurs, it is not unexpected that it might be less accurate for basal taxa. However, when taking growth marks into account the HOS classification was more accurate for taxa more closely related to the Sauropoda.

Growth mark variation

The most significant difference between the growth dynamics of basal Sauropodomorpha and derived Sauropodiformes is the number and location of the growth marks and the subsequent uninterrupted growth (Cerda *et al*. 2017). The growth marks in *Plateosauravus* are visible in the inner regions of the compactum and was the earliest out of our four dinosaurs. The cortex of Sauropodiforme indet. showed growth marks in the later portions of the mid cortex. *Melanorosaurus* had the latest deposition of growth marks throughout its ontogeny with all of them visible in the outermost region of the compacta. Lessemsauridae indet, the most derived taxon, did not have the latest deposition of growth marks as they are visible in the late-mid stage of

ontogeny. The variation in growth marks of the basal sauropodiforms in this study suggest that azonal growth was becoming increasingly more prevalent in the evolution towards the more derived Sauropoda. It is evident that there is considerably more uninterrupted growth deposited prior to the deposition of the first growth mark in the derived taxa. These features are similar to that observed in other basal Sauropodiformes such as, *Mussaurus* (Cerda *et al*., 2014; 2022), *Sefapanosaurus* (Botha *et al*., 2022), and *Aardonyx* (Yates *et al*., 2010; Botha *et al*., 2022) as well as lessemsaurids like *Antetonitrus* (Krupandan *et al*., 2018) and *Ledumahadi*, (McPhee *et al*., 2014) which all show substantial azonal growth prior to the development of zonal growth in their mid to late ontogenetic stages. However, it should be noted that some more derived Sauropodomorpha, such as some specimens of *Mussaurus*, *Patagosaurus* (Cerda *et al*., 2017), *Lessemsaurus* (Cerda *et al*., 2017; Cerda *et al*., 2022) and *Ingentia*, (Apaldetti *et al*., 2018) underwent zonal growth throughout their ontogeny. The two larger taxa, *Melanorosaurus* and Lessemsauridae indet. both show a decrease in distance between LAGs in the bone periphery and were likely much closer to skeletal maturity than *Plateosauravus* and Sauropodiforme indet..

This trait of relatively late deposition of growth marks (i.e., azonal growth during most of ontogeny) of our derived taxa, Sauropodiforme indet, *Melanorosaurus* and Lessemsauridae indet., studied here, agrees with observations made of other Sauropodiformes (Table 2; Krupandan *et al*., 2018; Cerda *et al*., 2017; 2022). The subsequent zonal growth as observed in *Plateosauravus* is commonly reported among basal Sauropodomorpha (Chinsamy, 1993, 1994; Klein & Sander 2007; Cerda *et al*., 2017) however, the rapid deposition of fibrolamellar tissue is generally uncommon in basal taxa (Table 2; Cerda *et al.*, 2017). The amount of azonal growth in Sauropodiforme indet., *Melanorosaurus* and Lessemsauridae indet. was variable but not to an extreme extent.

The interskeletal histovariation between the taxa is attributable to the differences in their individual life histories (such as the variation in vascular arrangement, amount of secondary reconstruction, regional growth rate variation, annuli surrounding LAGs), but the most distinctive characteristic between the basal sauropodomorph and sauropodiform dinosaurs studied here, is in the location of LAGs within the long bone compacta, and the amount of azonal and zonal growth that occurs. The amount of azonal growth is a key

factor in the evolution of gigantism but not an excluding factor in reaching large body sizes (Cerda *et al*., 2017; Apaldetti *et al*., 2018). Like Cerda and colleagues (2017) concluded, there does seem to be crossover between the growth dynamics of basal Sauropodomorpha and Sauropodiformes but the increase in uninterrupted growth tends to be more common nearing the Sauropoda clade in addition to the increase in growth rates via deposition of fibrolamellar bone (Apaldetti *et al*., 2018; Krupandan *et al*., 2018; Botha *et al*., 2022; Cerda *et al*., 2022).

Secondary reconstruction

Secondary reconstruction is often related to microdamage caused by biomechanical stressors (McFarlin *et al*., 2016; Montoya-Sanhueza & Chinsamy, 2018) and the age of the animals as older animals tends to have underwent more secondary reconstruction (Klinkhamer *et al*., 2018; Montoya-Sanhueza & Chinsamy, 2018). Secondary reconstruction is also related to life history events such as pregnancy or periods of low calcium (Montoya-Sanhueza & Chinsamy, 2018). This is evident when comparing *Plateosauravus* and Sauropodiforme indet. as these dinosaurs are roughly the same size and age but the discrepancy in the amount of secondary reconstruction is apparent. *Plateosauravus* displays minimal secondary reconstruction even in the inner cortex, whereas there is considerably more secondary osteons in the tibial compact bone of the Sauropodiforme indet. and considerable portions of the compacta of the fragmented fibula reconstructed. Generally, the femur had either the similar or more reconstruction than other long bones and this has been observed in the closely related *Mussaurus* as well (McPhee *et al*., 2014; Klinkhamer *et al*., 2018; Cerda *et al*., 2022). However, the tibia and fibula of Sauropodiforme indet. have both undergone more remodelling than the femur of *Plateosauravus*. As these two dinosaurs are similar in age and size, we would expect similar amounts of secondary reconstruction, but Sauropodiforme indet. clearly shows more secondary reconstruction.

Lessemsauridae indet. shows intensive secondary reconstruction to the point where dense Haversian bone is common in portions of the femora and tibia. However, we do not see more secondary reconstruction in the femur than the tibia and fibula. Unlike basal taxa that were bipedal or facultative quadrupeds, lessemsaurids was fully quadrupedal (Pol & Powell, 2007) and the elements of the legs would all have to bear similar loads.

However, due to no significant difference in the amount of secondary reconstruction, the cause would likely be due to either general resorption through aging (Padian *et al*., 2016) or microdamage through biomechanical stress (Frost, 1994; McFarlin *et al*., 2016). The same trend was not observed in *Melanorosaurus* which was an obligate quadruped and showed more localised secondary reconstruction within the femur which is most likely associated with biomechanical stress caused by locomotion (Petermann & Sander, 2013; McFarlin *et al*., 2016). However, Lessemsauridae indet. does show more overall secondary reconstruction than the other three dinosaurs sampled.

The secondary reconstruction observed in our four dinosaurs are most likely associated with internal requirements of calcium via phosphocalcic metabolism and other processes (Chinsamy, 1994; Cubo & Huttenlocker, 2020) except for Lessemsauridae indet. which underwent intensive secondary reconstruction throughout its elements suggesting that there were numerous internal and external impacts on the bone tissue leading to the extensive secondary remodelling of its bones.

4.3 Growth dynamics of Sauropodomorph dinosaurs

Our understanding of sauropodomorph growth dynamics has greatly improved as more recent, comprehensive studies have been conducted on various members of the clade (Cerda *et al*., 2017; Apaldetti *et al*., 2018; 2021; Krupandan *et al*., 2018; de Cerff *et al*., 2021; Chapelle *et al*., 2021; Cerda *et al*., 2022; Botha *et al*., 2022). Prior to the research of Cerda *et al*., (2017), there was paradigm of a binary distinction of zonal versus azonal growth when comparing basal to derived Sauropodomorpha. However, today we see a greater variability in the growth dynamics of sauropodomorph dinosaurs.

In the current study, it is evident that the basal sauropodomorph, *Plateosauravus*, has a common cyclical pattern of growth of basal Sauropodomorpha. The two closest taxa to *Plateosauravus* which have undergone histological analysis are *Saturnalia* (Stein, 2011) and *Plateosaurus* ((Klein & Sander 2007) both of which experienced interrupted growth throughout ontogeny. *Plateosauravus* did not show the predominant parallel-fibred bone of many other basal Sauropodomorpha (Cerda *et al*., 2017). Unlike its closest analysed relatives, parallel-fibred bone in *Plateosauravus* only becomes visible late in ontogeny when the growth rate slows down. There are LAGs visible throughout the *Plateosauravus* compacta which are shared with most of the

basal Sauropodomorpha such as *Massospondylus, Plateosaurus, Riojasaurus* (Yates, 2003; Cerda *et al*., 2017) and *Saturnalia*. These traits are a mix of the basal zonal growth and derived rapid growth especially when compared to other Elliot Formation sauropodomorph dinosaurs (de Cerff *et al*., 2021; Botha *et al*., 2022). The combined features of fibrolamellar tissue and deposition of growth marks throughout ontogeny is uncommon in the basal taxa. *Plateosauravus* shares its primarily rapid growth rate with derived taxa such as Sauropodiforme indet., *Melanorosaurus* and Lessemsauridae indet. sampled in this study. The presence of the rapidly growing *Plateosauravus* support conclusions by Cerda *et al*., (2017) which suggest a mosaic of growth dynamics specifically in the basal clades of the Sauropodomorpha.

The Sauropodiforme indet. specimen studied has been suggested to be related to *Melanorosaurus* and its bone histology and inferred growth dynamics appears to resemble the derived sauropodomorphs such as *Antetonitrus* (Krupandan *et al*., 2018); *Volkheimeria* (Cerda *et al*., 2017); some specimens of *Mussaurus* (Cerda *et al*., 2022) as well as the *Melanorosaurus* studied here. Thus, although its taxonomic assessment is lacking, the similarities in growth suggest that it is likely phylogenetically close to *Melanorosaurus*. The Sauropodiforme indet. resembles the derived sauropodiform dinosaurs due to the abundance of fibrolamellar bone prior to the first growth mark deposition and the late onset of LAG deposition. These specific features of its growth are much like sauropod dinosaurs like *Isanosaurus* (Jentgen-Ceschino *et al*., 2020) and *Patagosaurus* (Cerda *et al*., 2017). The dominant bone type in the first half of the ontogeny is fibrolamellar bone followed by growth mark deposition and continued fibrolamellar bone until late ontogenetic parallel-fibred bone deposition. The lack of a definitive taxonomic assignment, it is difficult to compare to sister taxa but the addition of Sauropodiforme indet. supports that the evolution of sauropod-like growth was present prior to the evolution of Sauropoda.

Melanorosaurus as a sauropodiform dinosaur is closely related as the direct outgroup to the Sauropoda and should be a suitable representative taxon for the transition from basal to derived sauropodomorph (Fig. 1). The compacta consist of fibrolamellar bone prior to the transition to parallel-fibred bone in the late stages of ontogeny. LAGs are seen in both the fibrolamellar and parallel-fibred tissue but only in outer third. Similar in femur size to our Lessemsauridae indet., *Melanorosaurus* exhibited six to seven LAGs in the tibia and femur

and these generally occurred later in ontogeny than those of the indeterminate lessemsaurid. *Melanorosaurus* shows the most sauropod-like growth via its uninterrupted growth until the very late stage of ontogeny where LAGs are visible in the outer cortex (Curry Rogers & Kulik, in press; Sander, 2000; Sander & Clauss, 2008; González *et al*., 2020). *Melanorosaurus* clearly shows that sauropod growth and increasing body sizes (Apaldetti *et al*., 2018) was present before the evolution of the Sauropoda (Figure 14: Cerda *et al*., 2017). This trait of rapid and extended uninterrupted growth becomes more common in the basal Sauropodiformes and basal Sauropoda as it is observed in *Antetonitrus* and some specimens of *Mussaurus* before becoming the norm in the Sauropoda but not in *Sefapanosaurus* (Botha *et al*., 2022) and *Aardonyx* (Yates *et al*., 2010; Botha *et al*., 2022).

Of all four dinosaurs in our study, Lessemsauridae indet. had the largest sample of elements and they are largest elements in general. LAGs are visible throughout the later portions of the outer half of long bones. As observed in various osteohistological studies of Sauropodomorpha (Table 2), fibrolamellar bone is deposited during the early stages of ontogeny. The continued uninterrupted deposition of fibrolamellar tissue through most of ontogeny is like that of the derived Sauropoda (Sander, 2000; González *et al*., 2020). The entire compacta of Lessemsauridae indet. consists of almost entirely fibrolamellar bone except when the growth rate slows down during the deposition of thin bands of lamellar bone and the very late-stage deposition of parallel-fibred bone. The initial azonal growth, followed by the relatively late deposition of growth marks are common features of derived Sauropoda (Sander *et al*., 2011; Cerda *et al*., 2017) and is expected of such a derived sauropodomorph dinosaur that is closely related to basal sauropods (Fig. 1; Cerda *et al*., 2017; Krupandan, 2018). The presence of the annuli formed by thin bands of lamellar tissue is likely formed due to environmental pressures causing a slow growth prior to LAG deposition (see Section 4.1.4). The absence of these thin lamellar bands in many other derived Sauropodomorpha suggest more abrupt interruptions in growth. *Lessemsaurus* (Cerda *et al*., 2017) would be very closely related to Lessamsauridae indet. and does show similar growth in that it reached large body size without exclusive uninterrupted growth to late ontogeny. The zonal growth observed in the mid ontogenetic stages of Lessemsauridae indet. is different to the primarily zonal growth of *Lessemsaurus* but it clear that they both show mostly rapidly deposited fibrolamellar bone tissue throughout their cortices. Thus, it seems that Lessemsauridae indet. was able to

reach a large body size without exclusive uninterrupted growth. These findings agree with those from Cerda *et al*., (2017) in which *Lessemsaurus* was also able to reach large body size via zonal growth. The variation between these two dinosaurs could be like the variation in growth dynamics (i.e., similar growth rates but different periods of growth) and plasticity observed in *Mussaurus* (Cerda *et al*., 2022) but this observation might be premature until more definitive phylogenetic placement of Lessemsauridae indet. is done.

The growth dynamics of the basal sauropodomorph, *Plateosauravus*, was somewhat expected as LAGs are present throughout the bone wall and the deposition of LAGs were earlier than all the derived sauripodiformes in this study. The derived taxa, Sauropodiforme indet., *Melanorosaurus* and Lessemsauridae indet. all present different delays in the first LAG deposition. Additionally, these taxa all show considerable amount of fibrolamellar bone as rapid growth is common in early ontogeny to reach sexual maturity (Griebeler *et al*., 2013; Chinsamy, 2023) and this deposition of fibrolamellar bone continues into the mid and late stages of ontogeny. Sauropodiforme indet., *Melanorosaurus* and Lessemsauridae indet. deposit parallel-fibred bone during the very late stages of their respective ontogeny which tends to start after multiple LAGs have been deposited. The decrease of growth rates in very late ontogeny and subsequent shift in bone type are suggested to be traits of the derived Sauropoda and observed in sauropod dinosaurs like *Volkheimeria* (Cerda *et al*., 2017), *Isanosaurus* (Jentgen-Ceschino *et al*., 2020) and *Patagosaurus* (Cerda *et al*., 2017) but not *Lessemsaurus* (Cerda *et al*., 2017) which underwent zonal growth throughout ontogeny.

The growth dynamics of the Sauropodiformes clade, that span the transition to the true Sauropoda, becomes even more variable with the addition of the current work on Sauropodiforme indet., *Melanorosaurus* and Lessemsauridae indet.. Our sauropodiform dinosaurs sampled are closely related to sauripodiformes *Mussaurus* (Cerda *et al*., 2017; 2022), *Aardonyx* (Yates *et al*., 2010; Botha *et al*., 2022), *Leonerasaurus* (Cerda *et al*., 2017), *Antetonitrus* (Krupandan *et al*., 2018), *Sefapanosaurus* (Botha *et al*., 2022) but only share similarities with some *Mussaurus* specimens which showed sauropod-like growth and *Antetonitrus*. Zonal growth is observed in *Aardonyx, Leonerasaurus,* and *Sefapanosaurus* but these three sauropodiform dinosaurs also show compacta dominated by a moderate rate of deposition leading to mostly parallel-fibred bone but it is worth noting that Botha *et al*. (2022) suggested an intermediate growth rate through the deposition of a woven

parallel-fibred bone matrix in *Sefapanosaurus* and *Aardonyx*. This mixture of rapidly deposited woven bone and moderately deposited parallel-fibred bone would suggest increases from the typical parallel-fibred bone observed in basal Sauropodomorpha (Table 1). It was worth noting that while *Mussaurus* shares this growth in some specimens, Cerda and colleagues (2022) note that this sauropodiform showed traits of both derived and basal growth patterns.

The changes in growth dynamics from basal to derived Sauropodomorpha does not follow a straightforward progression from slow, zonal growth to fast, azonal growth. The dichotomy suggested by early researchers has been refuted by extensive studies (Cerda *et al*., 2017; 2022; Krupandan *et al*., 2018; Chapelle *et al*., 2021; 2022; de Cerff *et al*., 2022; Botha *et al*., 2022). The latter is supported by the rapid growth in all four of our sampled dinosaurs and delayed deposition of LAGs in our three sauropodiform dinosaurs. The general trends in the basal Sauropodomorpha clade show the majority growing zonally (Table 2) with differences in growth rate and in the Sauropodiformes clade, the prevalence of early azonal growth increases as well (Cerda *et al*., 2017; 2022; Krupandan *et al*., 2018). There are some exceptions seen in the derived taxa *Lessemsaurus* and *Ingentia* which showed fast yet zonal growth throughout the cortex but did not impact the large body size it was able to achieve. Similarly, this growth pattern in seen in the studied *Plateosauravus* which happens to be a basal sauropodomorph dinosaur. As phylogenetic clades, there are very general shifts in the deposition of growth marks moving from the entire cortex to primarily the later stages of ontogeny. *Melanorosaurus, Antetonitrus, Volkheimeria* and some *Mussaurus* specimens show the most sauropod-like growth via the deposition of uninterrupted fibrolamellar bone growth from early to late stages of ontogeny in conjunction with the deposition of LAGs exclusively in the outer portions of the cortex. The presence of the partially derived growth dynamics in the basal sauropodomorph taxa suggest that traits of sauropod-like growth had already started to evolve early on in Sauropodomorpha (Cerda *et al*., 2017). The variation in growth dynamics throughout the Sauropodomorpha suggest variable growth trajectories. All sauropodomorph dinosaurs grow fast early in life but the variation is clear as they grow older. Growth varies between rapid, fibrolamellar bone or moderate, parallel-fibred bone and the timing of growth interruptions varies between throughout the whole compacta, mid-ontogeny and onwards or late ontogeny.

The overall changes in the growth dynamics of Sauropodomorpha to Sauropodiformes to Sauropoda shows the variation and mosaic nature of zonal and azonal growth in the sauropodomorph clade (Fig. 1; Cerda *et al*., 2017). Generally, the rates of bone growth increase from mostly moderate (i.e., parallel-fibred bone) to rapid deposition (i.e., fibrolamellar bone) as the taxa become more derived but it evident that derived traits can be observed in basal taxa. With the addition of these four sauropodomorph dinosaurs, we see a clear increase in the abundance of rapid azonal growth in the derived Sauropodiformes compared to basal sauropodomorph dinosaurs. We also see another basal sauropodomorph, *Plateosauravus*, able to grow at rapid rates into late ontogeny. The evolution of rapid rates of growth and trajectories are key factors in the evolution of gigantism in the Sauropoda. However, among the Sauropodomorpha it is evident that giant sizes can be obtained even with zonal growth although azonal growth appears to dominate among the relatively larger Sauropodiformes as they come close to reaching the derived gravisauran Sauropoda.

Chapter 5 Conclusions

5.1. Outcomes of the current study

Here, I summarise the outcomes of the investigation into the osteohistology of one basal sauropodomorph, *Plateosauravus*, and three sauripodiformes, Sauropodiforme indet., *Melanorosaurus* and Lessemsauridae indet.. In addition, I discuss how these findings relate to the hypotheses formulated at the onset of this study.

5.1.1. Bone microstructure and variation between sauropodomorph and sauropodiform dinosaurs

Osteohistology of the basal *Plateosauravus* consisted of primarily fibrolamellar bone with varying vascular arrangements. Parallel-fibred bone is observed in the very late stages of ontogeny. Seven LAGs are visible throughout the cortex signifying zonal growth throughout ontogeny. The rib of *Plateosauravus* showed good preservation of growth marks even when the femur failed to preserve some of them suggesting that ribs could be a better choice for skeletochronology.

The bone microstructure of Sauropodiforme indet. consists of mostly fibrolamellar bone followed by parallel-fibred in late ontogeny. Fibrolamellar bone is extensively vascularised but there is a slight decrease in vascularisation of the parallel-fibred bone in the outer cortex. Four LAGs are seen in the outer half of the cortex showing a notable amount of rapid, uninterrupted growth.

Melanorosaurus osteohistology is the most similar to the derived Sauropoda. The amount of fibrolamellar bone tissue is extensive and growth marks are present only in the outermost portions of the compacta bordering the bone wall. Six or seven LAGs are visible towards the bone periphery and a shift towards parallel-fibred bone occurs in this region. Pathological bone in the form of radial fibrolamellar bone is present in the outermost part of the femur compacta but is absent in the tibia.

Lessemsauridae indet. shows similar rate of bone growth to *Melanorosaurus* but a slightly earlier deposition of LAGs occurs in the compacta. The late deposition of LAGs in conjunction with the more sustained deposition of fibrolamellar bone are common traits of the growth dynamics of Sauropoda. There were also thin bands of lamellar tissue forming annuli in the outer half of the compacta but these episodes of slow

growth do not appear to have significantly impacted the general rapid growth of the long bones. The histology of the spinous process was also analysed and was generally not informative to ascertain the growth dynamics of this dinosaur.

The histovariation between long bones of different taxa depended primarily on life history and phylogenetic placement (i.e., basal versus derived taxa). Long bones all showed the same transition from early and mid-ontogeny fibrolamellar bone towards a late-stage ontogenetic shift to parallel-fibred bone. Femoral sections had considerably more secondary reconstruction than tibia and fibula sections. The *Melanorosaurus* femora had a distinct radial fibrolamellar pathology and the Lessemsauridae indet. and *Plateosauravus* elements showed annuli consisting of thin lamellar bone and a LAG. The caudal vertebrae and rib were the only non-long bone elements analysed and show vastly different histology than the long bones. The rib of *Plateosauravus* consisted of primarily lamellar and cancellous textured bone tissue whereas the caudal vertebrae of Lessemsauridae indet. consisted of cancellous bone except for the outermost layer of lamellar bone tissue.

Our findings show that there were very similar growth patterns within each respective taxon and that variation in growth dynamics does not differ within a skeleton. The similarities in growth support **Hypothesis I which stated that the different elements within each taxon will display similar growth dynamics**. However, there is notable intra- and interskeletal variation when comparing the different sauropodomorph dinosaurs in our study. These differences are most evident when comparing the long bones to other bones of the skeleton such as the rib and caudal vertebrae. The deposition of bone is far slower and does not preserve the growth dynamics of the individuals. The findings of the growth patterns preserved in the long bones give strong support to **Hypothesis I.**

Hypothesis II stated there will be notable intraspecific and interspecific histological variation between elements. In this study, variation was seen in the location of LAGs within the compacta and small-scale variation in their respective histology. The main differences observed related to variations in growth dynamics in addition to the unusual alternating fibrolamellar vascular arrangements in *Plateosauravus*, the presence of the pathology of *Melanorosaurus*, the thin annuli containing LAGs in *Plateosauravus* and Lessemsauridae

indet,. Small-scale variation includes the differing vascular arrangement and abundance of vascular canals between taxa and the differing amount secondary reconstruction between taxa. These are all considerable differences which support **Hypothesis II.**

5.1.2. Basal sauropodomorph and transitionary sauropodiform growth dynamics

Sander and colleagues (2004; 2008; 2011) had proposed that basal Sauropodomorpha grew slowly through interrupted growth whilst Sauropoda grew rapidly through uninterrupted growth. This paradigm has been upturned in recent years (Cerda *et al*., 2017; Apaldetti *et al*., 2018; 2021; Krupandan *et al*., 2018; de Cerff *et al*., 2021; Chapelle *et al*., 2021; Cerda *et al*., 2022; Botha *et al*., 2022). The current study of a basal sauropodomorph dinosaur and three representatives of the Sauropodiformes clade, the transitionary group between the basal Sauropodomorpha and the more derived gravisaurian Sauropoda, strengthens the argument against the proposed dichotomy of growth dynamics between basal and derived Sauropodomorpha. The findings of this study demonstrates that there is much more variation in the growth dynamics of basal Sauropodomorpha and the Sauropodiformes than initially expected.

Hypothesis III stated that *Plateosauravus* will show the characteristic zonal growth dynamics previously observed in majority of basal sauropodomorph taxa. This study found that *Plateosauravus* exhibited rapid growth unlike most basal sauropodomorph dinosaurs but still showed zonal growth throughout the compacta. Thus, the expected similarities in zonal growth shared by basal sauropodomorphs such as *Massospondylus* and *Plateosaurus* were found to be true and supports **Hypothesis III.** However, it should be noted that the unexpected abundance of fibrolamellar bone in the compacta makes *Plateosauravus* different to other basal Sauropodomorpha.

Hypothesis IV stated that Sauropodiforme indet., *Melanorosaurus* and Lessemsauridae indet. will show the characteristic azonal to late zonal shift in growth dynamics as observed in other sauropodiform dinosaurs. This study found that the rapid rates of growth coupled with uninterrupted growth in the Sauropodiformes taxa studied were shared with other Sauropodiformes and the Sauropoda. Variation in the deposition of LAGs in mid and late stages of ontogeny were also observed and implied different growth trajectories. These findings support the validity of **Hypothesis IV.**

5.2. Limitations & Future research

Osteohistological studies are highly informative to decipher growth and various aspects of the biology of extinct taxa. However, osteohistology often involves destructive analysis and therefore sample sizes are limited (Chinsamy, 2023). In the current study, although the number of elements were limited, they provided a good assessment of the growth dynamics of each of the taxa. Future research could undertake a more comprehensive sample across the skeleton to further assess variation within the skeleton.

One of the pertinent limitations of this study was the preservation of the bone microstructure some of the specimens. For example, the distal femur of *Plateosauravus* was anatomically well preserved, and it was expected that the histology would be good. However, upon sectioning, it was evident that the tissue had experienced intense diagenesis.

Another hindrance in this study was the lack of phylogenetic placement of the indeterminate specimens Sauropodiforme indet. and Lessemsauridae indet.. This was not ideal and constrains the overall deductions in terms of assessing the histological changes that occur in the evolution of the Sauropodomorpha.

Future studies on more sauropodomorph taxa, as well as more comprehensive sampling will permit a better assessment of the evolution of growth patterns among the Sauropodomorpha and will be particularly important for understanding the evolution of gigantism in the Sauropoda.

References

Allain, R. and Aquesbi, N., 2008. Anatomy and phylogenetic relationships of *Tazoudasaurus naimi* (Dinosauria, Sauropoda) from the late Early Jurassic of Morocco. Geodiversitas, 30(2), pp.345-424.

Apaldetti, C., Martínez, R.N., Cerda, I.A., Pol, D. & Alcober, O. 2018. An early trend towards gigantism in Triassic sauropodomorph dinosaurs. *Nature Ecology and Evolution*. 2(8):1227–1232. DOI: 10.1038/s41559-018-0599-y.

Apaldetti, C., Pol, D., Ezcurra, M.D. & Martínez, R.N. 2021. Sauropodomorph evolution across the Triassic–Jurassic boundary: body size, locomotion, and their influence on morphological disparity. *Scientific Reports*. 11(1):1–11. DOI: 10.1038/s41598-021-01120-w.

Apostolaki, N. 2019. The evolution of pneumaticity in Sauropodomorpha and its correlation to body size. *University of Bristol*. (PhD thesis).

Barrett, P.M. & Upchurch, P. 1994. Feeding mechanisms of *Diplodocus*. *Gaia*. 10:195–203.

Becerra, M.G., Gomez, K.L. & Pol, D. 2017. Une dent de sauropodomorphe augmente la diversité des morphotypes dentaires dans la formation Cañadón Asfalto (Jurassique inférieur – moyen) de Patagonie. *Comptes Rendus - Palevol*. 16(8):832–840. DOI: 10.1016/j.crpv.2017.08.005.

Bonaparte, J.F. 1999. Evolución de las vértebras presacras en Sauropodomorpha. *Ameghiniana*. 36(2):115–187.

Bonaparte, J.F. & Coria, R.A. 1993. A new and huge titanosaur sauropod from the Rio Limay Formation (Albian-Cenomanian) of Neuquen Province, Argentina. *Ameghiniana*. 30:271–282.

Bonaparte, J.F. & Martin, V. 1979. El hallazgo del primer nido de dinosaurios triasicos,(Saurischia, Prosauropoda), Triasico Superior de Patagonia, Argentina. *Ameghiniana*. 16(1–2):173–182.

Botha, J., Choiniere, J.N. & Benson, R.B.J. 2022. Rapid growth preceded gigantism in sauropodomorph evolution. *Current Biology*. 1–7. DOI: 10.1016/j.cub.2022.08.031.

Britt, B.B. 1994. Pneumatic postcranial bones in dinosaurs and other archosaurs.University of Calgary, Canada. PhD Thesis.

Bronzati, M., Müller, R.T. & Langer, M.C. 2019. Skull remains of the dinosaur *Saturnalia tupiniquim* (Late Triassic, Brazil): With comments on the early evolution of sauropodomorph feeding behaviour. V. 14. DOI: 10.1371/journal.pone.0221387.

Butler, R.J., Yates, A.M., Rauhut, O.W.M., Foth, C., Butler, R.J., Yates, A.M. & Rauhut, O.W.M. 2013. A pathological tail in a basal sauropodomorph dinosaur from South Africa : evidence of traumatic amputation ? 4634. DOI: 10.1080/02724634.2012.710691.

Button, D.J., Barrett, P.M. & Rayfield, E.J. 2016. Comparative cranial myology and biomechanics of *Plateosaurus* and *Camarasaurus* and evolution of the sauropod feeding apparatus. *Palaeontology*. 59(6):887–913. DOI: 10.1111/pala.12266.

Carrano, M.T. 2001. Implications of limb bone scaling, curvature and eccentricity in mammals and non-avian dinosaurs. *Journal of Zoology*. 254(1):41–55. DOI: 10.1017/S0952836901000541.

Carrano, M.T. 2005. The evolution of sauropod locomotion. *The Sauropods: Evolution and Paleobiology*. 229–249.

Woodruff, D., Fowler, D.W. & Horner, J.R. 2017. A new multi-faceted framework for deciphering diplodocid ontogeny. *Palaeontologia Electronica*. 20(3):1–53. DOI: 10.26879/674.

Castanet, J. 2006. Time recording in bone microstructures of endothermic animals; functional relationships.

Comptes Rendus - Palevol. 5(3–4):629–636. DOI: 10.1016/j.crpv.2005.10.006.

Cerda, I.A., Carabajal, A.P., Salgado, L., Coria, R.A., Reguero, M.A., Tambussi, C.P. & Moly, J.J. 2012. The first record of a sauropod dinosaur from Antarctica. *Naturwissenschaften*. 99(1):83–87. DOI: 10.1007/s00114-011-0869-x.

Cerda, I.A., Pol, D. & Chinsamy, A. 2014. Osteohistological insight into the early stages of growth in *Mussaurus patagonicus* (Dinosauria, Sauropodomorpha). *Historical Biology*. 26(1):110–121. DOI: 10.1080/08912963.2012.763119.

Cerda, I.A., Casal, G.A., Martinez, R.D. & Ibiricu, L.M. 2015. Histological evidence for a supraspinous ligament in sauropod dinosaurs. *Royal Society Open Science*. 2(10):1–17. DOI: 10.1098/rsos.150369.

Cerda, I.A., Chinsamy, A., Pol, D., Apaldetti, C., Otero, A., Powell, J.E. & Martínez, R.N. 2017. Novel insight into the origin of the growth dynamics of sauropod dinosaurs. V. 12. DOI: 10.1371/journal.pone.0179707.

Cerda, I.A., Pol, D., Otero, A. & Chinsamy, A. 2022. Palaeobiology of the early sauropodomorph *Mussaurus patagonicus* inferred from its long bone histology. *Palaeontology*. 65(4):1–48. DOI: 10.1111/pala.12614.

Cerda, I.A., Novas, F.E., Carballido, J.L. & Salgado, L. 2022. Osteohistology of the hyperelongate hemispinous processes of *Amargasaurus cazaui* (Dinosauria: Sauropoda): Implications for soft tissue reconstruction and functional significance. *Journal of Anatomy*. 240(6):1005–1019. DOI: 10.1111/joa.13659.

de Cerff, C., Krupandan, E. & Chinsamy, A. 2021. Palaeobiological implications of the osteohistology of a basal sauropodomorph dinosaur from South Africa. *Historical Biology*. 33(11):2865–2877. DOI: 10.1080/08912963.2020.1833000.

Chapelle, K.E.J., Barrett, P.M., Botha, J. & Choiniere, J.N. 2019. *Ngwevu intloko*: A new early sauropodomorph dinosaur from the Lower Jurassic Elliot Formation of South Africa and comments on cranial ontogeny in Massospondylus carinatus. PeerJ. 2019(8). DOI: 10.7717/peerj.7240.

Chapelle, K.E., Barrett, P.M., Choiniere, J.N. & Botha, J. 2022. Interelemental osteohistological variation in *Massospondylus carinatus* and its implications for locomotion . *PeerJ*. 10:e13918. DOI: 10.7717/peerj.13918.

Chapelle, K.E.J., Botha, J. & Choiniere, J.N. 2021. Extreme growth plasticity in the early branching sauropodomorph *Massospondylus carinatus*. *Biology Letters*. 17(5). DOI: 10.1098/rsbl.2020.0843.

Charig, A.J., Attridge, J., Crompton & W., A. 1965. On the origin of the sauropods and the classification of the Saurischia. *Proceedings of the Linnean Society of London*. 176(2):197–221. DOI: 10.1111/j.1095-8312.1965.tb00944.x.

Chinsamy-Turan, A. 2005. *The microstructure of dinosaur bone*. John Hopkins University Press.

Chinsamy, A. 1990. Physiological Implications of the Bone Histology of *Syntarsus rhodesiensis* (Saurischia: Theropoda). *Palaeontologia Africana*. 27:77–82.

Chinsamy, A. 1993. Bone histology and growth trajectory of the prosauropod dinosaur *Massospondylus carinatus* Owen. *Modern Geology*. 18(3):319–329.

Chinsamy, A. 1994. Dinosaur Bone Histology: Implications and Inferences. *The Paleontological Society Special Publications*. 7:213–228. DOI: 10.1017/s2475262200009539.

Chinsamy, A. 2023. Palaeoecological deductions from osteohistology. *Biology letters*. 19(8):20230245. DOI: 10.1098/rsbl.2023.0245.

Chinsamy, A. & Hurum, J.H. 2006. Bone microstructure and growth patterns of early mammals. *Acta Palaeontologica Polonica*. 51(2):325–338.

Chinsamy, A. & Raath, M. a. 1992. Preparation of fossil bone for histological examination. *Palaeontologia*

Africana. 29(I 992):39–44.

Chinsamy, A. & Tumarkin-Deratzian, A. 2009. Pathologic bone tissues in a Turkey vulture and a nonavian dinosaur: Implications for interpreting endosteal bone and radial fibrolamellar bone in fossil dinosaurs. *Anatomical Record*. 292(9):1478–1484. DOI: 10.1002/ar.20991.

Chinsamy, A., Martin, L.D. & Dodson, P. 1998. Bone microstructure of the diving *Hesperornis* and the volant Ichthyornis from the Niobrara Chalk of western Kansas. *Cretaceous Research*. 19(2):225–235. DOI: 10.1006/cres.1997.0102.

Chinsamy, A., Thomas, D.B., Tumarkin-Deratzian, A.R. & Fiorillo, A.R. 2012. Hadrosaurs Were Perennial Polar Residents. *Anatomical Record*. 295(4):610–614. DOI: 10.1002/ar.22428.

Chinsamy, A., Cerda, I. & Powell, J. 2016. Vascularised endosteal bone tissue in armoured sauropod dinosaurs. *Scientific Reports*. 6(April):1–9. DOI: 10.1038/srep24858.

Chinsamy, A., Marugán-Lobón, J., Serrano, F.J. & Chiappe, L. 2020. Osteohistology and Life History of the Basal Pygostylian, *Confuciusornis sanctus*. *Anatomical Record*. 303(4):949–962. DOI: 10.1002/ar.24282.

Chinsamy, A., Angst, D., Canoville, A. & Göhlich, U.B. 2021. Bone histology yields insights into the biology of the extinct elephant birds (Aepyornithidae) from Madagascar. *Biological Journal of the Linnean Society*. 130(2):268–295. DOI: 10.1093/BIOLINNEAN/BLAA013.

Christian, A., Peng, G., Sekiya, T., Ye, Y., Wulf, M.G. & Steuer, T. 2013. Biomechanical reconstructions and selective advantages of neck poses and feeding strategies of Sauropods with the example of *Mamenchisaurus youngi*. *PloS one*. 8(10). DOI: 10.1371/journal.pone.0071172.

Christiansen, P. 1999. On the head size of sauropodomorph dinosaurs: Implications for ecology and physiology. *Historical Biology*. 13(4):269–297. DOI: 10.1080/08912969909386586.

Clauss, M., Steuer, P., Müller, D.W.H., Codron, D. & Hummel, J. 2013. Herbivory and body size: Allometries of diet quality and gastrointestinal physiology, and implications for herbivore ecology and dinosaur gigantism. *PLoS ONE*. 8(10). DOI: 10.1371/journal.pone.0068714.

Cooper, M.R. 1984. A reassessment of *Vulcanodon karibaensis* (Dinosauria: Saurischia) and the origin of the Sauropoda.

Cubo, J. & Huttenlocker, A.K. 2020. Vertebrate palaeophysiology. *Philosophical Transactions of the Royal Society B: Biological Sciences*. 375(1793). DOI: 10.1098/rstb.2019.0130.

Curry Rogers, K. & Kulik, Z. (in press). Osteohistology of *Rapetosaurus krausei* (Sauropoda: Titanosauria) from the Upper Cretaceous of Madagascar. *Journal of Vertebrate Paleontology*. 38(4):(1)-(24). DOI: 10.1080/02724634.2018.1493689.

D'Emic, M.D., Whitlock, J.A., Smith, K.M., Fisher, D.C. & Wilson, J.A. 2013. Evolution of High Tooth Replacement Rates in Sauropod Dinosaurs. *PLoS ONE*. 8(7):1–7. DOI: 10.1371/journal.pone.0069235.

Enlow, D.H. 1962a. Functions of the Haversian system. *University of Michigan*.

Enlow, D.H. 1962b. A study of the post-natal growth and remodeling of bone. *American Journal of Anatomy*. 110(2):79–101.

Erickson, G.M., Rogers, K.C., Varricchio, D.J., Norell, M.A. & Xu, X. 2007. Growth patterns in brooding dinosaurs reveals the timing of sexual maturity in non-avian dinosaurs and genesis of the avian condition. *Biology Letters*. 3(5):558–561. DOI: 10.1098/rsbl.2007.0254.

Ezcurra, M.D. 2010. A new early dinosaur (Saurischia: Sauropodomorpha) from the Late Triassicof Argentina: A reassessment of dinosaur origin and phylogeny. *Journal of Systematic Palaeontology*. 8(3):371–425. DOI: 10.1080/14772019.2010.484650.

Ezcurra, M.D. & Apaldetti, C. 2012. A robust sauropodomorph specimen from the Upper Triassic of Argentina and insights on the diversity of the Los Colorados Formation. *Proceedings of the Geologists' Association*. 123(1):155–164. DOI: 10.1016/j.pgeola.2011.05.002.

De Fabrègues, C.P. & Allain, R. 2016. New material and revision of *Melanorosaurus thabanensis*, a basal sauropodomorph from the Upper Triassic of Lesotho. *PeerJ*. 2016(2):1–32. DOI: 10.7717/peerj.1639.

Fowler, D.W. & Sullivan, R.M. 2011. The first giant titanosaurian sauropod from the upper Cretaceous of North America. *Acta Palaeontologica Polonica*. 56(4):685–690. DOI: 10.4202/app.2010.0105.

Francillon-Vieillot, H., de Buffrénil, V., Castanet, J., Géraudie, J., Meunier, F.J., Sire, J.Y., Zylberberg, L. & de Ricqlès, A. 1990. Microstructure and mineralization of vertebrate skeletal tissues. *Skeletal biomineralization: patterns, processes and evolutionary trends*. 1:471–530.

Frost, H. M. (1994). Wolff's Law and bone's structural adaptations to mechanical usage: an overview for clinicians. The Angle Orthodontist 64, 175–188.

González, R., Cerda, I.A., Filippi, L.S. & Salgado, L. 2020. Early growth dynamics of titanosaur sauropods inferred from bone histology. *Palaeogeography, Palaeoclimatology, Palaeoecology*. 537(April 2019):109404. DOI: 10.1016/j.palaeo.2019.109404.

Griebeler, E.M., Klein, N. & Sander, P.M. 2013. Aging, Maturation and Growth of Sauropodomorph Dinosaurs as Deduced from Growth Curves Using Long Bone Histological Data: An Assessment of Methodological Constraints and Solutions. *PLoS ONE*. 8(6). DOI: 10.1371/journal.pone.0067012.

Harris, J.D. & Dodson, P. 2004. A new diplodocoid sauropod dinosaur from the Upper Jurassic Morrison Formation of Montana, USA. *Acta Palaeontologica Polonica*. 49(2):197–210.

Van Heerden, J. & Galton, P.M. 1997. The affinities of *Melanorosaurus* - A Late Triassic prosauropod dinosaur from South Africa. *Neues Jahrbuch fur Geologie und Palaontologie - Monatshefte*. (1):39–55. DOI: 10.1127/njgpm/1997/1997/39.

Hillenius, W.J. 2006. Dinosaur Physiology: Were Dinosaurs Warm-blooded? *Encyclopedia of Life Sciences*. (January 2006). DOI: 10.1038/npg.els.0003323.

Hone, D.W.E. & Benton, M.J. 2005. The evolution of large size: How does Cope's Rule work? *Trends in Ecology and Evolution*. 20(1):4–6. DOI: 10.1016/j.tree.2004.10.012.

Horner, J.R., De Ricqlès, A. & Padian, K. 2000. Long bone histology of the hadrosaurid dinosaur *Maiasaura peeblesorum*: growth dynamics and physiology based on an ontogenetic series of skeletal elements. *Journal of Vertebrate Paleontology*. 20(1):115–129.

Horner, J.R., Ricqls, A. De, Padian, K. & Scheetz, R.D. 2009. Comparative long bone histology and growth of the " hypsilophodontid" dinosaurs *Orodromeus makelai*, *Dryosaurus altus*, and *Tenontosaurus tillettii* (Ornithischia: Euornithopoda). *Journal of Vertebrate Paleontology*. 29(3):734–747. DOI: 10.1671/039.029.0312.

Hutchinson, J.R. 2005. Dinosaur Locomotion. *The Dinosauria*. V. 79. DOI: 10.1666/0022-3360(2005)079[1235:r]2.0.co;2.

Huttenlocker, A.K., Woodward, H.N. & Hall, B.K. 2013. The biology of bone. *Bone histology of fossil tetrapods*. 13–34.

Ibiricu, L.M., Lamanna, M.C., Martínez, R.D.F., Casal, G.A., Cerda, I.A., Martínez, G. & Salgado, L. 2017. A novel form of postcranial skeletal pneumaticity in a sauropod dinosaur: Implications for the paleobiology of Rebbachisauridae. *Acta Palaeontologica Polonica*. 62(X):221–236. DOI: 10.4202/app.00316.2016.

Jentgen-Ceschino, B., Stein, K. & Fischer, V. 2020. Case study of radial fibrolamellar bone tissues in the outer cortex of basal sauropods. *Philosophical Transactions of the Royal Society B: Biological Sciences*. 375(1793):1–12. DOI: 10.1098/rstb.2019.0143.

Klein, N. & Sander, P.M. 2007. Bone histology and growth of the prosauropod dinosaur *Plateosaurus Engelhardti* Von Meyer, 1837 from the Norian bonebeds of Trossingen (Germany) and Frick (Switzerland). *Special Papers in Palaeontology*. (77):169–206.

Klein, N. & Sander, M. 2008. Ontogenetic stages in the long bone histology of sauropod dinosaurs. *Paleobiology*. 34(2):247–263.

Klinkhamer, A.J., Mallison, H., Poropat, S.F., Sinapius, G.H.K. & Wroe, S. 2018. Three-Dimensional Musculoskeletal Modeling of the Sauropodomorph Hind Limb: The Effect of Postural Change on Muscle Leverage. Anatomical Record. 301(12):2145–2163. DOI: 10.1002/ar.23950.

Krupandan, E., Chinsamy-Turan, A. & Pol, D. 2018. The Long Bone Histology of the Sauropodomorph, *Antetonitrus ingenipes*. *Anatomical Record*. 301(9):1506–1518. DOI: 10.1002/ar.23898.

Lacovara, K.J., Lamanna, M.C., Ibiricu, L.M., Poole, J.C., Schroeter, E.R., Ullmann, P. V., Voegele, K.K., Boles, Z.M., *et al.* 2014. A gigantic, exceptionally complete titanosaurian sauropod dinosaur from southern Patagonia, Argentina. *Scientific Reports*. 4:1–9. DOI: 10.1038/srep06196.

Lambertz, M., Bertozzo, F. & Sander, P.M. 2018. Bone histological correlates for air sacs and their implications for understanding the origin of the dinosaurian respiratory system. *Biology Letters*. 14(1). DOI: 10.1098/rsbl.2017.0514.

Langer, M.C., Abdala, F., Richter, M. & Benton, M.J. 1999. A sauropodomorph dinosaur from the Upper Triassic (Carnian) of southern Brazil. *Comptes Rendus de l'Academie de Sciences - Serie IIa: Sciences de la Terre et des Planetes*. 329(7):511–517. DOI: 10.1016/S1251-8050(00)80025-7.

Langer, M.C., Ezcurra, M.D., Rauhut, O.W.M., Benton, M.J., Knoll, F., McPhee, B.W., Novas, F.E., Pol, D., e 2017. Untangling the dinosaur family tree. *Nature*. 551(7678):501–506. DOI: 10.1038/nature24011.

Lefebvre, R., Houssaye, A., Mallison, H., Cornette, R. & Allain, R. 2022. A path to gigantism: Three-dimensional study of the sauropodomorph limb long bone shape variation in the context of the emergence of the sauropod bauplan. *Journal of Anatomy*. (July 2021):297–336. DOI: 10.1111/joa.13646.

Lehrer HZ, Maxfield WS, Nice CM. 1970. The periosteal sunburst pattern in metastatic bone. *Am J Roentgenol* 108:154–161. Lenehan

Lockley, M.G., Meyer, C.A., Hunt, A.P. & Lucas, S.G. 1994. The distribution of sauropod tracks and trackmakers. *Gaia*. 10:233–248.

Lorigan JG, Libshitz HI, Peuchot M. 1989. Radiation-induced sarcoma of bone: CT findings in 19 cases. *Am J Roentgenol* 153:791–794

Makarieva, A.M., Gorshkov, V.G. & Li, B.L. 2005. Gigantism, temperature and metabolic rate in terrestrial poikilotherms. *Proceedings of the Royal Society B: Biological Sciences*. 272(1578):2325–2328. DOI: 10.1098/rspb.2005.3223.

De Margerie, E., Robin, J.P., Verrier, D., Cubo, J., Groscolas, R. & Castanet, J. 2004. Assessing a relationship between bone microstructure and growth rate: A fluorescent labelling study in the king penguin chick (*Aptenodytes patagonicus*). *Journal of Experimental Biology*. 207(5):869–879. DOI: 10.1242/jeb.00841.

McFarlin, S.C., Terranova, C.J., Zihlman, A.L. & Bromage, T.G. 2016. Primary bone microanatomy records developmental aspects of life history in catarrhine primates. *Journal of Human Evolution*. 92:60–79. DOI: 10.1016/j.jhevol.2015.12.004.

Mcphee, B.W., Yates, A.M., Choiniere, J.N. & Abdala, F. 2014. The complete anatomy and phylogenetic relationships of *Antetonitrus ingenipes* (Sauropodiformes, Dinosauria): Implications for the origins of Sauropoda. *Zoological Journal of the Linnean Society*. 171(1):151–205. DOI: 10.1111/zoj.12127.

McPhee, B.W., Benson, R.B.J., Botha-Brink, J., Bordy, E.M. & Choiniere, J.N. 2018. A Giant Dinosaur from the Earliest Jurassic of South Africa and the Transition to Quadrupedality in Early Sauropodomorphs. *Current*

Biology. 28(19):3143-3151.e7. DOI: 10.1016/j.cub.2018.07.063.

Montoya-Sanhueza, G. & Chinsamy, A. 2018. Cortical bone adaptation and mineral mobilization in the subterranean mammal *Bathyergus suillus* (Rodentia: Bathyergidae): Effects of age and sex. *PeerJ*. 2018(6). DOI: 10.7717/peerj.4944.

Müller, R.T. & Garcia, M.S. 2020. Rise of an empire: analyzing the high diversity of the earliest sauropodomorph dinosaurs through distinct hypotheses. *Historical Biology*. 32(10):1334–1339. DOI: 10.1080/08912963.2019.1587754.

Nacarino-Meneses, C., Jordana, X. & Köhler, M. 2016. First approach to bone histology and skeletochronology of *Equus hemionus*. *Comptes Rendus - Palevol*. 15(1–2):267–277. DOI: 10.1016/j.crpv.2015.02.005.

Nesbitt, S.J., Barrett, P.M., Werning, S., Sidor, C.A. & Charig, A.J. 2013. The oldest dinosaur? A Middle Triassic dinosauriform from Tanzania. *Biology Letters*. 9(1). DOI: 10.1098/rsbl.2012.0949.

Otero, A., Krupandan, E., Pol, D., Chinsamy, A. & Choiniere, J. 2015. A new basal sauropodiform from South Africa and the phylogenetic relationships of basal sauropodomorphs. *Zoological Journal of the Linnean Society*. 174(3):589–634. DOI: 10.1111/zoj.12247.

Otero, A., Cuff, A.R., Allen, V., Sumner-Rooney, L., Pol, D. & Hutchinson, J.R. 2019. Ontogenetic changes in the body plan of the sauropodomorph dinosaur *Mussaurus patagonicus* reveal shifts of locomotor stance during growth. *Scientific Reports*. 9(1):1–10. DOI: 10.1038/s41598-019-44037-1.

Otero, A., Carballido, J.L. & Moreno, A.P. 2020. The Appendicular Osteology of *Patagotitan mayorum* (Dinosauria, Sauropoda). *Journal of Vertebrate Paleontology*. 40(4). DOI: 10.1080/02724634.2020.1793158.

Padian, K., Werning, S. & Horner, J.R. 2016. A hypothesis of differential secondary bone formation in dinosaurs. *Comptes Rendus - Palevol*. 15(1–2):40–48. DOI: 10.1016/j.crpv.2015.03.002.

Petermann, H. & Sander, M. 2013. Histological evidence for muscle insertion in extant amniote femora: Implications for muscle reconstruction in fossils. Journal of Anatomy. 222(4):419–436. DOI: 10.1111/joa.12028.

Pol, D. & Powell, J.E. 2007. New information on *Lessemsaurus sauropoides* (Dinosauria: Sauropodomorpha) from the upper Triassic of Argentina. *Special Papers in Palaeontology*. 77:223.

Pol, D., Garrido, A. & Cerda, I.A. 2011. A new sauropodomorph dinosaur from the early Jurassic of Patagonia and the origin and evolution of the sauropod-type sacrum. *PLoS ONE*. 6(1). DOI: 10.1371/journal.pone.0014572.

Pol, D., Otero, A., Apaldetti, C. & Martínez, R.N. 2021. Triassic sauropodomorph dinosaurs from South America: The origin and diversification of dinosaur dominated herbivorous faunas. *Journal of South American Earth Sciences*. 107(June 2020):103145. DOI: 10.1016/j.jsames.2020.103145.

Prondvai, E., Stein, K., Osi, A. & Sander, M.P. 2012. Life history of *Rhamphorhynchus* inferred from bone histology and the diversity of pterosaurian growth strategies. *PLoS ONE*. 7(2). DOI: 10.1371/journal.pone.0031392.

Rauhut, O.W.M., Remes, K., Fechner, R., Cladera, G. & Puerta, P. 2005. Discovery of a short-necked sauropod dinosaur from the Late Jurassic period of Patagonia. *Nature*. 435(7042):670–672. DOI: 10.1038/nature03623.

Rauhut, O.W.M., Holwerda, F.M. & Furrer, H. 2020. A derived sauropodiform dinosaur and other sauropodomorph material from the Late Triassic of Canton Schaffhausen, Switzerland. *Swiss Journal of Geosciences*. 113(1). DOI: 10.1186/s00015-020-00360-8.

Reid, A.R.E.H. 1985. On Supposed Haversian Bone from the Hadrosaur Anatosaurus , and the Nature of Compact Bone in Dinosaurs Published by : SEPM Society for Sedimentary Geology Stable URL :

https://www.jstor.org/stable/1304832 REFERENCES Linked references are available on JST. 59(1):140–148.

Reid, R.E.H. 1990. Zonal “growth rings” in dinosaurs. *Modern Geology*. 15(1):19–48.

Ricqles De, A. 1983. Cyclical growth in the long limb bones of a sauropod dinosaur. *Acta Palaeontologica Polonica*. 28(1–2).

Sander, P.M. 2000. Longbone histology of the Tendaguru sauropods: implications for growth and biology. *Paleobiology*. 26(3):466–488. DOI: 10.1666/0094-8373(2000)026<0466:lhotts>2.0.co;2.

Sander, P.M. 2013. An evolutionary cascade model for sauropod dinosaur gigantism--overview, update and tests. *PloS one*. 8(10). DOI: 10.1371/journal.pone.0078573.

Sander, P.M. & Clauss, M. 2008. Paleontology: Sauropod gigantism. *Science*. 322(5899):200–201. DOI: 10.1126/science.1160904.

Sander, P.M. & Klein, N. 2005. Paleontology: Developmental plasticity in the life history of a prosauropod dinosaur. *Science*. 310(5755):1800–1802. DOI: 10.1126/science.1120125.

Sander, P.M. & Lallensack, J.N. 2018. Dinosaurs: Four Legs Good, Two Legs Bad. *Current Biology*. 28(19):R1160–R1163. DOI: 10.1016/j.cub.2018.08.025.

Sander, P.M., Klein, N., Buffetaut, E., Cuny, G., Suteethorn, V. & Le Loeuff, J. 2004. Adaptive radiation in sauropod dinosaurs: Bone histology indicates rapid evolution of giant body size through acceleration. *Organisms Diversity and Evolution*. 4(3):165–173. DOI: 10.1016/j.ode.2003.12.002.

Sander, P.M., Christian, A., Clauss, M., Fechner, R., Gee, C.T., Griebeler, E.M., Gunga, H.C., Hummel, J., *et al.* 2011. Biology of the sauropod dinosaurs: The evolution of gigantism. *Biological Reviews*. 86(1):117–155. DOI: 10.1111/j.1469-185X.2010.00137.x.

Sander, P.M., Klein, N., Stein, K. & Wings, O. 2011. Sauropod Bone Histology and Its Implications for Sauropod Biology. *Biology of the Sauropod Dinosaurs: Understanding the Life of Giants*. 276–302.

Schwarz-Wings, D., Meyer, C.A., Frey, E., Manz-Steiner, H.R. & Schumacher, R. 2010. Mechanical implications of pneumatic neck vertebrae in sauropod dinosaurs. *Proceedings of the Royal Society B: Biological Sciences*. 277(1678):11–17. DOI: 10.1098/rspb.2009.1275.

Seeley H. G. 1888. On the classification of the fossil animals commonly named Dinosauria. *Proc. R. Soc. Lond.*43: 165–171. http://doi.org/10.1098/rspl.1887.0117.

Sereno, P.C. 2007. Basal Sauropodomorpha: historical and recent phylogenetic hypotheses, with comments on Ammosaurus major (Marsh, 1889). *Special Papers in Palaeontology*. 77:261.

Seymour, R.S. 2016. Cardiovascular physiology of dinosaurs. *Physiology*. 31(6):430–441. DOI: 10.1152/physiol.00016.2016.

Smith, N.D. & Pol, D. 2007. Anatomy of a basal sauropodomorph dinosaur from the Early Jurassic Hanson Formation of Antarctica. *Acta Palaeontologica Polonica*. 52(4):657–674.

Stein, K. 2011. Long bone histology of basalmost and derived Sauropodomorpha: the convergence of fibrolamellar bone and the evolution of giantism and nanism. *Mathematisch-Naturwissenschaftlichen Fakultät*. 213. Available: http://hss.ulb.uni-bonn.de/2011/2714/2714.htm.

Stein, K. & Prondvai, E. 2014. Rethinking the nature of fibrolamellar bone: An integrative biological revision of sauropod plexiform bone formation. *Biological Reviews*. 89(1):24–47. DOI: 10.1111/brv.12041.

Stevens, K.A. 2013. The articulation of sauropod necks: methodology and mythology. *PloS one*. 8(10). DOI: 10.1371/journal.pone.0078572.

Taylor, M.P. & Wedel, M.J. 2013. Why sauropods had long necks; and why giraffes have short necks. *PeerJ*. 2013(1):1–41. DOI: 10.7717/peerj.36.

Tschopp, E. & Mateus, O. 2013. The skull and neck of a new flagellicaudatan sauropod from the Morrison Formation and its implication for the evolution and ontogeny of diplodocid dinosaurs. *Journal of Systematic Palaeontology*. 11(7):853–888. DOI: 10.1080/14772019.2012.746589.

Upchurch, P., Barrett, P.M. & Dodson, P. 2004. Sauropoda. *The Dinosauria*. 259–322.

Waskow, K. & Mateus, O. 2017. Histologie des côtes dorsales de dinosaures et d'un crocodile de l'Ouest du Portugal : implications squelettochronologiques sur la détermination de l'âge et des traits d'histoire de vie. *Comptes Rendus - Palevol*. 16(4):425–439. DOI: 10.1016/j.crpv.2017.01.003.

Waskow, K. & Sander, P.M. 2014. Growth record and histological variation in the dorsal ribs of *Camarasaurus* sp. (Sauropoda). *Journal of Vertebrate Paleontology*. 34(4):852–869. DOI: 10.1080/02724634.2014.840645.

Wilson, J.A. & Sereno, P.C. 1998. Early evolution and higher-level phylogeny of sauropod dinosaurs. *Journal of vertebrate paleontology*. 18(S2):1–79.

Wings, O. & Sander, P.M. 2007. No gastric mill in sauropod dinosaurs: New evidence from analysis of gastrolith mass and function in ostriches. *Proceedings of the Royal Society B: Biological Sciences*. 274(1610):635–640. DOI: 10.1098/rspb.2006.3763.

Yates, A.M. 2003. A definite prosauropod dinosaur from the Lower Elliot Formation (Norian: Upper Triassic) of South Africa. *Palaeontologia Africana*. (39):63–68.

Yates, A.M. 2007a. Solving a dinosaurian puzzle: The identity of *Aliwalia rex* Galton. *Historical Biology*. 19(1):93–123. DOI: 10.1080/08912960600866953.

Yates, A.M. 2007b. The first complete skull of the Triassic dinosaur *Melanorosaurus* haughton (Sauropodomorpha: Anchisauria). *Evolution and palaeobiology of early sauropodomorph dinosaurs*. (77):9–55.

Yates, A.M. & Kitching, J.W. 2003. The earliest known sauropod dinosaur and the first steps towards sauropod locomotion. *Proceedings of the Royal Society B: Biological Sciences*. 270(1525):1753–1758. DOI: 10.1098/rspb.2003.2417.

Yates, A.M., Bonnan, M.F., Neveling, J., Chinsamy, A. & Blackbeard, M.G. 2010. A new transitional sauropodomorph dinosaur from the Early Jurassic of South Africa and the evolution of sauropod feeding and quadrupedalism. *Proceedings of the Royal Society B: Biological Sciences*. 277(1682):787–794. DOI: 10.1098/rspb.2009.1440.

Yates, A.M., Wedel, M.J. & Bonnan, M.F. 2012. The early evolution of postcranial skeletal pneumaticity in sauropodomorph dinosaurs. *Acta Palaeontologica Polonica*. 57(1):85–100. DOI: 10.4202/app.2010.0075.

Young, M.T., Rayfield, E.J., Holliday, C.M., Witmer, L.M., Button, D.J., Upchurch, P. & Barrett, P.M. 2012. Cranial biomechanics of *Diplodocus* (Dinosauria, Sauropoda): Testing hypotheses of feeding behaviour in an extinct megaherbivore. *Naturwissenschaften*. 99(8):637–643. DOI: 10.1007/s00114-012-0944-y.

Ziv, V., Wagner, H.D. & Weiner, S. 1996. Microstructure-microhardness relations in parallel-fibered and lamellar bone. *Bone*. 18(5):417–428. DOI: 10.1016/8756-3282(96)00049-X.

Appendix

Table 3: General measurements of each long bone of *Plateosauravus*, Sauropodiforme indet., *Melanorosaurus* and Lessemsauridae indet. Provided measurements of pre-sectioned bones prior to thin section preparation*. All measurements are in millimetres. Abbreviations: MS – Midshaft; DS – Distal head.

Specimen number	Bone type	Bone length	MS circumference	MS diameter	DH circumference	DH diameter
SAM-PK-K382	Femur	506.89	359.42	125.72	^	^
	Tibia	516.76	254.35	98.55	^	^
	Tibia	554.86	171.59	61.31	^	^
SAM-PK-3603	Femur	580.01	219.5	75.50	^	^
SAM-PK-2780	Distal femur head	226.00	^	^	238.50	103.00
NMQR-1551	Femur	600.00	^	180.00	^	^
	Tibia	493.00	^	170.00	^	^
NMQR-3314	Fibula	431.00	68.00	149.1*	^	^
	Tibia	442.00	50.03	201.5*	^	^

Table 4: General measurements for non-long bones of *Plateosauravus* and Lessemsauridae indet. All measurements are in millimetres.

Specimen number	Bone type	Length	Circumference	Width
SAM-PK-K382	Caudal vertebrae	445.58	102.48	119.00
	Spinous process	169.86	^	70.83
SAM-PK-3341	Rib	345.50	80.00	^